INTERNATIONAL ATOMIC ENERGY AGENCY

INDC(CCP)-440
Distr.: L0

I N D C INTERNATIONAL NUCLEAR DATA COMMITTEE

Articles Translated from Journal Yadernye Konstanty (Nuclear Constants)

(Series: Nuclear Constants, Issue No. 1-2, 2003)

Translated by the IAEA

September 2004

IAEA NUCLEAR DATA SECTION, WAGRAMER STRASSE 5, A-1400 VIENNA

Nuclear Data Section
International Atomic Energy Agency
P.O. Box 100
Wagramer Strasse 5
A-1400 Vienna
Austria

Produced by the IAEA in Austria
September 2004

INDC(CCP)-440
Distr.: L0

Articles Translated from Journal Yadernye Konstanty (Nuclear Constants)

(Series: Nuclear Constants, Issue No. 1-2, 2003)

Abstract

This report contains the translation of four papers published in the Nuclear Constants journal (Voprosy Atomnoj Nauki I Teknniki, seriya: Yadernye Konstanty (YK), vypusk 1-2, 2003). Other three papers from this report ("Evaluation of Value and Localization of Systematic Errors for Level Densities and Radiative Strength Functions extracted from (n,2γ) Reaction" by A.M. Sukhovoi and V.A. Khitrov; "On Conservative Multigroup Methods" by B.D. Abramov and "Evaluation of Some Contribution Sources of Systematic Errors in Determination of the Level Densities and Strength Functions from the Gamma-Spectra in Nuclear Reactions" by A.M. Sukhovoi et al.) are available only in Russian.

September 2004

Contents

NEUTRON CONSTANTS AND PARAMETRS

04-10281 (199) [1]
Translated from Russian

UDC 539.163

EVALUATION OF THE RESOLVED RESONANCE REGION FOR ^{233}Pa

G.B. Morogovskij, L.A. Bakhanovich
Sosny Joint Institute for Energy and Nuclear Research, Belarus National Academy of Sciences

EVALUATION OF THE RESOLVED RESONANCE REGION FOR ^{233}Pa. Thermal cross-sections and Breit-Wigner parameters have been obtained for the representation of total cross-section energy dependence in the 0.01–107 eV region as a result of evaluating ^{233}Pa experimental capture cross-sections at E=0.0253 eV and Simpson's total cross-section σ_t(E) in the resolved resonance region.

Since ^{233}Pa is one of the elements of the U-Th fuel cycle, its neutron cross-sections in the thermal and resonance regions are of some interest. In the existing files of evaluated nuclear data on this nucleus (JENDL-3.2 [1], ENDF/B-VI [2] and JEF-2 [3]), the parameters of Simpson et al. [4] are used to represent cross-sections in the 10^{-5}–17 eV energy range with an appropriate modification to obtain the required cross-section values at energy 0.0253 eV. Moreover, in the evaluations of Refs [2, 3] the resolved resonance region is expanded to 38.5 eV by the use of Harris's parameters [5] above 18 eV. We will not consider Refs [1, 3] further since in file [1] the upper limit of the resolved resonance region is taken to be 16.5 eV, which is substantially lower than in evaluations [2, 3], while in file [3] the region of interest to us is the same as in [2]. An evaluation carried out by us on the experimental measurements of σ_t(E) in [4] and test calculations using the parameters of [2] showed that:

1. The ENDF/B-VI parameters [2] need revision, especially in the 16–38.5 eV energy range, where some resonances have clearly been omitted.
2. The resolved resonance region can be expanded to ~100 eV.
3. An evaluation of the experimental measurements of σ_t and σ_γ in the thermal region needs to be carried out to obtain reliable self-consistent values for these cross-sections at E=0.0253 eV and to refine the parameters of the negative resonance, which substantially affect the energy dependence of the cross-sections in the 0.01–0.8 eV energy range.

The present paper addresses the above problems.

Firstly, note that there is only one experimental measurement of the energy dependence of the ^{233}Pa cross-section in the thermal and resolved resonance regions. This is the aforementioned study by Simpson et al. [4] on the determination of σ_t(E). The evaluations in [1–3], up to 17 eV, are based on resonance parameters obtained by the authors of [4] as a result of analysing their own measurements. Our study is based directly on the measurements

of $\sigma_t(E)$ in [4]. In addition, to refine the description of the total cross-section energy dependence in the regions between resonances, we initially used a potential scattering radius value of ~10 fm rather than the value of 8.9184 fm adopted in [2]. In obtaining self-consistent values for the thermal cross-sections (see section 3) the value of the scattering radius was refined.

1. Re-evaluation of parameters taking into account the omission of resonances in the 0.01–38.5 eV energy range

Comparison of the experimental measurements of $\sigma_t(E)$ in [4] with the calculation using the parameters of the evaluation in [2] shows that up to 17 eV these parameters on the whole describe the total cross-section dependence of [4] fairly well. Exceptions are the 0.01–1 eV range and the gaps between resonances above 5.5 eV, where the calculated curve is rather low (see Fig. 1). We used the parameters of [2] as a starting set to carry out parametrization in the 0.01–38.5 eV energy range. However, preliminary calculations already showed that an improved description of the dependence $\sigma_t(E)$ in [4] in the 0.01–17 eV range results directly from refining a number of the resonance energies of [2] (see Table 1). We also think that the total cross-section energy dependence of [4] in the 16.1–16.9 eV range is largely determined by two previously unidentified resonances at energies of 16.2 and 16.8 eV.

Table 1

E_r, eV [2]	-0.20	0.795	10.89	12.15	14.80	15.96	17.00
E_r, eV – present study	-0.18	0.789	10.87	12.13	14.75	15.92	17.02

The parameters calculated by us for the 24 resonances in the 0.01–17.5 eV range describe the total cross-section dependence of [4] taking into account the energy resolution of the experiment substantially better than do the parameters of [2], as can be seen from Fig. 1 and the comparison of several mean values. Thus, for E_1 and E_2 equal to 0.01 and 16.5 eV respectively, the area under the total cross-section curve $A_t = \int_{E_1}^{E_2} \sigma_\tau(E)dE$ for [4] is 2373 b·eV, whereas in the calculation using the parameters of [2] we obtain 2420 b·eV (2% discrepancy) and with our own parameters 2364 b·eV (0.4% discrepancy). However, what is more significant is the discrepancy between the areas A_t for each resonance calculated from the experimental total cross-sections of [4], the evaluation of [2] and the parameters of the present study. The magnitude of this discrepancy between the experimental and calculated values of A_t in the 0.01–16.5 eV range is, on average, 4.4% for each resonance with the parameters of [2] and 1.2% with our parameters.

Above 17.5 eV, the omission of resonances in the parameters of [2] is easily noticeable even visually (see Fig. 2). A comparison of the mean resonance parameters calculated from this set for the regions 0.01–18 eV and 18–38.5 eV (see Table 2) also justifies the assertion that at least 50% of the resonances above 18 eV have been omitted. Based on an analysis of the dependence $\sigma_t(E)$ from [4] and the dependence calculated using the parameters from the evaluation of [2], we have obtained resonance energies for 11 omitted resonances up to 39.1 eV which are necessary for an adequate description of the experimentally measured total

cross-section dependence of [4] in the 18–38.5 eV energy range. The resonance energies of four resonances of the set from [2] (20.95, 21.81, 22.85 and 28.17 eV) have also been refined, and three resonances (24.23, 26.9 and 31.05 eV) from [2] we regard as experimentally unresolved doublets. Thus, according to our evaluation, there are at least 23 resonances in the 18–39.3 eV region. With the parameters calculated by us for these resonances the dependence $\sigma_t(E)$ of [4] in the 18–38.5 eV range can be described much more accurately than with the parameters of [2], as shown clearly in Fig. 2. Furthermore, a comparison of the resonance areas obtained from the experimental total cross-sections of [4] with those calculated using the evaluation of [2] and the parameters from our study shows that the mean deviation from experiment for each resonance is 17.9% for the parameters of [2] and 3.4% for our parameters. A comparison of the mean resonance parameters obtained on the basis of our calculations for the 0.01–18 eV and 18–38.5 eV regions (see Table 2) also indicates some omission of resonances above 18 eV. However, the existing experimental measurements of $\sigma_t(E)$ [4] do not allow this omission to be repaired.

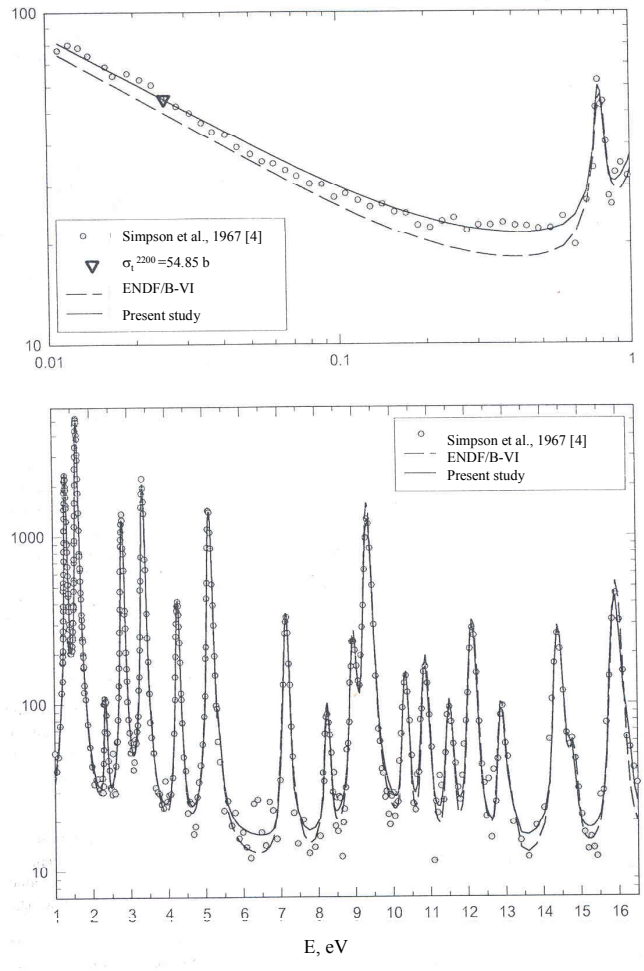

Fig. 1. Comparison of the experimentally measured total cross-section of [4] with total cross-sections calculated using the ENDF/B-VI file and the parameters in Table 3 for the 0.01 eV–16.5 eV energy range

2. Obtaining resonance parameters in the region above 38.5 eV

As already noted, above 38.5 eV resonance parameters have not previously been used in evaluations. In [2] this energy is considered the beginning of the unresolved resonance region, in which mean resonance parameters are used to describe the cross-sections. Figure 2 shows a calculated total cross-section obtained from the mean resonance parameters of [2] above 38.5 eV. In the present study we determined the resonance energies and obtained resonance parameters to describe $\sigma_t(E)$ of [4] above 38.5 eV taking into account the energy resolution of the experiment.

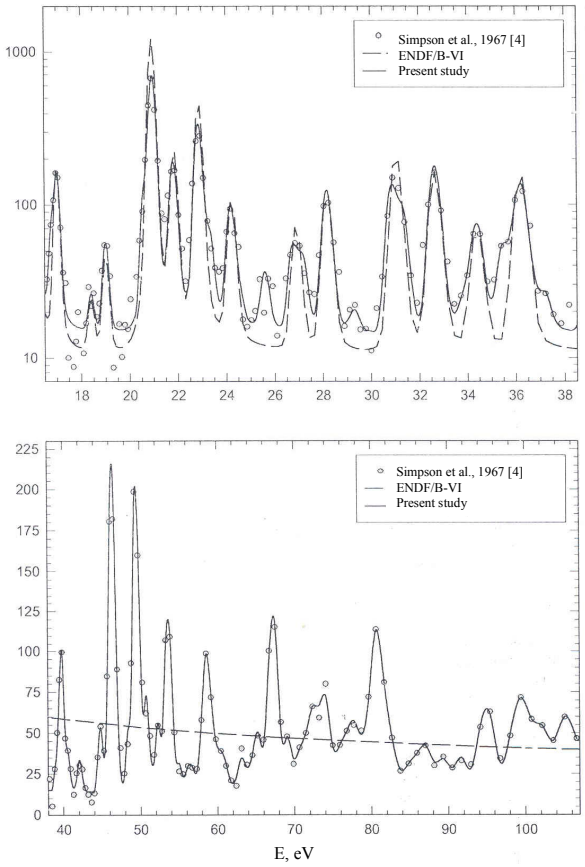

Fig. 2. Comparison of total cross-sections measured experimentally in [4] and calculated using the ENDF/B-VI file and the parameters in Table 3 in the 16.5–106.6 eV energy range

Based on an analysis of the total cross-section energy dependence of [4] and the iterative procedure used by us to calculate resonance parameters, we obtained resonance energies and corresponding parameters for a set of 46 resonances which allowed us to reproduce fairly reliably the dependence $\sigma_t(E)$ of [4] over the 38.5–106.6 eV energy range (see Fig. 2). Thus, the area A_t for the 38.5–106.6 eV region calculated from the data of [4] is 3625 b·eV, whereas calculations using the mean resonance parameters of [2] and the parameters of the present study give 3219 b·eV (discrepancy with [4] 11%) and 3611 b·eV (discrepancy with [4] 0.4%), respectively, and the mean deviation for the region of one resonance is 1.3% with our parameters.

The mean resonance parameters calculated from this set (see Table 2) demonstrate that in our evaluation there is a noticeable omission of resonances in comparison with the preceding energy regions; however, the existing experimental data provide no basis for increasing the number of resonances in the range in question. Our calculation of potentially omitted resonances in the 0.01–106.6 eV range allowed us to obtain the following evaluated mean resonance parameters: $\langle g\Gamma_n^0 \rangle$ = 0.043±0.002 meV, $\langle \Gamma_\gamma \rangle$ = 53.86 meV, $\langle D \rangle$ = 0.609±0.024 eV and $S_0 = (0.711 \pm 0.018) \cdot 10^{-4}$. It should be noted that this evaluation is fairly stable and weakly dependent on the upper limit of the range over which it was carried out.

Table 2

Comparison of mean resonance parameters in various energy ranges

Parameter	ENDF/B-VI [2] Energy range, eV		Present study Energy range, eV		
	0.01–18	18–38.5	0.01–18	18–38.5	38.5–106.6
$\langle \Gamma_n^0 \rangle$, meV	0.122	0.234	0.1045	0.1114	0.2316
$\langle \Gamma_\gamma \rangle$, meV	56.48	55.0	53.92	61.78	50.04
$\langle D \rangle$, eV	0.81	1.618	0.74	0.89	1.478

Thus, based on the analysis of the experimentally measured total cross-section of [4], the parameters of 93 resonances were calculated allowing the energy dependence $\sigma_t(E)$ to be described reliably over the 0.01–106.6 eV range. The parameters of the negative resonance obtained by us were refined after evaluating the thermal cross-sections (see section 3).

The evaluation of the capture resonance integral which we carried out based on the measurements in Refs [6–10] gave us a weighted mean value I_γ = 843.63±29.59 b, while the calculation of I_γ using our parameters in the 0.5–106.6 eV region gives a value of 779.56 b. If we use the value I_γ = 53.88 b obtained from [2] for the 106.6 eV–20 MeV range, then for the 0.5–20 MeV region taking into account the value of I_γ obtained using our parameters we get I_γ = 833.44 b, which is in good agreement with the weighted mean value.

3. Evaluation of the cross-sections σ_t^{2200} and σ_γ^{2200} and refinement of the parameters obtained

The reason why the thermal cross-sections needed to be evaluated is that these cross-sections differ in files [1, 2], even though these evaluations are based on the same source data. Thus, calculation based on file [1] gives σ_t^{2200} = 53.05 b, σ_γ^{2200} = 40.03 b and I_γ = 863 b, which are reasonably close to the reference values for this study [11]: σ_t^{2200} = 55±3 b, σ_γ^{2200} = 39.5±1.2 b and I_γ = 860±35 b. In the evaluation of [2] the reference values used are σ_γ^{2200} = 39.79 b and I_γ = 859.69 b (up to 10 MeV), and from calculation based on file [2] we obtain σ_γ^{2200} = 41.46 b and I_γ = 856.63 b (up to 20 MeV). Furthermore, σ_t^{2200} [2] = 49.80 b, which is 9.5% lower than for the measurements in [4].

For the present study we used the following assumptions:

- The experimental measurements of $\sigma_t(E)$ in [4] for the 0.01–0.1 eV region are sufficiently reliable for determining σ_t^{2200};

- The evaluated value of σ_γ^{2200} should be obtained taking into account all existing measurements of this value;
- Since the contribution of the negative resonance is approximately 40% to the total cross-section and around 50% to the radiative capture cross-section, its parameters should allow us (taking into account the contribution of all the other resonances) to obtain both the total cross-section energy dependence in the thermal region and evaluated values of σ_t^{2200} and σ_γ^{2200}.

Since we have no reason to question the measurements of the total cross-section in [4], the value of σ_t^{2200} was evaluated based on these data. Our calculations in the thermal point area gave a value of σ_t^{2200} = 54.85 b, which essentially agreed with the evaluation given by the authors of [4] (σ_t^{2200} = 55±3 b) and which we used in subsequent calculations as the evaluated value.

The value of σ_γ^{2200} was evaluated on the basis of Refs [6–9]. Note that the experiments of [6, 8, 9] were performed in a Maxwellian spectrum, with T = 343 K for the measurement in [9]. The anomalously high cross-section value σ_γ = 68±8 b [6] and the anomalously low value σ_γ = 31.4±1 b [9] compensate each other, although Connor's study [9] requires separate consideration. The first thing to be noted is the very small measurement error. Thus, while in [6–8] the errors are 12–18%, in this study they are only 3.2%, which, alongside the anomalously low value of σ_γ, hardly corresponds to reality. Furthermore, in [9] it is stated that using the g-factor obtained on the basis of the data from [4] gives a value σ_γ^{2200} = 39.5±1.2 b, i.e. study [9] uses a value g_γ = 0.795. However, our calculations based on both file [2] and the parameters of the present study do not support such a value for g_γ. To obtain the evaluated cross-section σ_γ^{2200} we calculated the values of σ_γ^{2200} from the Maxwellian cross-sections σ_γ of [6, 8, 9] using the g_γ values for our set of parameters at the corresponding temperatures and attributing an error of ~16% to the measurement in [9]. Such an error makes it possible to 'hook up' the measurements of [8] and [9] one to the other. As a result, the weighted mean value of σ_γ^{2200} was found to equal 42.53±3.03 b, which was taken by us as the evaluated value. Since σ_f^{2200} was taken as zero, the evaluated value of σ_n^{2200} = 12.32 b.

Once the evaluated values of the thermal cross-sections had been obtained, a final refinement was made in the value of the potential scattering radius R and the resonance parameters in order to describe the energy dependence $\sigma_t(E)$ of [4] adequately and to reproduce the values of σ_t^{2200} and σ_γ^{2200} evaluated by us. Such a procedure is especially important for the negative resonance because of its influence on the cross-section dependence in the thermal region, as already noted above. The refined values of the parameters are given in Table 3. Note also that calculations in the present study based on our parameters were performed using values from this table.

Study [4] discusses in some detail the possible existence of an anomalously broad, weak resonance in the 0.4 eV region (see Fig. 1) and concludes that the irregularity of the dependence $\sigma_t(E)$ of [4] in this region is most probably due to a systematic measurement error. Since no new information on this question has come to light so far, we did not think it possible to link the total cross-section energy dependence in this region to the presence of a resonance there.

Table 3

Resonance parameters for ^{233}Pa

E_r, eV	J	Γ_n, meV	Γ_γ, meV
-0.180	3/2	0.005024	35.00
0.789	3/2	0.001084	32.65
1.341	3/2	0.134980	43.32
1.644	3/2	0.386760	40.56
2.356	3/2	0.009299	35.20
2.830	3/2	0.194424	45.93
3.386	3/2	0.394440	40.01
4.288	3/2	0.109480	48.40
5.152	3/2	0.498440	47.34
7.181	3/2	0.173844	41.04
8.260	3/2	0.050114	41.17
8.970	3/2	0.197020	77.32
9.370	3/2	1.313480	86.99
10.350	3/2	0.130738	48.11
10.870	3/2	0.190512	78.30
11.520	3/2	0.110748	78.62
12.130	3/2	0.413420	70.90
12.900	3/2	0.102380	26.05
14.420	3/2	0.498020	68.15
14.750	3/2	0.063478	53.96
15.920	3/2	0.924340	56.17
16.200	3/2	0.120216	59.53
16.800	3/2	0.141248	73.71
17.020	3/2	0.313980	46.77
18.400	3/2	0.029814	46.60
19.000	3/2	0.122350	45.55
20.600	3/2	0.313480	47.69
20.950	3/2	2.491400	57.66
21.810	3/2	0.724920	89.27
22.850	3/2	1.374120	62.53
23.300	3/2	0.206640	73.19
24.180	3/2	0.408320	71.08
24.500	3/2	0.047658	46.06
25.600	3/2	0.116788	74.22
26.750	3/2	0.220000	49.00
27.150	3/2	0.192538	73.65
28.170	3/2	0.720020	65.38
29.300	3/2	0.037284	46.51
30.850	3/2	0.890340	43.10
31.300	3/2	0.604080	44.40
32.650	3/2	1.492720	61.58

E_r, eV	J	Γ_n, meV	Γ_γ, meV
33.900	3/2	0.097156	85.32
34.400	3/2	0.604740	66.57
35.500	3/2	0.433200	70.04
36.200	3/2	1.403660	61.89
37.100	3/2	0.139772	77.95
39.100	3/2	0.276940	45.41
39.750	3/2	1.198160	42.04
40.500	3/2	0.324100	72.09
42.050	3/2	0.308460	72.96
44.750	3/2	0.707380	44.25
46.000	3/2	1.991480	58.44
46.500	3/2	3.148200	57.22
48.500	3/2	0.884860	60.58
49.450	3/2	4.453000	32.36
50.700	3/2	1.342640	61.98
52.300	3/2	1.061060	63.53
53.600	3/2	3.167800	56.45
54.900	3/2	0.418520	54.87
56.400	3/2	0.529560	65.90
57.800	3/2	0.446520	69.11
58.500	3/2	2.444000	35.92
59.350	3/2	1.122740	63.53
60.600	3/2	0.784600	44.01
61.500	3/2	0.098720	73.75
63.100	3/2	0.778980	25.12
64.500	3/2	0.618860	66.99
65.400	3/2	1.397460	61.94
67.200	3/2	5.469800	56.43
69.100	3/2	1.573940	61.41
71.000	3/2	1.465040	39.31
72.400	3/2	2.586200	38.43
73.900	3/2	3.285600	34.23
75.700	3/2	1.142640	63.08
76.800	3/2	1.523760	38.86
78.000	3/2	2.297200	58.20
79.500	3/2	1.331280	47.34
80.600	3/2	6.117000	37.38
81.800	3/2	2.153800	47.78
82.700	3/2	0.990940	42.35
84.800	3/2	0.825660	43.48
85.750	3/2	0.765240	44.31
87.000	3/2	2.019000	37.63

E_r, eV	J	Γ_n, meV	Γ_γ, meV
89.250	3/2	1.648820	38.14
91.750	3/2	1.969800	61.32
94.900	3/2	5.839400	27.80
98.100	3/2	2.185400	58.07
99.400	3/2	5.049400	31.50
100.800	3/2	1.909560	37.92
102.200	3/2	3.437200	34.06
103.600	3/2	1.319880	40.30
105.600	3/2	6.203800	53.97
110.000	3/2	5.243400	53.07

Given that the parametrization of the resolved resonance region was carried out solely on the basis of the total cross-section measurements of [4], the values given in Table 3 for Γ_n and Γ_γ (or to be more precise Γ_a, since there is no information on a possible contribution of the fission cross-section to the total cross-section, although there may be such a contribution) are preliminary and subject to refinement when experimental measurements of $\sigma_f(E)$ and $\sigma_\gamma(E)$ in the resolved resonance region become available.

REFERENCES

1. Japanese Evaluated Data Library, Version 3, JAERI 1319, 1990.
2. Dunford, C.L., Nuclear Data for Science and Technology, Proc. Int. Conf., Jülich, 1991, 788, Springer-Verlag, 1992, Berlin.
3. Nordborg, C., Salvatores, M., Nuclear Data for Science and Technology, Proc. Int. Conf. Gatlinburg, Tennessee, USA, May 9–13, 1994, v. 2 p. 680.
4. Simpson, F.B., Codding J.W., Nucl. Sci. Eng., 1967, v. 28, p. 133.
5. Harris, DR., R,WAPD-TM-814, 1969.
6. Smith, R.R., Passel, T.O., Reeder, S.D., Alley, N.P., Heath, R.L., R, IDO-16226, 1955.
7. Eastwood, T.A., Werner, R.D., Can. Journ. of Phys., 1960, v. 38, p. 751.
8. Halperin, J., Stoughton, R.W., Druschel, R.E., Cameron, A.E., Walker, R.L., R, ORNL-3320, 1962.
9. Connor, J.C., R,WAPD-TM-837, 1970.
10. Yurova, L.N., Polyakov, A.A., Rukhlo, V.P. et al., Voprosy atomnoj nauki i tekhniki, Ser.: Yadernye konstanty, 1984, No.1, (55) p.3.
11. Mughabghab, S.F., Neutron cross-sections, 1984, v. 1, Part B, Academic Press.

NUCLEAR REACTOR DATA

04-10281 (203) [2]
Translated from Russian

UDC 621.039.51

MODELLING REACTOR KINETICS USING DIFFERENT SETS OF DELAYED NEUTRON DATA

B.D. Abramov
Institute for Physics and Power Engineering, Obninsk, Russia

MODELLING REACTOR KINETICS USING DIFFERENT SETS OF DELAYED NEUTRON DATA. Some reactor kinetics mathematical modelling problems are considered in the framework of the standard 6-group delayed neutron constants (Keepin, ABBN, JENDL, ENDF/B6) with energy and isotope dependent precursor half-lives, and the new 8-group delayed neutron data (Spriggs, Campbell, Piksaikin) with 'universal' precursor decay constant (or half-life) groups identical for all isotopes and energies.

Much work has been done on developing and validating algorithms for the mathematical modelling of transient neutron physics processes in nuclear reactors (see, for example [1-33]), and today these problems have largely been solved. However, a number of important questions remain regarding various improvements, corrections, the review of obsolete assumptions, etc., for both conventional and, in particular, advanced nuclear and electronuclear reactors with a complex, heterogeneous arrangement of various non-standard fuel compositions.

These include the selection and validation of delayed neutron characteristics (number of groups, decay constants, fractions, energy spectra), which have recently attracted heightened interest [20-26].

This study examines the methodology for mathematical modelling of distributed neutron kinetics as part of a generalized point model of a reactor [26-33] using arbitrary libraries of delayed neutron constants, including the well-known 6-group constants systems of Keepin [3], ABBN-78, [7], ABBN-93 [19, 20], JENDL [17], ENDF/B6 [18], and the new 8-group constants system in paper [22] with 'universal' decay constants (or half-lives), identical for all isotopes and energies, for the precursors in the groups.

Algorithms are formulated for calculating the coefficients of the generalized point kinetics equations for the general case of dependence of the precursor decay constants on the type of parent isotope generating them and the neutron energy initiating its fission, a link is established between these coefficients and the constants in [22], and some specific cases and applications are examined.

The comparative accuracy of the standard 6-group and the new 8-group constants [22] is studied on the basis of numerical solution of a number of model problems.

1. Distributed reactor kinetics equations

Let us consider, using the denotations in [28-33], a relatively general system of equations

$$\frac{1}{v}\frac{\partial\varphi}{\partial t} + M\varphi = F\varphi + \sum_{l}\sum_{m'} (\lambda_{(l)}^{(m')} R_{(l)}^{(m')} - F_{(l)}^{(m')}\varphi) + Q, \tag{1a}$$

$$\frac{\partial R_{(l)}^{(m')}}{\partial t} = -\lambda_{(l)}^{(m')} R_{(l)}^{(m')} + F_{(l)}^{(m')}\varphi, \tag{1b}$$

describing the changes in the neutron flux $\varphi(x,E,\Omega,t)$ in a reactor, where $Q(x,E,\Omega,t)$ is an external neutron source; v is the neutron velocity; $R_{(l)}^{(m')} = \chi_{(l)}^{(m')} C_{(l)}^{(m')}$; $\chi_{(l)}^{(m')}(E)$ is the spectrum; $C_{(l)}^{(m')}(x,t)$ is the concentration of delayed neutron precursors with a decay constant $\lambda_{(l)}^{(m')}$ and number $m' = m'(l)$, produced by the isotope l; $\beta_{(l)}^{(m')}$ is their fraction; and M, F, $F_{(l)}^{(m')}$ are the operators, given by the formulas:

$$M = \Omega\nabla + C, \quad C = \Sigma - S, \quad S = K_s, \quad F = K_f,$$

$$K_b\varphi = \int dE' \int d\Omega' \omega_b(x,E,E',\Omega,\Omega')\varphi(x,E',\Omega',t), \quad b = s,f,$$

$$F_{(l)}^{(m')}\varphi = \chi_{(l)}^{(m')}(E) \int dE' \beta_{(l)}^{(m')}(E') \nu_{fl}(E') \Sigma_{fl}(x,E') \int d\Omega' \varphi(x,E',\Omega',t)/4\pi$$

for the functions $\varphi(x,E,\Omega,t)$, satisfying the specific conditions of smoothness inside, and the vacuum boundary condition at the surface Γ of, a reactor volume G. Here the time dependence of the coefficients of equations (1) is not indicated,

$$\omega_{b'l}(x,E,E',\Omega,\Omega') = \nu_{b'l}(E')\Sigma_{b'l}(x,E')W_{b'l}(E',E,\Omega',\Omega) \quad \omega_s = \sum_{b'\neq c,f}\sum_{l} \omega_{b'l}$$

$$\omega_f = \sum_{l} \omega_{fl} \quad \int dE \int W_{b'l}(E',E,\Omega',\Omega)d\Omega = 1, \quad \Sigma(x,E) = \sum_{b'}\sum_{l} \Sigma_{b'l}(x,E),$$

$\nu_{b'l}(E), W_{b'l}(E',E,\Omega',\Omega)$ is the number of secondary neutrons and their distribution probability density at energies E and divergence directions of Ω, formed in a type b' reaction of a neutron with the nucleus of the lth isotope; $\Sigma_{b'l}(x,E') = N_l(x)\sigma_{b'l}(E')$ is the macroscopic cross-section of this reaction; $\sigma_{b'l}(E')$ is the microscopic cross-section;

$N_l(x)$ is the nucleus density of the lth isotope; summation is performed for isotope numbers l and process types b': elastic scattering $(b'=e)$, inelastic scattering $(b'=i)$, radiative capture $(b'=c)$, fission $(b'=f)$, etc. [4].

These equations have a somewhat unusual appearance since they take into account possible dependence of emitter decay constants on the number l of the parent isotope. Although theoretically absent owing to the prompt nature of emitter decay, this dependence appears, as is known from [3, 12–26], when effective group decay constants are determined in practice, and is a function of both the isotope number and the energy that initiated its neutron fission.

In fact, since in experimental determination the constants $\lambda_{(l)}^{(m')}$ usually acquire a parametric dependence on the energy spectrum of the neutrons that initiated the fission of the parent nuclei then, for example, in measurements using thermal or fast neutrons the constants $\lambda_{(r,l)}^{(m')}$ appear, corresponding to the thermal ($r=t$) or the fast $r=f$ spectra, etc. [3, 12-26].

Also, equations (1) make no provision for the dependence of $\lambda_{(l)}^{(m')}$ on r and, in this respect, require some revision. We shall do this assuming that the neutron energy spectrum in a reactor splits into several subspectra (test spectra) X_r, each of which has its own concentration of precursors $C_{(r,l)}^{(m')}(x,t)$, decaying with constants $\lambda_{(r,l)}^{(m')}$, so that equations (1) are recast into the form:

$$\frac{1}{v}\frac{\partial\varphi}{\partial t}+M\varphi=F\ \varphi+\sum_l\sum_{m'}\sum_r(\lambda_{(r,l)}^{(m')}R_{(r,l)}^{(m')}-F_{(r,l)}^{(m')}\varphi)+\ Q\quad , \tag{2a}$$

$$\frac{\partial R_{(r,l)}^{(m')}}{\partial t}=-\lambda_{(r,l)}^{(m')}R_{(r,l)}^{(m')}+F_{(r,l)}^{(m')}\varphi, \tag{2b}$$

where $R_{(r,l)}^{(m')}=\chi_{(r,l)}^{(m')}C_{(r,l)}^{(m')},\chi_{(r,l),}^{(m')}\beta_{(r,l)}^{(m')}$ are the corresponding partial values,

$$F_{(r,l)}^{(m')}\varphi=\chi_{(r,l)}^{(m')}(E)\int dE'\beta_{(r,l)}^{(m')}(E')\nu_{fl}(E')\Sigma_{fl}(x,E')\Phi_r(x,E',t)/4\pi,$$

and Φ_r is the contribution of flux $\Phi=\int d\Omega\varphi\approx\sum_r\Phi_r$ to test spectrum X_r. Here for Φ_r we can use, for example, the separable functions $\Phi_r=\theta_r\Phi$, where $\theta_r(E)$ is the range's characteristic function, into which the region of neutron energy change under investigation is divided, or, in the more general case of the sample spectra lying on top of each other, functions in the form $\Phi_r = a_rX_r$, where $X_r(E)$ are the given spectra, and $a_r(x,t)$ several coefficients which can be determined from the square deviation minimization condition $<(\Phi-\sum_r a_rX_r)^2>$, in accordance with which, for example, in the important case of

splitting the source spectrum into thermal and fast spectra X_t, X_f, the coefficients a_t, a_f are calculated using the formula:

$$a_i = \frac{< X_i \Phi >< X_j^2 > - < X_j \Phi >< X_i X_j >}{< X_i^2 >< X_j^2 > - < X_i X_j >^2}, \quad i, j = t, f, \qquad (2c)$$

where the brackets < > denote the integral for all values of E examined, etc.

Equations (2) are also one possible expansion of the standard distributed reactor kinetics equations to take into account the parametric dependence of the precursor decay constants on neutron energy. If there is no such dependence they are converted into equations (1). In turn, when the numeration order is changed $l, m' \to j$, equations (1) are converted into the normal kinetics equations

$$\frac{1}{v}\frac{\partial \varphi}{\partial t} + M\varphi = F\varphi + \sum_j (\lambda_j R_j - F_j \varphi) + Q, \; \frac{\partial R_j}{\partial t} = -\lambda_j R_j + F_j \varphi,$$

which are accurate only when all the possible precursors (of which there are around 270 [22]) are taken into account with their true decay constants λ_j, formed only directly during the fission process. The latter is because there is no direct calculation of successive beta decay chains in these equations [3].

2. Generalized point kinetics equations

Equations (1) (or, even more so, (2)) are generally extremely complex. Therefore they are usually rendered more tractable by conversion into somewhat simplified reactor point model equations excluding spatial, energy and angular dependence. The various ways of achieving this are described, for example, in [1-6]. A generalization following [30-33], of equations (2) is given below.

Generalized point kinetics equations are understood here to be the following equations [30-33]. If we assume $\psi, \psi^* \geq 0$ the solutions to the equations

$$M\psi = F\psi / k_{эф}, \qquad (3a)$$

$$M^*\psi^* = F^*\psi^* / k_{эф}, \qquad (3b)$$

where M^*, F^* are linked to the operators M, F and k_{ef} is the effective multiplication factor. Multiplying equations (2) by ψ^*, equation (3b) by φ, integrating with respect to $x \in G$ and all of E, Ω and subtracting the results from each other, it is not difficult to write the integrated identities as:

$$(\psi^*, \frac{1}{v}\frac{\partial\varphi}{\partial t}) = \rho(\psi^*, F\varphi) + \sum_{r,l,m'}(\psi^*, \lambda^{(m')}_{(r,l)} R^{(m')}_{(r,l)} - F^{(m')}_{(r,l)}\varphi) + (\psi^*, Q),$$

$$(\psi^*, \frac{\partial R^{(m')}_{(r,l)}}{\partial t}) = -\lambda^{(m')}_{(r,l)}(\psi^*, R^{(m')}_{(r,l)}) + (\psi^*, F^{(m')}_{(r,l)}\varphi),$$

where $\rho = 1 - 1/k_{ef}$ is the reactivity. Using the representation of flux in the form:

$$\varphi(x,E,\Omega,t) = P(t)\tilde{\psi}(x,E,\Omega,t)/(p,\tilde{\psi}) = P(t)\xi(x,E,\Omega,t), \quad (4)$$

these identities can be converted into the generalized equations

$$[\frac{d}{dt} + (\overline{\alpha} - \frac{\rho - \overline{\beta}}{\Lambda})]P = [\sum_{m=1}^{\overline{m}} \overline{\lambda}^{(m)}\overline{C}^{(m)} + \overline{Q}]/k_p\Lambda, \quad (5a)$$

$$[\frac{d}{dt} + (\overline{\lambda}^{(m)} - \alpha^{(m)})]\overline{C}^{(m)} = \overline{\beta}^{(m)} k_p P \quad (5b)$$

of point kinetics (reactor point model) relative to the unknowns

$$P(t) = (p,\varphi),\ \overline{C}^{(m)}(t) = \sum_{r;l,m'\in m}(\psi^*, R^{(m')}_{(r,l)}) \quad (6)$$

with the coefficients

$$\overline{\alpha} = \frac{(\psi^*, v^{-1}\partial\xi/\partial t)}{(\psi^*, v^{-1}\xi)},\ \Lambda = \frac{(\psi^*, v^{-1}\tilde{\psi})}{(\psi^*, F\tilde{\psi})},\ k_p = \frac{(\psi^*, F\tilde{\psi})}{(p,\tilde{\psi})}, \quad (7a)$$

$$\overline{\lambda}^{(m)} = \frac{\sum_{r;l,m'\in m}(\psi^*, \lambda^{(m')}_{(r,l)} R^{(m')}_{(r,l)})}{\sum_{r;l,m'\in m}(\psi^*, R^{(m')}_{(r,l)})},\ \alpha^{(m)} = \frac{\sum_{r;l,m'\in m}(\partial\psi^*/\partial t, R^{(m')}_{(r,l)})}{\sum_{r;l,m'\in m}(\psi^*, R^{(m')}_{(r,l)})}, \quad (7b)$$

$$\overline{\beta}^{(m')}_{(r,l)} = \frac{(\psi^*, F^{(m')}_{(r,l)}\tilde{\psi})}{(\psi^*, F\tilde{\psi})},\ \overline{\beta}^{(m')}_{(l)} = \sum_r \overline{\beta}^{(m')}_{(r,l)},\ \overline{\beta}^{(m)} = \sum_{l,m'\in m}\overline{\beta}^{(m')}_{(l)}, \quad (7c)$$

$$\overline{\beta} = \beta_{эф} = \sum_{m=1}^{\overline{m}} \overline{\beta}^{(m)},\quad \overline{Q} = (\psi^*, Q),\ \xi = \tilde{\psi}/(p,\tilde{\psi}), \quad (7d)$$

where m is the number of the effective group of delayed neutrons; $\overline{m}$ is the number of groups; $m' \in m$ is the set of numbers $m' = m'(l)$ of the precursors attributed to the m th group; $(\,,\,)$ is the symbol of the integral for all of $x \in G$ and E, Ω; $p(x,E,\Omega,t) \geq 0$ is the 'density' of the unknown functional $P = (p, \varphi)$; $\widetilde{\psi}(x,E,\Omega,t) \geq 0$ is the shape function, selected from various calculations of the approximation, for example $\widetilde{\psi} = \psi$, etc.

Equations (5) and (7) are also unknown generalized point kinetics equations equivalent to distributed kinetics equations (2) as regards calculation of the functionals (6). They generalize the equations of L.N. Usachev [1], A.F. Henry [2-6] and others [5] regarding the introduction of the coefficient $k_p = (\psi^*, F\xi)$, characterizing the difference between the target weighted function $_p$ and $F^*\psi^*$, and also the corrections $\overline{\alpha}, \alpha^{(m)}$, taking into account changes in the shape of functions $\widetilde{\psi}, \psi^*$ during the process under examination, and are an expansion of them for calculating the arbitrary functionals $P = (p, \varphi)$ in the general case of dependence of the shape-functions $\psi^*, \widetilde{\psi}$ on time t and the dependence of the decay constants $\lambda_{(r,l)}^{(m')}$ on the numbers l of isotopes and the numbers r of spectra. See [30] for a more complete description of the features and methods for solving equations (5)-(7).
The coefficients (7) of these equations depend on what functions $\psi^*, \widetilde{\psi}$ are selected and can usually be calculated only approximately. For example, assuming in (7) that

$$R_{(r,l)}^{(m')} \approx F_{(r,l)}^{(m')} \varphi / \lambda_{(r,l)}^{(m')}, \tag{8}$$

and selecting for $\widetilde{\psi}$ the solution $\psi \geq 0$ of equation (3a) (or, when $Q \neq 0$, of an equation of the type $(M - F)\widetilde{\psi} = Q$), we arrive at a certain variety in the appearance of the adiabatic approximation [2, 3, 8, 10], when the flux shape instantaneously follows a change in the reactor properties. This approximation from (7) yields generalizations of the corresponding coefficient determinations of the kinetics equations in [1] in terms of taking these factors into account, and supplementing them, in particular, by means of the formula

$$\frac{1}{\overline{\lambda}^{(m)}} = \frac{1}{\overline{\beta}^{(m)}} \sum_{r;\, l, m' \in m} \frac{\overline{\beta}_{(r,l)}^{(m')}}{\lambda_{(r,l)}^{(m')}} \tag{9}$$

to calculate $\overline{\lambda}^{(m)}$ in a fissile isotope mixture, which is, in turn, a generalization of the well-known results of [3-6, 9, 28-32].

The standard point kinetics equations follow from equations (5)-(7) when any fixed solutions of ψ^*, ψ in equations (2) are selected as shape-functions within the scope of the additional assumptions $p = F^*\psi^*, \quad \partial p / \partial t = 0$, when the coefficients $\Lambda, \overline{\lambda}^{(m)}, \overline{\beta}^{(m)}, \overline{\beta}$

lose their time-dependence and the additional correlations $\overline{\alpha} = \alpha^{(m)} = 0,\ k_p = 1$ come to bear.

We note that in the case of $Q = 0$, equations (2) (in the standard 41.1 type condition limits of [4]) have a positive solution in the form

$$\varphi(x,E,\Omega,t) = \psi_o(x,E,\Omega)\exp(\alpha_o t),\ \alpha_o > -\lambda_{(r,l)}^{(m')},\ \psi_o \geq 0, \quad (10)$$

in accordance with which the so-called inhour equation holds

$$\alpha_o \Lambda = \rho - \overline{\beta} + \sum_{r,l,m'} \frac{\lambda_{(r,l)}^{(m')} \overline{\beta}_{(r,l)}^{(m')}}{\lambda_{(r,l)}^{(m')} + \alpha_o} = \rho - \alpha_o \sum_{r,l,m'} \frac{\overline{\beta}_{(r,l)}^{(m')}}{\lambda_{(r,l)}^{(m')} + \alpha_o}, \quad (11)$$

with coefficients $\Lambda,\ \overline{\beta}_{(r,l)}^{(m')}, \overline{\beta}$, calculated using formulas (7) with weighting of the functions ψ^*, ψ_o. These assumptions from (7b) yield the formula

$$\overline{\lambda}^{(m)} = [\sum_{r;l,m' \in m} \frac{(\psi^*, \lambda_{(r,l)}^{(m')} F_{(r,l)}^{(m')} \psi_o)}{\alpha_o + \lambda_{(r,l)}^{(m')}}] / [\sum_{r;l,m' \in m} \frac{(\psi^*, F_{(r,l)}^{(m')} \psi_o)}{\alpha_o + \lambda(_{(r,l)}^{(m')}}] \quad (12)$$

improving the accuracy of (9) for the case $\alpha_o \neq 0$.

3. Interpolation formulas $\lambda_{(r,l)}^{(m)}, \beta_{(r,l)}^{(m)}$

When performing reactor calculations with spectra $X(E)$, differing from the standard test spectra $X_r(E),\ r = t, f$ used when measuring the constants $\lambda_{(r,l)}^{(m)}, \beta_{(r,l)}^{(m)}$, the question arises as to which of these constants should be used. For example, in the ABBN-78 system designed for BN-type fast reactor calculations, Keepin's data are taken for ^{235}U and ^{239}Pu when $r = t$, and, in the latest ABBN-93 version, when $r = f$. However, it is known that for such reactors several intermediate values for these constants are more suitable. The approach proposed, in principle, allows these to be determined.

Let us take, for example, the calculation formulas $\overline{\lambda}_{(l)}^{(m)}, \overline{\beta}_{(l)}^{(m)}$ for reactors with the (integral) spectrum $X(E)$, intermediate in "hardness" between the spectra $X_r, r = t, f$ used to obtain experimental data for $\lambda_{(r,l)}^{(m)}, \beta_{(r,l)}^{(m)}$. Assuming that the regrouping of the precursors does not take place and using formulas (2) for expansion of the flux into the sum $\Phi \approx X \approx a_t X_t + a_f X_f$ of the test spectra, we can deduce the following approximated formulas

from determination of (2), (7c) and (9) for homogeneous zones, neglecting the dependence of the function ψ^* on its independent variables

$$\bar{\lambda}_{(l)}^{(m)} \approx \bar{\beta}_{(l)}^{(m)} / (\sum_{r=t,f} \bar{\beta}_{(r,l)}^{(m)} / \lambda_{(r,l)}^{(m)}), \qquad \bar{\beta}_{(l)}^{(m)} = \sum_{r=t,f} \bar{\beta}_{(r,l)}^{(m)}, \tag{13a}$$

$$\bar{\beta}_{(r,l)}^{(m)} \approx \beta_{(r,l)}^{(m)} \, (a_r < \nu_{fl} \Sigma_{fl} X_r >) / (a_t < \nu_{fl} \Sigma_{fl} X_t > + a_f < \nu_{fl} \Sigma_{fl} X_f >) \tag{13b}$$

which can be used to calculate the $\bar{\lambda}_{(l)}^{(m)}, \bar{\beta}_{(l)}^{(m)}$ of a given reactor for known $\lambda_{(r,l)}^{(m)}, \beta_{(r,l)}^{(m)}, X_r$ and X, where the coefficients a_r are calculated using (2c) replacing $\Phi \to X$.

Formulas (13) also give one possible interpolation of $\bar{\lambda}_{(l)}^{(m)}, \bar{\beta}_{(l)}^{(m)}$ between the values $\lambda_{(r,l)}^{(m)}, \beta_{(r,l)}^{(m)}, r = t, f$ for a given spectrum X when $< X_r X > \neq 0, r = t, f$.

4. Inverse kinetics equations

Inverse kinetics equations (or the inverse solutions to kinetics equations [8]) are usually used to determine reactivity for a known flux. Let us recall how they are derived. Writing the solution to equation (2b) in the form

$$R_{(r,l)}^{(m')}(t) = \int_{-\infty}^{t} dt' e^{-\lambda_{(r,l)}^{(m')}(t-t')} F_{(r,l)}^{(m')} \varphi_{t'}$$

and substituting it in equation (2a), it is not difficult to obtain, just like equations (5), the integral identity

$$\rho = \bar{\beta} + \alpha\Lambda - [\bar{Q} + \sum_{r,l,m'} \lambda_{(r,l)}^{(m')} \int_{-\infty}^{t} dt' e^{-\lambda_{(r,l)}^{(m')}(t-t')} (\psi^*, F_{(r,l)}^{(m')} \varphi_{t'})] / (\psi^*, F\varphi_t),$$

which holds for all solutions to equations (2), where the denotations used are

$$\psi^* = \psi_t^*, \ \varphi_{t'} = \varphi(x, E, \Omega, t'), \ \alpha_p = (dP/dt)/P,$$

$$\alpha_\xi = \bar{\alpha}, \quad \alpha = \alpha_\xi + \alpha_p = (\psi^*, v^{-1} \partial\varphi/\partial t) / (\psi^*, v^{-1}\varphi).$$

The latter, introducing the functions (of the "detector efficiencies" type) in [8])

$$\varepsilon_{(r,l)}^{(m')}(t,t') = (\psi_t^*, F_{(r,l)}^{(m')}\xi_{t'}), \quad \varepsilon(t) = k_p\overline{\beta} = \sum_{r,l,m'} (\psi_t^*, F_{(r,l)}^{(m')}\xi_t) \tag{14}$$

and neglecting the (usually rapidly decreasing) term $\Lambda\alpha(t)$, can be written, for example, in the form of the following generalization of inverse kinetics equation (4.37) in [8]:

$$\rho/\overline{\beta} = 1 - \{\overline{Q} + \sum_{r;l,m'} \lambda_{(r,l)}^{(m')} \int_{-\infty}^{t} dt' \varepsilon_{(r,l)}^{(m')}(t,t')P(t')e^{-\lambda_{(r,l)}^{(m')}(t-t')}\} / \varepsilon(t)P(t) \tag{15}$$

in the case of the arbitrary functionals P in the form of (6) and dependence $\lambda_{(r,l)}^{(m')}$ on l and r assuming

$$\Lambda|\alpha| << \overline{\beta} = \beta_{эф}. \tag{16}$$

We note that to calculate the right side of (15) we need to know not only the values $P(t')$ at all preceding moments $t' < t$, but also the values of a rather large — generally speaking — number of coefficients (14) which are dependent on the two variables t', t. The number of these coefficients, however, drops noticeably for

$$\lambda_{(r,l)}^{(m')} = \lambda_{(l)}^{(m')} = \overline{\lambda}^{(m)} \forall m' \in m, \tag{17}$$

when $\lambda_{(r,l)}^{(m')}$ depends neither on the number m' within the boundaries of the group, nor on the number of the test spectra r, and instead of $\varepsilon_{(r,l)}^{(m')}(t,t')$ only coefficients in the form $\varepsilon^{(m)}(t,t') = \sum_{r;l;m' \in m} \varepsilon_{(r,l)}^{(m')}$ are required.

5. The approach taken by Spriggs G.D, Campbell I.M and Piksaikin V.M [22]

The conditions of (17) are achieved in the 8-group system of constants [22] with 'universal', identical for all isotopes and energies, precursor group decay constants. In this system the decay constants in the first three groups agree with the corresponding data for ^{87}Br, ^{137}I and ^{88}Br. In the other groups, the decay constants are determined by weighting of the decay constants of several dominant precursors in the group using a type (9) formula (without summing for *r*, *1*) .

The relative yields are then determined using the least-squares method from analysis of the calculated delayed neutron decay curves that are obtained using the known 6-group data (Keepin et al.), after preliminary revision to reject inaccurate data. It is claimed that the method used for "equivalent conversion" from 6-group to 8-group data conserves the positive reactivity scale [22].

This method for preparing the constants (see also [12-15]) can obviously be considered an approximate method of performing the algorithms in section 2 to calculate the coefficients of point kinetics equations for a single isotope fuel with no spatial dependence through special selection of precursor distribution in groups.

In actual fact, if all the precursors are distributed into groups in accordance with their true decay constants and the indicators in paper [22], and formula (9) is used to calculate the decay constants, then in the first three groups, where there will be one precursor each, the values obtained for $\overline{\lambda}^{(m)}$ will agree with the $\overline{\lambda}^{(m)}$ of [22] precisely. In the other groups the agreement will be, generally speaking, only approximate.

In this connection we note the following. Assuming that the true characteristics $\lambda_{(r,l)}^{(m')}$, of all the delayed neutron precursors (of which there are approximately 271 [22]) are known and have to be convoluted into a given number $\overline{m}$ of groups such that the functionals (4) are conserved for all values of t during the transition from the original distributed model (2) to the group point model (5). Then the group values $\overline{\lambda}^{(m)}$,… must clearly be calculated using formulas (7).

Thus, these formulas also yield an accurate solution to the problem under investigation. Since the coefficients $\overline{\lambda}^{(m)}$,… will generally depend on both time and the specifics of the task (reactor configuration, fuel type, etc.), this, in turn, means that there are, in principle, no genuinely universal 8-group systems of constants. However, there would clearly appear to exist an approximately similar universality.

6. Calculation of reactivity dependence on the inverse period

Let us turn to the comparative properties of the 6-group constants of Keepin, ABBN-78, ABBN-93, JENDL and ENDF/B6 and the new 8-group constants proposed in [22]. We shall confine ourselves, as usual [20-26], to an examination of models that omit details related to prompt neutron production time, delayed neutron spectra and the energy dependence of delayed neutron yields, i.e. models described by a type (5) point kinetics equations system in an approximation of an instantaneous step [3-6]

$$0 = (\rho - \overline{\beta})n + \sum_{l,m'} \lambda_{(l)}^{(m')} C_{(l)}^{(m')}\,,\quad \frac{dC_{(l)}^{(m')}}{dt} = -\lambda_{(l)}^{(m')} C_{(l)}^{(m')} + \overline{\beta}_{(l)}^{(m')} n\,, \tag{18}$$

where, in this instance, n(t) is the neutron flux, $\overline{\beta}$ is calculated using a type (7c) formula, and index r of the only sample spectrum $r = f$ is omitted for simplicity's sake.

The particular case of the inhour equation (11) follows from (18)

$$\rho/\bar{\beta} = \alpha \sum_{l,m'} (\bar{\beta}_{(l)}^{(m')}/\bar{\beta})/(\lambda_{(l)}^{(m')} + \alpha), \qquad (19)$$

linking reactivity ρ and the inverse period α in the approximation $\Lambda = 0, r = f$.

Tables 1-3 contain the results of calculations $(\rho/\bar{\beta})(\alpha)$ using (19) with Keepin's constants [3] for ^{235}U, ^{238}U and ^{239}Pu and the relative deviations in percentages

$$\delta\rho_k(\alpha) = \{[(\frac{\rho}{\bar{\beta}})_k(\alpha) - (\frac{\rho}{\bar{\beta}})(\alpha)]/[(\frac{\rho}{\bar{\beta}})(\alpha)]\} \cdot 100 \qquad (20)$$

of the reactivities $(\rho/\bar{\beta})_k(\alpha)$, calculated using the 8-group constants (k=1) proposed in [22] and the 6-group constants of ABBN-78 [7] (k=2), JENDL [17] (k=3) and ENDF/B6 [18] (k=4) from the reactivities $(\rho/\bar{\beta})(\alpha)$ (of Keepin).

Table 1

$\delta\rho_k(\alpha)$ dependence for ^{235}U

α	-0.012	-0.010	-0.008	-0.004	0.000	0.004	0.008	0.012
ρ	-0.821	-0.271	-0.162	-0.061	0.000	0.045	0.081	0.111
$\delta\rho_1$	30.64	3.218	2.540	2.797	2.967	3.034	3.047	3.036
$\delta\rho_2$	43.02	2.639	1.622	1.941	2.204	2.341	2.400	2.432
$\delta\rho_3$	-9.952	-5.691	-3.847	-2.176	-1.407	-0.957	-0.673	-0.477
$\delta\rho_4$	-43.29	-20.17	-16.27	-14.06	-13.18	-12.60	-12.15	-11.77

Table 2

$\delta\rho_k(\alpha)$ dependence for ^{238}U

α	-0.012	-0.010	-0.008	-0.004	0.000	0.004	0.008	0.012
ρ	-0.243	-0.128	-0.086	-0.035	0.000	0.028	0.051	0.071
$\delta\rho_1$	36.52	-1.100	-1.409	-0.716	-0.394	-0.245	-0.179	-0.142
$\delta\rho_2$	0.000	0.000	0.000	0.000	0.000	0.000	0.000	0.000
$\delta\rho_3$	0.000	0.000	0.000	0.000	0.000	0.000	0.000	0.000
$\delta\rho_4$	-14.65	-7.446	-6.654	-6.447	-6.349	-6.209	-6.041	-5.855

Table 3

$\delta\rho_k(\alpha)$ dependence for ^{239}Pu

α	-0.012	-0.010	-0.008	-0.004	0.000	0.004	0.008	0.012
ρ	-0.717	-0.292	-0.182	-0.069	0.000	0.051	0.094	0.127
$\delta\rho_1$	38.15	1.241	0.870	1.693	2.136	2.353	2.450	2.488
$\delta\rho_2$	5.787	3.678	4.488	5.202	5.375	5.380	5.312	5.221
$\delta\rho_3$	-4.097	-0.817	0.490	1.656	1.989	2.196	2.293	2.338
$\delta\rho_4$	-27.09	-13.05	-10.84	-9.689	-9.239	-8.929	-8.672	-8.444

The corresponding graphical representation of these data is given in Figs 1-3, where the abbreviation SCP refers to the data from [22].

In the examples examined, the 8-group constants were obtained in [22] in the course of the aforementioned equivalent conversion of the 6-group constants of Piksaikin (1997) for ^{235}U, Keepin (1957) for ^{238}U, and Besant (1997) for ^{239}Pu, respectively.

From Fig. 2 and the data in Table 2 we can see that there is no strict conservation of the reactivity scale during the transition from Keepin's 6-group constants for ^{238}U to the 8-group constants. The weighted average half-lives $T_{(l)} = ln\,2 \sum_{m'} (\bar{\beta}_{(l)}^{(m')} / \bar{\beta}) / \lambda_{(l)}^{(m')}$ are not even conserved. Let us say that in this instance $\delta\rho_1(0) = 100(T_1 - T)/T$, according to the data in Table 2, is 0.39% (according to the data in [3] and [22], where $T = 5.32$ and $T_1 = 5.3$, respectively, $\delta\rho_1(0)$ is evaluated at the somewhat different value of 0.37%, which is clearly caused by rounding errors in the transition from λ to T).

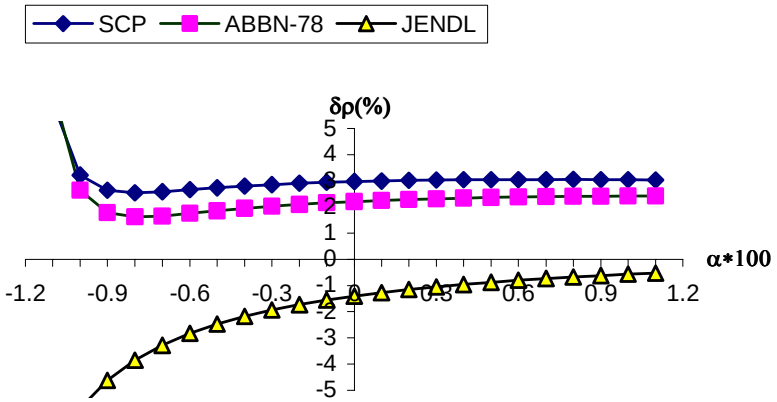

Fig. 1. δρ/α dependence for ^{235}U

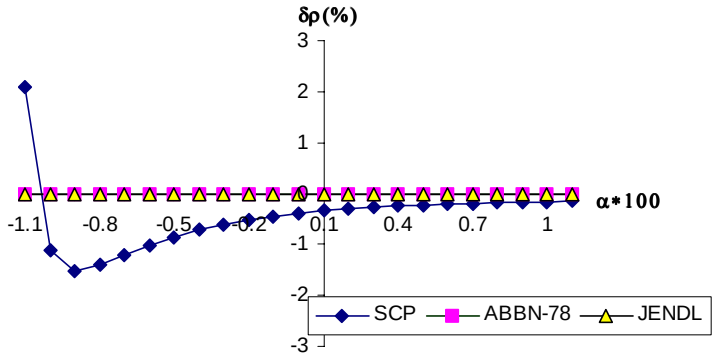

Fig. 2. δρ/α dependence for ^{238}U

The data further show that, for subcriticalities that are not too low (when $\alpha \geq -0.010$), the spread of reactivity values between the constants examined and Keepin's constants is approximately 2.5 – 3.2% for ^{235}U, 0.14 – 1.4% for ^{238}U and 0.8 – 2.5% for ^{239}Pu.

For the ABBN-78 constants these deviations are 1.6 – 2.6%, 0.0% and 3.7 – 5.4%, respectively, whereby the zero deviation for ^{238}U is simply because the relevant constants agree. This is also true for the JENDL constants, where these deviations are somewhat larger. However, the largest deviations are characteristic of the ENDF/B6 constants. As regards the ABBN-93 constants, in these examples they agree with Keepin's constants [3].

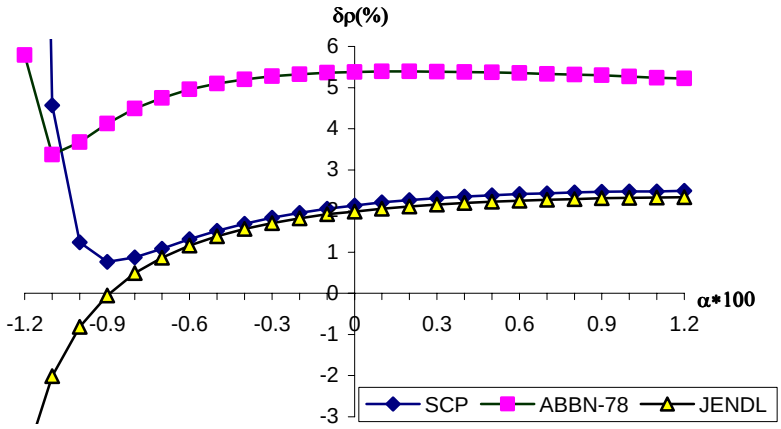

Fig. 3. δρ/α dependence for ^{239}Pu

Let us turn to the kinetics for a mixed, multi-isotope fuel. Let us consider the following two versions of standard, idealized fuel mixtures approximately modelling the medium enrichment zone (MEZ) 3 and zone 4 with MOX fuel in a BN-600 reactor loaded with hybrid uranium-plutonium [27]:

1) Uranium fuel (MEZ): 0.19 ^{235}U; 0.8 ^{238}U; 0.01 ^{239}Pu;
2) MOX fuel: 0.01 ^{235}U; 0.8 ^{236}U; 0.19 ^{239}Pu,

where the first figures are the relative isotope concentrations in the mixture.

Tables 4 and 5 contain, just like Tables 1–3, the results of calculations of the relative deviations $\delta\rho_k(\alpha)$ calculated using (19) and (20) with the use of different sets of constants for the fuel compositions indicated.

These show that in region $\alpha \geq -0.010$ the difference between Keepin's constants and the constants in [22] ranges from -0.17 to +0.75% for uranium systems and from -0.6 to +0.7% for MOX fuel. This is noticeably less than for the partial components of the mixture, which clearly indicates error compensation.

The results for the JENDL constants are close. The ABBN-78 constants are characterized by some large differences (0.5 – 0.8% for mixture No. 1 and 1.3 – 1.7% for mixture No. 2) and, finally, the ENDF/B6 constants yield the largest differences.

The preceding results were obtained without averaging of the decay constants. Let us now turn to an examination of the accuracy of type (9) and (12) formulas for averaging of the group isotope decay constants. For this, transforming (19) into the form:

$$\frac{\rho}{\overline{\beta}} = \alpha \sum_{m=1}^{\overline{m}} \frac{\overline{\beta}^{(m)} / \overline{\beta}}{\overline{\lambda}^{(m)} + \alpha}, \tag{21}$$

let us examine the following ways of averaging the isotope decay constants:

$$\overline{\lambda}^{(m)} = [\sum_{l} \overline{\beta}_{(l)}^{(m)}] / [\sum_{l} \overline{\beta}_{(l)}^{(m)} / \lambda_{(l)}^{(m)}], \tag{22a}$$

$$\overline{\lambda}^{(m)} = [\sum_{l} \lambda_{(l)}^{(m)} \overline{\beta}_{(l)}^{(m)} / (\alpha + \lambda_{(l)}^{(m)})] / [\sum_{l} \overline{\beta}_{(l)}^{(m)} / (\alpha + \lambda_{(l)}^{(m)})], \tag{22b}$$

where, in this case, according to (7c),

$$\overline{\beta}_{(l)}^{(m)} = \beta_{(l)}^{(m)} W_l, \quad \overline{\beta}^{(m)} = \sum_{l} \overline{\beta}_{(l)}^{(m)}, \quad \overline{\beta} = \sum_{m=1}^{\overline{m}} \overline{\beta}^{(m)},$$

$\beta_{(l)}^{(m)}$ is the yield of the precursor in the mth group, formed during fission of the lth isotope; W_l is the relative concentration (importance) of this isotope in the mixture.

Table 4

$\delta\rho_k(\alpha)$ dependence for mixture 1

α	-0.012	-0.010	-0.008	-0.004	0.000	0.004	0.008	0.012
ρ	-0.357	-0.157	-0.101	-0.040,	0.000	0.031	0.057	0.079
$\delta\rho_1$	33.98	0.363	-0.168	0.333	0.582	0.692	0.731	0.745
$\delta\rho_2$	18.88	0.930	0.575	0.645	0.793	0.727	0.731	0.729
$\delta\rho_3$	-4.428	-1.886	-1.168	-0.596	-0.359	-0.224	-0.145	-0.089
$\delta\rho_4$	-27.40	-11.73	-9.662	-9.684	-8.299	-8.001	-7.729	-7.474

Table 5

$\delta\rho_k(\alpha)$ dependence for mixture 2

α	-0.012	-0.010	-0.008	-0.004	0.000	0.004	0.008	0.012
ρ	-0.338	-0.161	-0.105	-0.042	0.000	0.032	0.059	0.082
$\delta\rho_1$	37.03	-0.218	-0.592	0.096	0.429	0.583	0.646	0.672
$\delta\rho_2$	3.372	1.313	1.509	1.668	1.683	1.657	1.611	1.563
$\delta\rho_3$	-1.890	-0.379	0.105	0.464	0.591	-0.651	-0.671	-0.679
$\delta\rho_4$	-20.35	-9.592	-8.183	-7.578	-7.335	-7.118	-6.905	-6.694

Table 6

$\delta\rho_k(\alpha)$ dependence for mixtures 1 and 2

α	-0.012	-0.010	-0.008	-0.004	0.000	0.004	0.008	0.012
$\delta\rho_1$	-4.017	-0.217	-0.049	-0.007	3E-05	0.003	0.007	0.012
$\delta\rho_2$	-1.303	-0.087	-0.019	-0.002	5E-04	0.003	0.003	0.004

The errors levels of $\delta\rho_k(\alpha)$ for reactivity calculation using formulas (21) and (22a) for mixtures 1 (k=1) and 2 (k=2) are shown in Table 6.

This Table shows that the simplest averaging of decay constants using (22a), when α≥–0.008, leads to smaller deviations than the 8-group system of constants [22] with 'universal' decay constants that do not have to be averaged (Tables 4 and 5). Formula (22b) yields more or less exact results. In this regard see also [9].

This means that the problem of the increase in the number of equations when moving from a single isotope to a multi-isotope fuel has a comparatively simple solution, generally speaking, outside the framework of the 8-group system of constants [22].

7. Calculation of reactivity using the inverse kinetics equations method

Let us look at the influence of the choice of delayed neutron parameters on the effectiveness of the inverse kinetics equations method for determining reactivity. Limiting ourselves to model (18), we derive from it an equation for determining the neutron flux

$$n(t)=\frac{1}{1-\rho/\overline{\beta}}\sum_{l,m'}\lambda_{(l)}^{(m')}a_{(l)}^{(m')}e^{-\lambda_{(l)}^{(m')}t}\left[\frac{n(o)}{\alpha_{-}+\lambda_{(l)}^{(m')}}+\int_0^t dt'n(t')e^{\lambda_{(l)}^{(m')}t'}\right], \qquad (23)$$

where $a_{(l)}^{(m')}=\overline{\beta}_{(l)}^{(m')}/\overline{\beta}$, and its corresponding type (15) inverse kinetics equation

$$\frac{\rho}{\overline{\beta}}=1-\sum_{l}\lambda_{(l)}^{(m')}a_{(l)}^{(m')}e^{-\lambda_{(l)}^{(m')}t}\left[\frac{n(o)}{\alpha_{-}+\lambda_{(l)}^{(m')}}+\int_0^t dt'n(t')e^{\lambda_{(l)}^{(m')}t'}\right]\frac{1}{n(t)}, \qquad (24)$$

for determining of $\rho/\overline{\beta}$, making the usual assumptions that when $t<0$ the reactor was starting up: $n(t)\approx n(0)\exp\alpha_{-}t$, and at $t=0$ was shut down.

If we consider equation (23), say, with Keepin's constants as the generator for the given ρ, n(0), α_{-} of the neutron flux 'experimental' values and equation (24) with other constants as the inverse kinetics equation to determine the reactivity $\rho/\overline{\beta}$ for the given $n(t)$, we can check how far the different systems of constants correspond to each other for the task of measuring reactivity.

Tables 7 and 8 contain the results of calculating n(t) for $\alpha_{-}=0$, $\rho/\overline{\beta}$ = -0.1 at times t = 0.01, 0.10, 1.00, 10.0 and 100 seconds using equation (23) with Keepin's constants, and

for 'reactivities' $Rk = (\rho/\bar{\beta})_k(t)$, 'reconstructed' using (24) on the basis of these fluxes and the 8-group constants [22] (k=1), and also the 6-group constants in ABBN-78 (k=2), JENDL (k=3) and ENDF/B6 (k=4).

These data as a whole confirm the deviation pattern seen above in the results of calculations using the different systems of constants in their 'pure form', i.e. without using procedures for the convolution of precursors in the mixture.

Let us now examine the convolutions. Table 9 shows the results of calculating $\delta\rho_k(t)$ using the inverse kinetics equation (24) with Keepin's constants when ρ= -0.1 with averaged isotope decay constants $\bar{\lambda}_{(l)}^{(m)} = \bar{\lambda}^{(m)}$ of the type (22a) for mixtures 1 (k=1) and 2 (k=2).

It can be seen that convolution within a group of decay constants for the isotopes in the fuel mixture does not lead to errors exceeding fractions of a percent.

Table 7

$(\rho/\bar{\beta})_k(t)$ for mixture No. 1 when $\rho/\bar{\beta}$ = -0.1

t	0.01	0.10	1.00	10.0	100
n(t)	0.90880	0.90384	0.87120	0.73054	0.30457
R1	-0.09999	-0.10003	-0.10017	-0.10089	-0.10083
R2	-0.09999	-0.10005	-0.10028	-0.10071	-0.10079
R3	-0.09999	-0.09993	-0.09989	-0.10015	-0.09958
R4	-0.10003	-0.10052	-0.10079	-0.09384	-0.09100

Table 8

$(\rho/\bar{\beta})_k(t)$ for mixture No. 2 when $\rho/\bar{\beta}$ = -0.1

t	0.01	0.10	1.00	10.0	100
n(t)	0.90880	0.90390	0.87173	0.73462	0.31627
R1	-0.10000	-0.10003	-0.10015	-0.10074	-0.10070
R2	-0.10000	-0.10012	-0.10088	-0.10382	-0.10654
R3	-0.99999	-0.10006	-0.10063	-0.10318	-0.10521
R4	-0.10004	-0.10062	-0.10139	-0.09692	-0.09620

Table 9

$\delta\rho_k(t)$ for mixtures 1 and 2

t	0.01	0.10	1.00	10.0	100
$\delta\rho_1$	-0.3E-02	0.2E-02	0.5E-01	0.6E-01	-0.1E-01
$\delta\rho_2$	0.1E-02	0.9E-02	0.2E-01	0.1E-01	-0.8E-01

Conclusion

This paper examines methods for mathematical kinetics modelling for delayed neutrons, taking into account the possible dependence of delayed neutron emitter decay constants on the type of parent nucleus producing them and the energy initiating its neutron fission.

One of these methods, based on transformation of the input of distributed reactor kinetics equations into equivalent reactor point model equations [30], is an accurate method in principle and allows us to make approximations of any order. However, it is generally more complex to perform.

The other method, based on the transition from the conventional 6-group systems of delayed neutron constants to a new 8-group system [22] with 'universal' precursor decay constants, identical for all the isotopes and energies in the groups, is, in principle, approximate but simpler to perform.

In this paper these methods were compared on the basis of numerical analysis of several simplified tasks. The results obtained show that:

- The process used in [22] for equivalent conversion of 6-group to 8-group constants in fact leads only to an approximated conservation of the positive reactivity scale, with a relative error not exceeding, say, 0.4% for ^{238}U. In so doing, however, such important functionals as weighted average precursor half-lives may not be conserved;

- In the examples examined, the deviations in the reactivity values calculated using the 8-group constants from the corresponding values calculated using Keepin's 6-group constants are, on the whole, close to the deviations characteristic of the ABBN-78 and JENDL 3.2 6-group constants;

- The corresponding deviations for the ENDF/B6 constants are considerably higher;

- Its main advantage is simplification of the dynamic model through transition from the conventional 6-group constants systems to an 8-group constants system with universal decay constants;

- A generally similar simplification can also be achieved in the conventional 6-group models by assimilating the aforementioned supplementary computing procedures for interpolation and averaging out of the group half-lives.

In summary, we can assume that the 8-group approach in [22], being simpler algorithmically, and also apparently no less accurate than the conventional 6-group approach, is promising for practical applications. Its possibilities and limitations must, however, be clearly identified. For this, generally speaking, further investigation is required.

REFERENCES

1. Usachev, L.N., Equation for neutron importance, reactor kinetics and perturbation theory, Reactor Construction and Theory of Reactors, USSR Academy of Sciences, Moscow, 1955.
2. Henry, A.F., The Application of Reactor Kinetics to the Analysis of Experiments, Nucl. Sci. and Eng., v.3, No. 1, p. 52–70 (1958).
3. Keepin, G.R., Physics of nuclear reactor kinetics, Atomizdat, Moscow, 1967.

4. Shikhov, S.B., Mathematical theory of reactors, Atomizdat, Moscow, 1973.
5. Bell, D., Glasstone S., Nuclear reactor theory, Atomizdat, Moscow, 1974.
6. Hedrick, D., Nuclear reactor dynamics, Atomizdat, Moscow, 1975.
7. Abagyan, L.P., Bazazyants, N.O., Nikolaev, M.N., Tsibulya, A.M., Group constants for reactor and shielding calculations, Ehnergoatomizdat, Moscow, 1981.
8. Kazanskij, Yu.A., Matusevich, E.S., Experimental methods for reactor physics, Energoatomizdat, Moscow, 1984.
9. Shokod'ko, A.G., Zhuravlev, V.I., Sluchevskaya, V.M., Representation of several fissile isotopes by one effective isotope when determining reactivity by the inverse kinetic method, Voprosy atomnoj nauki i tekhniki, Ser. Fiz. i tekh. yad. reaktorov, No. 9 (6), p. 69–71 (1984).
10. Gulevich, A.V., Kukharchuk, O.F., Polevoj, V.B., Pupko, S.V., Application of an integral neutron kinetics model to the calculation of multiregion multiplying systems, Preprint IPPE-2129, Obninsk, 1990.
11. Bezborodov, A.A., Volkov, A.V., Ganina, S.M., Ginkin, V.P., Kuznetsov, I.A., Troyanova, N.M., Shvetsov, Yu.E., Programme for a joint solution to spatial-time neutron transport equations and thermohydraulic transient and emergency processes in fast reactors, Preprint IPPE-2637, Obninsk, 1997.
12. Maksyutenko, B.P., Relative delayed neutron yields for fast neutron induced fission of ^{238}U, ^{235}U and ^{232}Th, Zhurnal Ehksperimental'noj i Teoreticheskoj Fisiki, v. 35, p. 815 (1958).
13. Tarasko, M.Z., Maksyutenko, B.P., A new approach to the search for the distribution of delayed neutron precursors, Yadernaya Fizika, v. 17, No. 6, p. 1149–1155 (1973).
14. Meneley, D.A., The Effective Delayed Neutron Fraction in Fast Reactors, ANL-7410, 198 (1970).
15. Cahalan, J.E., Ott, K.O., Delayed Neutron Data for Fast Reactor Analysis, Nucl. Sci. Eng., 70, 184, (1973).
16. Tuttle, R.J., Delayed Neutron Data for Reactor Physics Analysis, Nucl. Sci. Eng., 56, p. 37–71 (1975).
17. JENDL-3.2, JAERI-DATA/CODE97-044.
18. Brady, M.C., England, T.R., Delayed Neutron Data and Group Parameters for 43 Fissioning Systems, Nucl. Sci. Eng., 103, p.129–149 (1989).
19. Manturov, G.N., Nikolaev, M.N., Tsibulya, A.M., ABBN-93 Group constants system, Voprosy atomnoj nauki i tekhniki, Ser. Yadernye konstanty, No. 1, p. 59–98 (1996).
20. Zabrodskaya, S.V., Nikolaev, M.N., Tsibulya, A.M., Data on delayed neutrons in the ABBN-93 constants system, Voprosy atomnoj nauki i tekhniki, Ser. Yadernye konstanty, No. 1, p. 21 (1998).
21. Spriggs, G.D., In-Pile Measurement of the Decay Constants and Relative Abundances of Delayed Neutrons, Nucl. Sci. Eng., 114, 342 (1993).
22. Spriggs, G.D., Campbell, I.M., Piksaikin, V.M., An 8-Group Neutron Model Based on a Consistent Set of Half-Lives, Report LA-UR-98-1619, LANL, Distributed to the OECD/NEA's Working Party in Delayed Neutrons (WPEC/SG6), 1999.
23. Piksaikin, V.M., Kazakov, L.E., Isaev, S.G., Korolev, G.G., Roshchenko, V.A., Tertychnyj, R.G., 8-group relative delayed neutron yields for monoenergetic neutron induced fission of ^{239}Pu, Voprosy atomnoj nauki i tekhniki, Ser. Yadernye konstanty, No. 1, p. 66–67 (2001).

24. Piksaikin, V.M., Kazakov, L.E., Isaev, S.G., Korolev, G.G., Roshchenko, V.A., Tertychnyj, R.G., 8-group relative delayed neutron yields for epithermal neutron induced fission of ^{238}U and ^{239}Pu, ibid, p. 67–72 (2001).
25. Doroshenko, A.Yu., Piksaikin V.M., Tarasko M.Z., The Energy Spectrum of Delayed Neutrons from Thermal Neutron Induced Fission on ^{235}U and Its Analytical Approximation, Voprosy atomnoj nauki i tekhniki, Ser. Yadernye konstanty, No. 1, p. 87–93 (2001).
26. Borzakov, S.B., Zamyatin, Yu.S., Panteleev, Ts., et al., Study of delayed neutron decay curves during thermal neutron fission, Voprosy atomnoj nauki i tekhniki, Ser. Yadernye konstanty, No. 2, p. 5–11 (1999).
27. Updated Codes and Methods to Reduce the Calculational Uncertainties of the LMFR Reactivity Effects, Working Material, First Research Co-ordination Meeting, Vienna, 24–26 November 1999, p.11.
28. Abramov, B.D., Some questions on mathematical modelling of reactor kinetics, Preprint IPPE-2778, Obninsk, 1999.
29. Abramov, B.D., Danilychev, A.V., Stogov, V.Yu., Suslov, I.P., Questions on modelling the kinetics of heterogeneous regions with various types of fuel using point approximation, Preprint IPPE-2855, Obninsk, 2000.
30. Abramov, B.D., Some generalizations of reactor kinetics equations, Preprint IPPE-2875, Obninsk, 2001.
31. Abramov, B.D., Some modifications to the theory of coupled reactors, Atomnaya energiya, Vol. 90, No. 5, p. 337–345 (2001).
32. Abramov, B.D., Some modifications to point kinetics equations, Yadernaya energetika, No. 2, p. 52–59 (2001).
33. Abramov, B.D., Some generalizations of reactor inverse kinetics equations, Preprint IPPE-2970, Obninsk, 2003.

THE CONSTANTS AND PARAMETERS OF NUCLEAR STRUCTURE AND NUCLEAR REACTIONS

04-10281 [3]
Translated from Russian

UDC 539.17

Consistent evaluation of photoneutron reaction cross-sections using data obtained in experiments with quasimonoenergetic annihilation photon beams at Livermore (USA) and Saclay (France)

V. V. Varlamov, N.N. Peskov, D.V. Rudenko, M.E. Stepanov
M.V. Lomonosov Moscow State University
D.V. Skobel'tsyn Scientific Research Institute for Nuclear Physics
Centre for Photonuclear Experiment Data

CONSISTENT EVALUATION OF PHOTONEUTRON REACTION CROSS-SECTIONS USING DATA OBTAINED IN EXPERIMENTS WITH QUASIMONOENERGETIC ANNIHILATION PHOTON BEAMS AT LIVERMORE (USA) AND SACLAY (FRANCE). A detailed, systematic analysis of the (γ,xn), (γ,n) and (γ,2n) reaction cross-section data obtained using quasimonoenergetic annihilation photon beams at Livermore (USA) and Saclay (France) was carried out for 19 nuclei (7 initially): ^{51}V, ^{75}As, ^{89}Y, ^{90}Zr, ^{115}In, ^{116,117,118,120,124}Sn, ^{127}I, ^{133}Cs, ^{159}Tb, ^{165}Ho, ^{181}Ta, ^{197}Au, ^{208}Pb, ^{232}Th, ^{238}U. It was observed that the (γ,xn) reaction cross-section data obtained at both laboratories without using a neutron multiplicity determination procedure disagreed by 10–15%. Additionally, it was found that the disagreement of the (γ,n) and (γ,2n) partial reaction cross-sections obtained at both laboratories using a neutron multiplicity determination procedure was significantly greater (up to 30–40%), and as a rule in different directions. These disagreements were interpreted as being the result of differences in the neutron multiplicity determination procedures used in both laboratories: the procedure at Saclay was incorrect, resulting in the incorrect attribution of part of the (γ,2n) reaction cross- section to the (γ,n) reaction. A special method was used to make the data consistent. This involved recalculating the part of the (γ,n) reaction cross-section determined to be 'false' and moving it back to the (γ,2n) reaction cross-section. For all 19 nuclei listed above, the jointly corrected (γ,xn), (γ,n) and (γ,2n) reaction cross-sections were evaluated and prepared for inclusion in the EXFOR nuclear reaction database.

Introduction

One of the main problems of experimental research in nuclear physics has been and remains obtaining information on the structure of the atomic nucleus. Such information can be obtained primarily from nuclear reactions. Information on the structure of a target nucleus can be obtained by analysing the angular, energy, mass and other distributions of product particles

and the excitation energies of the final nucleus measured at different energies of different incident particles. Among the vast variety of nuclear reactions, those induced by electromagnetic interactions occupy a not insignificant position. Such reactions [1–4] are caused by the electromagnetic field whose properties have been thoroughly studied, and the mechanism by which energy is transferred from an incident gamma ray to the nucleus under investigation is accurately known. In such reactions, effects due to the structure of the nucleus can be distinguished more easily from nucleus excitation mechanisms than in reactions induced by neutrons and charged particles.

Absorption by a nucleus of a γ-ray with an energy of up to ~50 MeV leads to the emission by the nucleus of individual nucleons and their combinations. The energy dependence of the photonuclear reaction cross-section for all atomic nuclei except the lightest — deuteron, triton and the ^{3}He nucleus — exhibits a clearly expressed powerful and broad maximum called the giant dipole resonance. The nucleus is most likely to emit one nucleon and less likely to emit two or more. This fact, and the relation of the energy thresholds of the relative reactions, determines the main decay channels of the giant dipole resonance. A reaction corresponding to a decay channel of the giant dipole resonance where a particular nucleon or combinations thereof are produced ((γ,n), (γ,p), (γ,np), (γ,2n), (γ,3n) etc.)) is known as a partial reaction. The sum of all the partial reactions describes all possible channels (except scattering) for photons exiting from the primary beam — the total photoabsorption reaction:

$$(\gamma,\mathrm{abs}) = (\gamma,1n) + (\gamma,np) + (\gamma,2n) + (\gamma,3n) + (\gamma,1p) + (\gamma,2p) + \ldots + (\gamma,f), \quad (1)$$

where (γ,f) is the fission reaction which is only possible in relatively heavy nuclei.

In the energy region at the giant dipole resonance maximum the photoabsorption cross-section for the majority of nuclei mainly comprises the (γ,n), (γ,p) and (γ,np) reaction cross-sections, while beyond the giant dipole resonance maximum reactions with a higher emitted multiplicity nucleon can make a significant contribution, notably the (γ, 2n) reaction. The relation of the cross-sections of reactions involving emission of one and two neutrons is an important characterizing feature of the photodisintegration process which is dependent on the mechanism of excitation and decay of the nucleus. Thus, for example, a discrepancy between the energy dependence of the cross-section of the reaction involving emission of a single neutron and the predictions of the statistical model could serve as evidence of processes involving direct knock-out of neutrons from the nucleus by gamma rays, and the extent of the discrepancy as a measure of the relations between the different reaction mechanisms [5].

However, the validity of such conclusions depends to a significant extent on how accurately and reliably the cross-section of the reaction involving emission of a single neutron (γ,n) is determined in the energy region where a process involving emission of two neutrons in the (γ,2n) reaction is possible. Owing to various factors, the principal of which will be examined below, in many cases the data for the (γ,n) and (γ,2n) reactions are interlinked and influence one another. Unfortunately, there are significant disagreements between data of this type obtained in different experiments. The majority of the data on the (γ,n) and (γ,2n) reactions was obtained in experiments with quasimonoenergetic annihilation photons at Livermore (USA) and Saclay (France), and the reason for the significant disagreements

between them [6] is certain shortcomings in the procedures used in the experiments to determine photoneutron multiplicity.

Moreover, earlier research [e.g. 7–9] shows that, in many cases, even data which are free from error connected with the determination of product multiplicity, obtained indirectly in various experiments, such as the total photoneutron reaction cross-sections

$$(\gamma,xn) = (\gamma,1n) + (\gamma,np) + 2(\gamma,2n) + 3(\gamma,3n) + \ldots + \nu(\gamma,f), \qquad (2)$$

also differ appreciably from one another. The aforementioned research studied the main reasons for these discrepancies and proposed ways of making the data consistent. This paper focuses on this research, particularly as regards the data on the cross-sections of the partial photoneutron reactions (γ,n) and (γ,2n). The data on the cross-sections of the total photoneutron reaction (γ,xn) are also studied.

In producing this paper, we used the full database of nuclear reactions induced by photons, neutrons, charged particles and heavy ions [10–13] created through the network [14] of IAEA Nuclear Data Centres in accordance with the requirements and recommendations [15] of the IAEA Nuclear Data Section based on an EXFOR [16].

1. Analysis of systematic differences in data on photoneutron reaction cross-sections

Clearly, for reliable research on the giant dipole resonance, its various decay channels and their competition in giant dipole resonance formation processes, we need primarily to be able to determine in a detailed and accurate manner both the total photoabsorption cross-section, total (γ, xn), and the partial cross-sections, in particular the photoneutron cross-sections, such as (γ,n),(γ,np),(γ,2n),(γ,3n), and other photonuclear reactions. Isolating one of these reactions experimentally and determining its cross-section is far from being always possible. The difficulties of experimental research on photonuclear reactions (lack of intense monoenergetic photon beams, low reaction cross-section values, relatively close energy threshold values of the different reactions, high background levels, inadequate detector efficiency, etc.) frequently compel experimenters to use far from optimal experimental conditions. The main problems which substantially increase the difficulty of obtaining reliable information on photonuclear reaction cross-sections, and present the greatest difficulties as regards a unique interpretation of the results when comparing different experiments, include the following:

- non-monochromatic photon beams;
- multiplicity of products of many reactions, principally neutrons from the (γ, 2n) reaction.

The first difficulty is connected with a lack of sufficiently intense monoenergetic photon beams and, hence with the problems of creating the special conditions in photonuclear experiments which would allow us to view the effective spectrum of the photons inducing the reaction as quasimonoenergetic, i.e. to some degree close to a monoenergetic spectrum. The second difficulty is caused by the characteristics of the various methods used to identify and register the different reaction products.

A lack of due attention to even one of these difficulties in specific experiments, let alone to both, brings with it the risk of significant divergences in the interpretation of the results obtained in the experiment. In many cases, this gives rise to significant systematic disagreements between the results of different experiments. These systematic disagreements can only be detected, and their effect on the result of each individual experiment eliminated, through detailed and systematic overall analysis of the results of numerous experiments, accurately taking account of exactly what was obtained under exactly what conditions.

A whole series of such systematic studies has been carried out [e.g. 7–9] using relational databases created [e.g. 10–13] at the Centre for Photonuclear Experiments Data of the Moscow State University Scientific Research Institute for Nuclear Physics. This research has helped elucidate the causes of some of the notable systematic disagreements and allowed a whole series of cross-sections of various photonuclear reactions to be obtained (evaluated) in a form which is virtually free of certain systematic errors.

1.1. Systematic errors in reaction cross-sections obtained using gamma bremsstrahlung and quasimonoenergetic annihilation photons

Of the disagreements mentioned above, the most significant are the notable disagreements in the results of experiments performed using beams of gamma bremsstrahlung (GB) and quasimonoenergetic photons formed by the annihilation of relativistic positrons (QMA photons), which experiments — taken together — have provided us with the majority of data on photonuclear reaction cross-sections. These disagreements are as follows: photonuclear reaction cross-sections obtained using QMA photon beams, by comparison with the cross-sections of similar reactions obtained from GB experiments:

- have a smoother shape in the vast majority of cases;
- have a lower absolute value in many cases.

These disagreements can be illustrated using the fairly accurate data on the cross-sections of the total photoneutron reaction $(\gamma,xn) = [(\gamma,n) + (\gamma,np) + 2(\gamma,2n)]$ on the two isotopes of oxygen $^{16,18}O$.

The $^{16}O(\gamma,xn)$ reaction. The cross-sections of the $^{16}O(\gamma,xn)$ reaction obtained in three different experiments (one GB experiment [17] and two QMA experiments: at Saclay (France) [18] and Livermore (USA) [19]) are shown in Fig. 1. We can see clearly that almost all the characteristic features (clearly expressed maxima and minima) appear in all three cross-sections compared. It is easy to see that, in all three cross-sections compared, these features are close (though they do not coincide) in terms of energy position, but differ quite appreciably in terms of their absolute value. We may say that the nature of these differences is almost the same over the whole energy range studied.

Notably, the result of the GB experiment [17] and the QMA data obtained at Saclay [18] disagree essentially only in the shape (the latter cross-section looks like an appreciably smoother version of the former), but they are close to one another as regards the absolute value. By contrast, the QMA cross-section obtained at Livermore [19] is appreciably lower than the other two previous ones (by ~ 15%) in terms of the absolute value.

The ^{18}O(γ,xn) reaction. A more accurate quantitative representation of the scale of these divergences can be obtained, for example, using the data in Ref. [20], which gives detailed data on the ratios of the amplitudes (A_{GB}/A_{QMA}) and widths ($<G_{QMA}/G_{GB}>$) of the resonances in the (γ,xn) reaction cross-sections identified in experiments employing GB [20] and QMA photons [21, Livermore] on the oxygen isotope ^{18}O. However arbitrary the procedure for determining the amplitudes (and widths) of the resonances in the cross-sections, which have a complex structure, lower amplitude values were obtained for almost all resonances in the QMA cross-section (mean value of the ratio of the amplitudes $<A_{GB}/A_{QMA}>$ = 1.17; ratio of the integral cross-section values in the 8–28 MeV interval $\sigma^{int}_{GB}/\sigma^{int}_{QMA}$ = 1.16). In line with the statement above that the QMA cross-sections look like smoothed versions of the GB cross-sections, the mean value for the ratios of the widths of the corresponding resonances is appreciably greater than 1: $<\Gamma_{QMA}/\Gamma_{GB}>$ = 1.35.

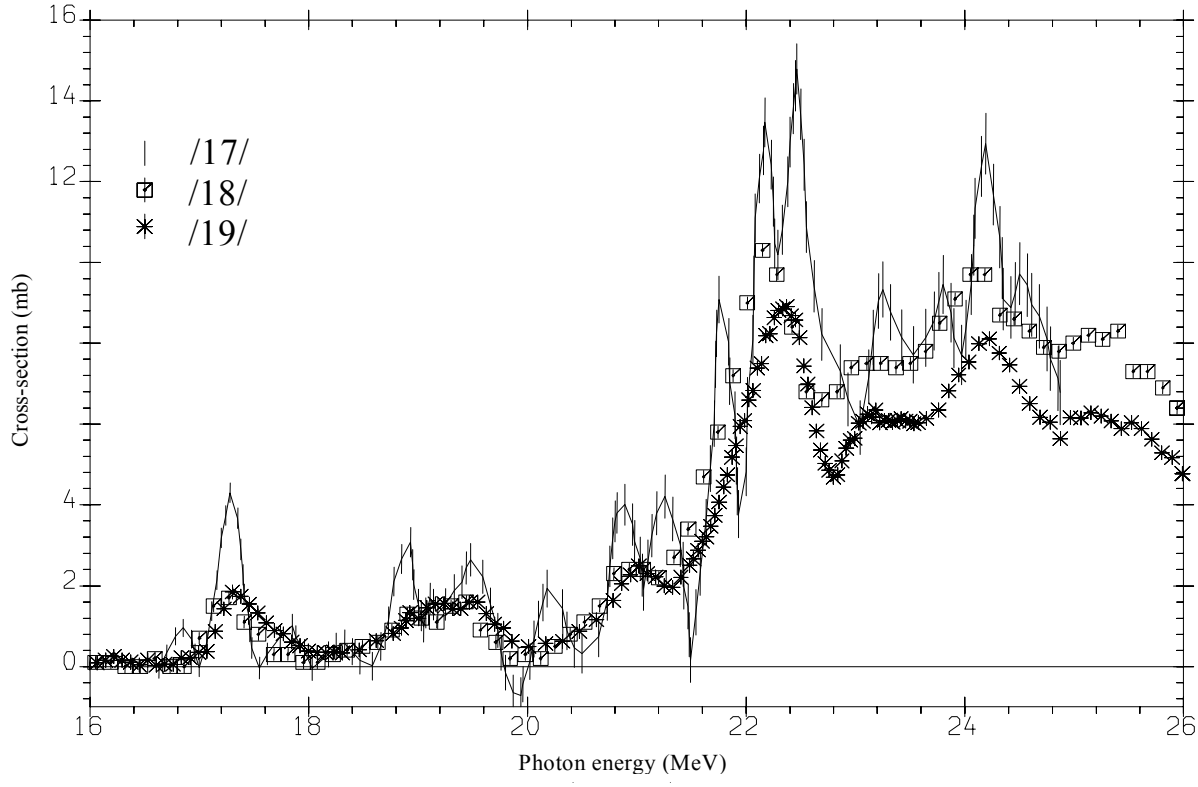

Fig. 1. Comparison of ^{16}O(γ,xn) reaction cross-sections obtained in a GB experiment [17] and in two typical experiments using QMA photons performed at Saclay (France) [18] and Livermore (USA) [19]

An analysis [22] of existing experimental data [1–4] for over 500 (γ,xn) total photoneutron reaction cross-sections on nuclei from ^{3}H to ^{238}U gives us some idea of the systematic nature of the divergences in the results of the different experiments. Fig. 2 shows the values of the ratios of the integral cross-sections

$$r = R^{int}_{syst} = \sigma^{int}_{various\ laboratories}(\gamma,xn)/\sigma^{int}_{Livermore}(\gamma,xn), \qquad (3)$$

obtained using various methods in different laboratories to the QMA data obtained in one of them (to be specific, Livermore). In order to avoid as far as possible problems [6] related to measuring the photoneutron multiplicity, the integral cross-sections were calculated for the (γ,xn) reaction, in the incident photon energy region between the energy thresholds of the (γ,n) and (γ,2n) reactions; thus, in effect, the data on the (γ,n) reaction in the energy region up to the (γ,2n) reaction threshold were analysed (compared).

The results given show a clear disagreement between the Livermore data and the data from most laboratories: the mean value of the ratio $\langle R^{int}_{syst} \rangle \neq 1$. Despite the fact that there are also some disagreements between the data from the various laboratories, the values for the ratio in question clearly cluster around a mean value of $\langle R^{int}_{syst} \rangle = 1.122 \pm 0.243$. It is particularly important to note that, in terms of the absolute value, the Saclay QMA data do not agree with the Livermore QMA data of the same type but with the data obtained using quasimonoenergetic photons in other laboratories (General Atomic (USA), Pennsylvania (USA), Illinois (USA), Giessen (Germany)), and with the data from experiments using gamma bremsstrahlung (performed mainly in Moscow and Melbourne (Australia)).

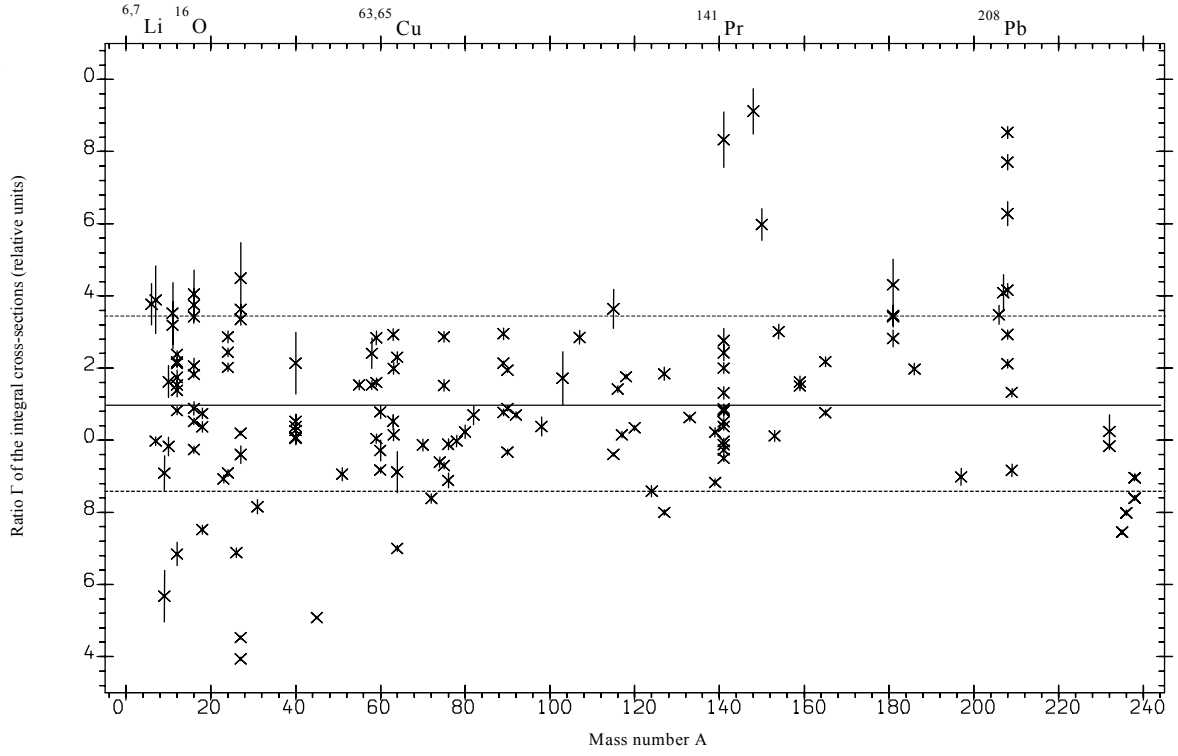

Fig. 2. Systematics [22] of the values of the ratio
$r = R^{int}_{syst} = \sigma^{int}_{various\ laboratories}(\gamma,xn)/\sigma^{int}_{Livermore}(\gamma,xn)$ of the integral cross-section values for the total photoneutron reaction up to the (γ,2n) reaction threshold for various nuclei, obtained using various photon beams in various laboratories and using quasimonoenergetic photons at Livermore. Continuous line — mean value of the ratio $r = R^{int}_{syst}$, dotted lines — boundaries of the standard deviation range.

Similar divergences in the absolute values of the reaction cross-sections could be caused, for example, by differences in the energy calibrations of the experimental facilities and the error levels of the absolute normalizations.

1.2 Systematic errors of the total photoneutron reaction cross-sections obtained using QMA photons at Saclay and Livermore

1.2.1. Integral reaction cross-sections

In addition to the disagreements mentioned above in the data from similar QMA experiments performed using similar methodologies at Saclay and Livermore, using as an example data on the $^{16}O(\gamma,xn)$ total photoneutron reaction cross-section, we can give a large number of other examples.

Table 1, for example, gives data from Ref. [1] on the integral cross-sections of the total photoneutron reaction (γ,xn) also obtained at Saclay and Livermore for five intermediate and heavy nuclei. These data were selected from the extensive data in Ref. [1] for reasons of ease of comparison owing to the closeness of the integration limits. We can see clearly that, for all five nuclei, the data on the integral cross-sections of identical reactions obtained at Saclay are higher than the data obtained at Livermore by ~6–16%. Thus, in the case of the ^{51}V nucleus, where the integration limits E_γ^{max} practically coincide, the ratio $R^{int}(\gamma,xn) = \sigma^{int}{}_S(\gamma,xn)/\sigma^{int}{}_L(\gamma,xn)$ is 689/654 = 1.06. For the nuclei ^{75}As, ^{90}Zr and ^{165}Ho, where the integration limits stand in the relation to one another $E_\gamma^{max}{}_S < E_\gamma^{max}{}_L$, the ratios cannot be lower than 1306/1130 = 1.16, 1309/1158 = 1.13 and 3667/3385 = 1.08 respectively.

Table 1

Comparison of the integral cross-sections (data from Ref. [1]) for the total photoneutron reaction (γ,xn) obtained at Saclay (upper values) and Livermore (lower values)

Nucleus	^{51}V	^{75}As	^{90}Zr	^{133}Cs	^{165}Ho
E_γ^{max}, MeV	27.8 27.8	26.2 29.5	25.9 27.6	24.2 29.5	26.8 28.9
σ^{int}, MeV·mb	689 654	1306 1130	1309 1158	2484 2505	3667 3385

Many other examples of similar disagreements in the data in Ref. [1] are less clear, simply because the integration limit used when calculating the integral cross-sections differ appreciably, but they clearly confirm the tendency observed.

1.2.2. Absolute magnitudes of the reaction cross-sections

These disagreements in the data from the same types of QMA experiments performed at Livermore and Saclay have been known for quite some time and have been the subject of much research and discussion.

Thus, for example, the cross-sections of photoneutron reactions on the nuclei ^{nat}Zr, ^{127}I, ^{141}Pr, ^{197}Au and ^{nat}Pb obtained previously at Livermore at different times, were redetermined at that laboratory in 1987 [23] with the specific aim of identifying possible ways of eliminating the striking disagreements between those data and the data from Saclay. New data for both the absolute values and the integral cross-section values for various photoneutron reactions on 14 nuclei were compared with one another in detail and were used to elaborate

recommendations for eliminating these discrepancies. The introduction of a special factor F (Table 2) was recommended for additional reciprocal normalization of the data from the two laboratories.

Table 2

The factor F (Livermore/Saclay ratio) recommended in Ref. [23] to normalize the Saclay data in order to eliminate disagreements with the Livermore data

Nucleus	Laboratory	Factor F, relative units	Factor 1/F, relative units
^{nat}Rb	S	0.85 ± 0.03	1.18
^{89}Sr	S	0.85 ± 0.03	1.18
^{89}Y	S	0.82	1.22
^{89}Y	L	1.0	
^{90}Zr	S	0.88	1.14
^{90}Zr	L	1.0	
^{91}Zr	L	1.0	
^{92}Zr		1.0	
^{93}Nb	S	0.85 ± 0.03	1.18
^{94}Zr	L	1.0	
^{127}I	S	0.8	1.25
^{197}Au	S	0.93	1.08
^{206}Pb	L	1.22	
^{207}Pb	L	1.22	
^{208}Pb	L	1.22	
^{208}Pb	S	0.93	1.08
^{209}Bi	L	1.22	

The dual nature of the recommendations elaborated in Ref. [23] is striking. In the case of the cross-sections of the reactions on the nuclei ^{206,207,208}Pb, ^{209}Bi, where these can be compared with the Saclay data, it is proposed that the latter be reduced (by multiplying by F ~0.8). Where there are no Saclay data, it is proposed that the Livermore data be increased (by multiplying by F ~1.2).

We would point out once again that the authors of Ref. [23] attribute the striking disagreements (up to ~25%) in the data from the same types of QMA experiments performed at Saclay and Livermore to possible errors at Livermore in determining the photon flux and the neutron detector efficiency.

1.3. Systematic errors of the absolute values of the (γ,n) and (γ,2n) partial reaction cross-sections obtained using QMA photons at Saclay and Livermore

Fig. 3, which shows the cross-sections of the reaction ^{75}As(γ,xn) from two experiments using QMA photon beams at Saclay (France) [24] and Livermore (USA) [25], shows how different not only the absolute values, but also the shape of the cross-sections for the same types of reactions obtained in the same types of QMA experiments but in different laboratories, can be. Fig. 3 clearly shows that, over the whole energy region studied, the first cross-section's absolute value is appreciably higher than the second's.

Fig. 3 also shows how the same types of QMA data differ appreciably from each other in different ways in different energy regions. While the cross-sections which are being compared are very similar in shape in the energy region below ~18 MeV, in the higher energy region the cross-section in Ref. [24] by comparison with the cross-section in Ref. [25], has a rather pronounced additional maximum. The closeness of the energy where this disagreement occurs to the threshold of the $^{75}As(\gamma,2n)^{73}As$ reaction (18.2 MeV), and the closeness of the value for the contribution this additional maximum makes to the $^{75}As(\gamma,xn)$ reaction cross-section to the value for the $^{75}As(\gamma,2n)^{73}As$ reaction cross-section also obtained in Ref. [24], suggests that such disagreements might also be connected in some way with the processes for registering neutrons with a multiplicity other than one, i.e. products of the (γ,2n) reaction in particular.

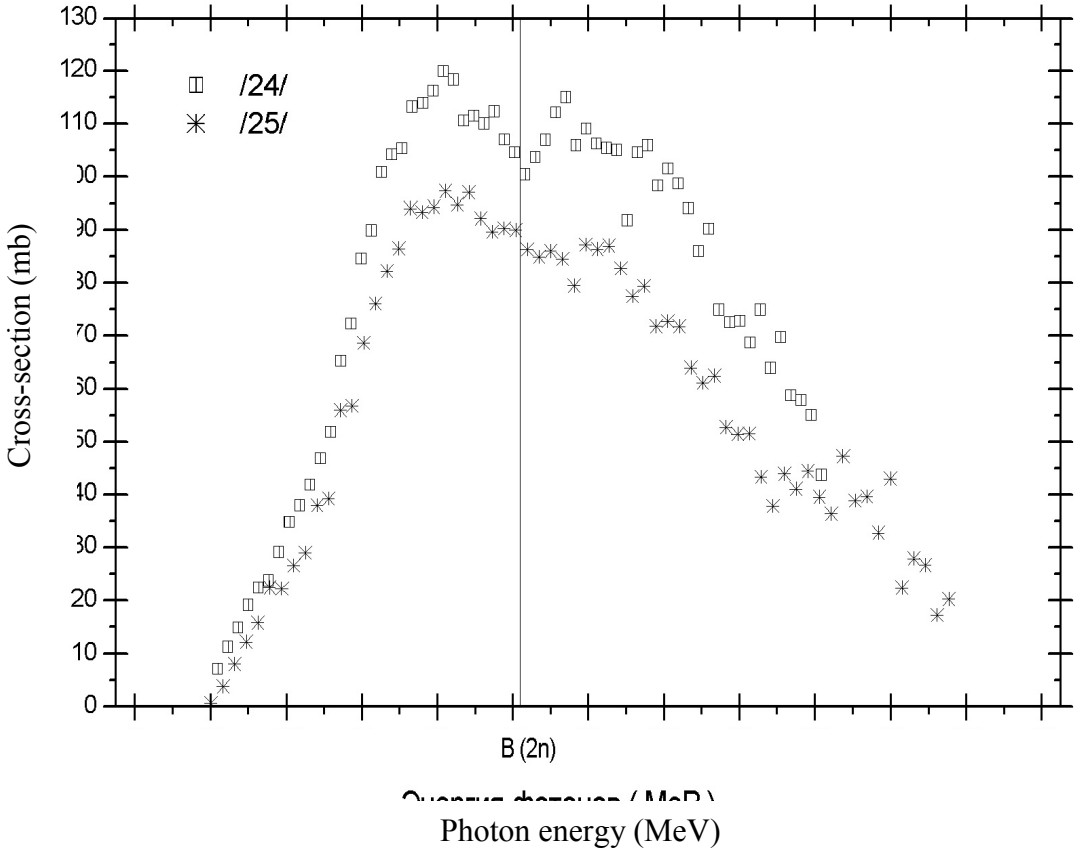

Fig. 3. Comparison of the ^{75}As (γ,xn) reaction cross-sections obtained in two typical experiments using QMA photons at Saclay [24] and Livermore [25]

Detailed systematic analysis of the disagreements between the Saclay and Livermore data on the partial photoneutron reaction cross-sections, particularly the (γ,2n) reaction, reveals the even more serious (dramatic) nature of these disagreements which are clearly systematic. Thus, Ref. [6], in addition to analysing the ratios of the integral cross-sections for the total photoneutron reaction (γ,xn) obtained directly in experiments, also examined the relations of the absolute values from Ref. [1] for the (γ,n) and (γ,2n) partial reaction cross-sections for 12 intermediate and heavy nuclei from ^{89}Y to ^{208}Pb. The following patterns were found:

- the cross-sections for the total photoneutron reaction (γ,xn) obtained at Saclay and Livermore are slightly shifted relative to one another in terms of the energy;
- the (γ,xn) reaction cross-sections obtained at Saclay are ~8–15% higher in terms of their absolute value than the cross-sections obtained at Livermore (closely in line with the systematics from Ref. [22] shown in Fig. 2);
- the (γ,n) and (γ,2n) reaction cross-section values obtained at Saclay and Livermore relate to one another in a substantially different way:
  - the (γ,n) reaction cross-section values obtained at Saclay are, on the whole, also higher than the cross-section values for the same reactions obtained at Livermore, but their ratio greatly exceeds the 10–15% divergence between the (γ,xn) reaction cross-section values; thus, for example, for the nucleus ^{159}Tb, the divergence determined in Ref. [6] using the data from Ref. [1] is 37% — 1936/1413 (Saclay data higher);
  - the (γ,2n) reaction cross-section values are related to each other in the opposite manner; thus, again for ^{159}Tb, the ratio of the cross-section values is 605/887 (Livermore data higher), i.e. the discrepancy is 47% [1,6]!

The quantitative data from Ref. [1] for all 12 nuclei studied in Ref. [6] are given in Table 3.

Here and below we should remember that, as the direct photoneutron registration method was used in the experiments performed at Saclay and Livermore which are being discussed in detail, and the B(np) thresholds of the (γ,np) reactions are low (Table 3), it is more correct to designate the single-neutron reaction as [(γ,n) + (γ,np)] rather than (γ,n).

Thus, the results of the experiments performed at both laboratories for identical total photoneutron reactions (γ,xn), which do not take into account photoneutron multiplicity, differ by ~8–15% (Saclay data higher); while the results obtained for the partial reaction cross-sections, which do take into account multiplicity, disagree in completely different ways and dramatically (the disagreements are substantially greater (up to 50%) and so in different directions). Based on an analysis of the characteristics of the procedures for determining the photoneutron multiplicity at Saclay and Livermore, these disagreements were interpreted in Ref. [6] as being the result of errors in the procedure used at Saclay to determine the photoneutron multiplicity: a portion of the neutrons from the (γ,2n) reaction was erroneously attributed to the (γ,n) reaction. A special method was proposed to overcome such disagreements in the data from the two laboratories on partial photoneutron reactions. In essence, it involves using a special formula to recalculate the data for the (γ,2n) reaction cross-sections obtained at Saclay where the photoneutron multiplicity was incorrectly determined: the portion of the (γ,n) reaction cross-section which was erroneously attributed to the single-neutron reaction is reattributed to the two-neutron reaction cross-section.

Table 3

Comparison from Ref. [6] of integral cross-section values from Ref. [1] for the (γ,n), (γ,2n) and (γ,xn) reactions obtained using QMA photon beams (Saclay/Livermore values)

Nucleus	B(np) threshold of the (γ,np) reaction, MeV	$\sigma^{int}_S(\gamma,n)/\sigma^{int}_L(\gamma,n)$, both — MeV·mb	$\sigma^{int}_S(\gamma,2n)/\sigma^{int}_L(\gamma,2n)$, both — MeV·mb	R(xn) = $\sigma^{int}_S(\gamma,xn)/\sigma^{int}_L(\gamma,xn)$, relative units
^{89}Y	18.2	1279/960 = 1.33	74/99 = 0.75	1.255 ± 0.005
^{115}In	15.9	1470/1354 = 1.09	278/508 = 0.55	0.942 ± 0.004
^{117}Sn	16.2	1334/1380 = 0.97	220/476 = 046	1.012 ± 0.007
^{118}Sn	18.8	1377/1302 = 1.06	258/531 = 0.49	1.056 ± 0.005
^{120}Sn	19.0	1371/1389 = 0.99	399/673 = 0.59	0.987 ± 0.004
^{124}Sn	20.0	1056/1285 = 0.82	502/670 = 0.75	0.929 ± 0.006
^{133}Cs	15.0	1828/1475 = 1.24	328/503 = 0.65	1.106 ± 0.007
^{159}Tb	14.0	1936/1413 = 1.37	605/887 = 0.68	1.062 ± 0.001
^{165}Ho	13.9	2090/1735 = 1.20	766/744 = 1.03	1.136 ± 0.007
^{181}Ta	13.3	2180/1300 = 1.68	790/881 = 0.90	1.218 ± 0.018
^{197}Au	13.7	2588/2190 = 1.18	479/777 = 062	1.004 ± 0.013
^{208}Pb	14.9	2731/1776 = 1.54	328/860 = 0.38	1.296 ± 0.011

The situation as regards the (γ,n) and (γ,2n) partial photoneutron reaction cross-sections looks very complex:

- on the one hand, the Livermore data for both the total reaction (γ,xn) and the (γ,n) and (γ,2n) partial reactions, which stand in a correct relationship to one another, cannot be used [6, 8, 9] without a correction — multiplication by a coefficient that brings these data into line with the data from other laboratories; this coefficient should, in principle, be calculated using the Saclay QMA data for the (γ,xn) reaction cross-section for each nucleus individually; where the relevant Saclay data are missing, the coefficient $<R^{int}_{syst}> = 1.122$ can be used [8, 9], which was obtained in Ref. [22] on the basis of an extensive (almost comprehensive) systematics of the data on the total photoneutron reaction cross-sections;
- on the other hand, while the Saclay data for the (γ,xn) reaction may be used [22] directly (without additional normalization), the Saclay data for the (γ,n) and (γ,2n) reactions cannot be used: they differ significantly (and in a different direction!) from the corresponding Livermore data and must be recalculated using the special relation from Ref. [6].

Unfortunately, in Ref. [6], when determining the values of the special coefficient for determining the proportion of the (γ,n) reaction cross-section which should be attributed to the (γ,2n) reaction cross-section, some inaccuracies occurred, the energy scales were corrected for energy regions where there are already shortcomings in the photoneutron multiplicity determination procedure, some data were used in error and the reaction cross-sections were not analysed for all the nuclei for which data were obtained at Saclay and Livermore.

Thus there is a pressing need for more detailed research and more accurate and comprehensive joint processing of the results of the QMA experiments performed at both laboratories, which is of course the purpose of this paper. A comprehensive system for joint correction of the data on the partial photoneutron reaction cross-sections was produced for all the 12 nuclei from Ref. [6] included in Table 3, and for the seven nuclei ^{51}V, ^{75}As, ^{90}Zr, ^{116}Sn, ^{127}I, ^{232}Th, ^{238}U, i.e. for most of the nuclei for which data of the same type were obtained at both laboratories (Saclay and Livermore).

2. Substantiation of the method for reciprocally harmonizing the absolute values of the QMA partial photoneutron reaction cross-sections obtained at Saclay and Livermore

2.1. Detailed analysis of the relation of the data on the partial photoneutron reaction cross-sections

The relational database created on nuclear reaction cross-sections [13] was used to obtain all the required systematics of the relevant data on the total and partial photoneutron reaction cross-sections for the 19 nuclei which were subsequently used to study the interrelations of the cross-section values for single- and two-neutron reactions obtained at Livermore and Saclay. In order to study and describe the systematic disagreements in the QMA data obtained at Saclay and Livermore more accurately, we analysed them in detail in several stages:

- to check for possible disagreements of the type noted above (Fig. 3) for the ^{75}As nucleus, over the whole energy range studied, we obtained the energy dependences of the ratio

$$R(E) = \sigma_{Saclay}(\gamma,xn)/\sigma_{Livermore}(\gamma,xn) \qquad (4)$$

- based on the systematics (Fig. 2) of the disagreements between the Livermore data and those of other laboratories, all the reaction cross-sections obtained at Livermore were shifted (the procedure was iterative, the coefficient R(E) was calculated each time after both cross-sections to be compared had been transferred to a common scale (Gauss interpolation was used for this)) to the Saclay data by a ΔE value which was such that, in the energy region from the (γ,n) reaction threshold up to the (B(2n)) threshold of the $(\gamma,2n)$ reaction, i.e. in the region where the photoneutron multiplicity is exactly 1, the coefficient R(E) was as close as possible to a constant value;

- after this correction of the energy scales (shifting of the Livermore cross-sections to the Saclay cross-sections):

  - using the data for the (γ,n) reaction, again in the energy region up to the $(\gamma,2n)$ reaction threshold, we determined the coefficient

$$R(n) = \sigma^{int}_{Saclay}(\gamma,n)/\sigma^{int}_{Livermore}(\gamma,n), \qquad (5)$$

which, given the conditions that this is being determined in the energy region up to B(2n), is the same as the coefficient

$$R(xn) = \sigma^{int}_{Saclay}(\gamma,xn)/\sigma^{int}_{Livermore}(\gamma,xn), \quad (6)$$

which is entirely similar to the coefficients used in Refs. [6, 22];

– in the overlapping energy regions, we calculated the coefficient

$$R(2n) = \sigma^{int}_{Saclay}(\gamma,2n)/\sigma^{int}_{Livermore}(\gamma,2n). \quad (7)$$

The coefficients R(n) and R(2n), which were thus obtained more accurately than in Ref. [6], describe the interrelations between the cross-sections of the single- and two-neutron reactions determined at Saclay and Livermore.

The systematics of the values obtained for the coefficients R(n) and R(2n) for all 19 nuclei studied are shown in Fig. 4 and Table 4. They clearly confirm the dramatic situation noted above (Table 3) with respect to the relations between the values for the cross-sections of partial photoneutron reactions with a different photoneutron multiplicity.

The data obtained indicate that, for most of the nuclei studied:

- the values of the coefficient $R(n) = \sigma^{int}_{Saclay}(\gamma,n)/\sigma^{int}_{Livermore}(\gamma,n)$ are appreciably higher than the values of the coefficient $R(2n) = \sigma^{int}_{Saclay}(\gamma,2n)/\sigma^{int}_{Livermore}(\gamma,2n)$, which is in effect a quantitative indication of a direct connection between the systematic disagreements noted above and the procedure for determining the photoneutron multiplicity;
- the R(n) coefficients mostly have values greater than 1 (roughly 10–25% more); overall, this agrees with the systematics (Fig. 2) of the R^{int}_{syst} values, which correspond to them in terms of how they were determined (the other laboratory is Saclay, the integration region is the same — between the thresholds of the (γ,n) and (γ,2n) reactions);
- the values of the R(2n) coefficients are mostly appreciably lower than 1;
- several cases stand out where the data do not fit into the general picture:
  - for the nuclei ^{75}As, ^{127}I and ^{165}Ho R(2n)>1, i.e. the ratios for the two-neutron reaction are in a region which is ‘typical’ for the single-neutron reaction;
  - for the nuclei ^{124}Sn and ^{238}U R(n) < 1, i.e. the ratios for the single-neutron reaction are in a region which is ‘typical’ for the two-neutron reaction; in the case of ^{124}Sn, both coefficients (R(n) and R(2n)), while less than 1, are very close to unity.

The ratios of the integral cross-sections of the relevant reactions given in Table 4, averaged for the data for all 19 nuclei, are <R(n)> = 1.09 and <R(2n)> = 0.8, which agrees on the whole with the data averaged for 12 nuclei in Ref. [6].

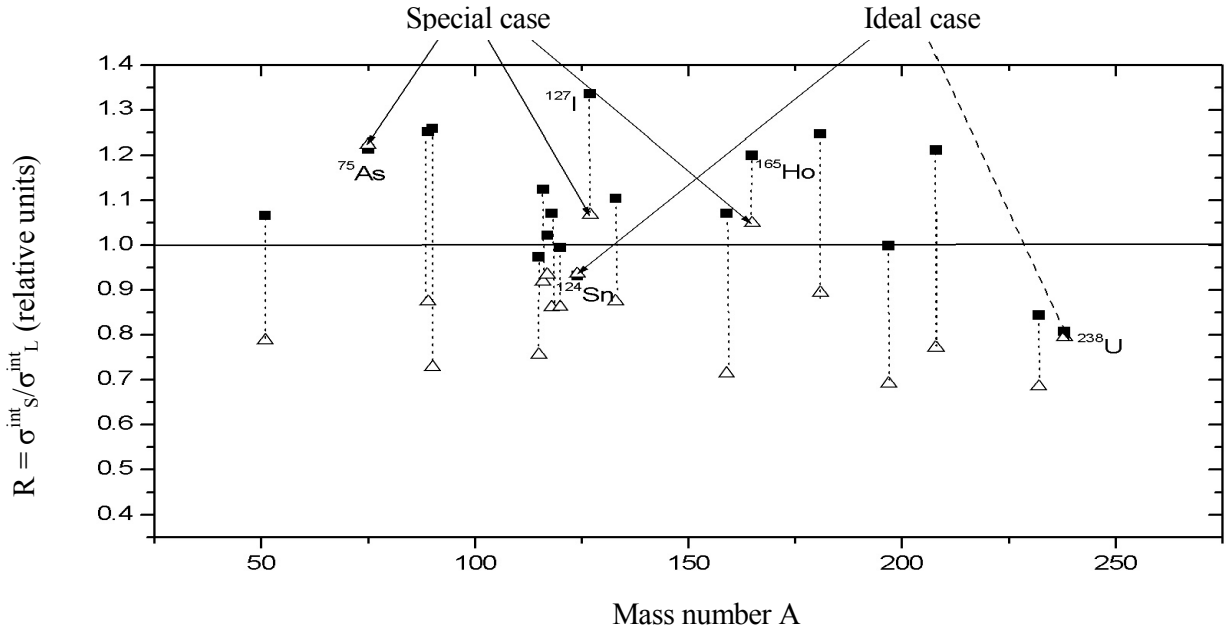

Fig. 4. Systematics of the values (Table 4) of the ratios R(n) = $\sigma^{int}_{Saclay}(\gamma,n)/\sigma^{int}_{Livermore}(\gamma,n)$ (squares) and R(2n) = $\sigma^{int}_{Saclay}(\gamma,2n)/\sigma^{int}_{Livermore}(\gamma,2n)$ (triangles) obtained after appropriate correction of the energy scales to achieve harmonized integration ranges using the data from the experiments performed at Saclay and Livermore.

Table 4

Main data for the comparison of the QMA data obtained at Saclay and Livermore (E^{int}_{min} and E^{int}_{max} are the lower and upper integration limits of the (γ,2n) reaction cross-sections respectively

No.	Nucleus	ΔE shift, MeV	(γ,2n) reaction threshold, MeV	R(n) = $\sigma^{int}_{Saclay}(\gamma,n)/\sigma^{int}_{Livermore}$ (γ,n), relative units	E^{int}_{min}, MeV	E^{int}_{max}, MeV	R(2n) = $\sigma^{int}_{Saclay}(\gamma,2n)/\sigma^{int}_{Livermore}$ (γ,2n), relative units
1	$^{51}_{23}$V	0.2	20.4	[18]/[26] 1.066	20.4	27.78	[18]/[26] 0.788
2	$^{75}_{33}$As	-0.07	18.2	[24]/[25] 1.214	18.2	26.2	[24]/[25] 1.223
3	$^{89}_{39}$Y	-0.08	20.8	[27]/[28] 1.252	21.03	27.02	[27]/[28] 0.874
4	$^{90}_{40}$Zr	-0.2	21.3	[27]/[28] 1.259	21.57	25.93	[27]/[28] 0.728
5	$^{115}_{49}$In	0.1	16.3	[29]/[30] 0.974	16.46	24.05	[29]/[30] 0.756
6	$^{116}_{50}$Sn	-0.1	17.1	[29]/[30] 1.103	17.1	22.12	[29]/[30] 0.919
7	$^{117}_{50}$Sn	-0.04	16.5	[29]/[30] 1.022	16.73	21.06	[29]/[30] 0.934
8	$^{118}_{50}$Sn	-0.4	16.3	[29]/[30] 1.071	16.3	21.57	[29]/[30] 0.861
9	$^{120}_{50}$Sn	-0.2	15.6	[29]/[30] 0.995	15.6	22.39	[29]/[30] 0.862
10	$^{124}_{50}$Sn	0.15	14.4	[29]/[30] 0.932	14.56	21.61	[29]/[30] 0.936
11	$^{127}_{53}$I	-0.2	16.3	[31]/[32] 1.336	16.3	29.54	[31]/[32] 1.067
12	$^{133}_{55}$Cs	-0.05	16.2	[29]/[25] 1.104	16.2	24.16	[29]/[25] 0.875
13	$^{159}_{65}$Tb	-0.3	14.9	[5]/[19] 1.071	14.9	27.99	[5]/[19] 0.714
14	$^{165}_{67}$Ho	-0.05	14.7	[5]/[33] 1.2	14.7	28.48	[5]/[33] 1.049
15	$^{181}_{73}$Ta	-0.5	14.2	[5]/[34] 1.247	14.2	24.58	[5]/[34] 0.894
16	$^{197}_{79}$Au	-0.35	14.7	[35]/[36] 0.999	14.7	24.70	[35]/[36] 0.691
17	$^{208}_{82}$Pb	-0.2	14.1	[35]/[37] 1.212	14.1	26.33	[35]/[37] 0.771
18	$^{232}_{90}$Th	-0.05	11.6	[38]/[39] 0.844	11.6	16.33	[38]/[39] 0.685
19	$^{238}_{92}$U	-0.15	11.3	[38]/[39] 0.762	11.3	18.26	[38]/[39] 0.793

Table 4 also contains the other parameters used in the joint processing of the data: the energy shifts ΔE of the Livermore cross-sections to the Saclay cross-sections, the B(2n) values of the (γ,2n) reaction thresholds, the integration limits of the cross-sections, and references to the relevant source data (the numerical data on the reaction cross-sections for the numerical processing were taken from the collections in the nuclear reaction database created which is described above [13]).

Thus a detailed and accurate analysis of the data for the 19 nuclei (Table 4) confirms the main conclusion of Ref. [6] that there is a line between the disagreements found in the partial photoneutron reaction cross-section data obtained at Saclay and Livermore and the characteristics of the procedures used to determine the photoneutron multiplicity.

2.2. Analysis of the reliability of the procedures for identifying photoneutron reactions with different multiplicities

As Ref. [6] shows that the systematic disagreements in the QMA cross-sections of the (γ,n) and (γ,2n) partial photoneutron reactions obtained at Saclay and Livermore are directly dependent on the correctness of the procedure used to determine the multiplicity of the photoneutrons generated, it would seem useful to look at the main characteristics of both procedures used.

For direct photoneutron registration used at both laboratories, the contribution to the total photoabsorption cross-section of reactions where several neutrons are generated is multiplied by the relevant coefficient — the photoneutron multiplicity. To distinguish between the contributions of the reactions where one, two, three (and more) neutrons are generated, special methods must be used.

The need to distinguish between the contributions of the (γ,n) and (γ,2n) reactions in particular, bearing in mind that the registration efficiency for two particles is equal to the square of the registration efficiency for one, meant that special 4π neutron detectors had to be created which were designed to measure the neutron multiplicity. Highly efficient (40–60%) detectors of the slowing-down type were developed in which the neutrons generated during the short duration of the accelerator gamma-ray pulse were slowed down and detected during the time between the short accelerator pulses. BF_3 counters in the form of long tubes placed in paraffin or polyethylene (Livermore) and a large-volume liquid scintillator enriched with gadolinium (Saclay) were used to detect the slowed-down photoneutrons.

Determining the photoneutron multiplicity using the ring-ratio technique employed at Livermore. In order to distinguish between the contributions of the (γ,n), (γ,2n) and (γ,3n) reactions, a highly effective neutron detector was constructed at Livermore allowing slowed-down neutrons to be recorded at various distances from the target. The BF_3 counters were placed in concentric rings around the target. The ring-ratio technique used is based on measuring the mean neutron energy and exploiting the fact that the ratio of the number of counts in the inner and outer rings of BF_3 counters is a monotonically increasing function of the mean photoneutron energy. The registration efficiency for neutrons of different energies is determined using calibrated neutron sources. Thus, using the ring ratios the mean energies of the neutrons and, hence, the ratios for reaction events involving one and two neutrons can be determined independently and fairly precisely. Thus, using the data on

the registration efficiency for neutrons of different energies, the cross-sections of the partial reactions can be determined fairly accurately for any multiplicity (1, 2, 3).

Precision calibration of the energy dependence of the neutron registration efficiency employed at Saclay. The method developed at Saclay is based on precision calibration of a Gd large-volume liquid scintillator using a ^{252}Cf source. A calibration curve is used to determine the region where the registration efficiency is virtually independent of the neutron energy. Although the dependence of detector efficiency on neutron energy published in Ref. [38] is not in fact a constant in any region, it was stated that (substantial) deviations in the registration efficiency from the required constant only occur for neutrons with an energy of E_n~5 MeV. It was also assumed that the photoneutron energy in the giant resonance region does not exceed E_n~3 MeV. This assumption is not sufficiently well-founded as we know that the spectra of photoneutrons from the (γ,n) and (γ,2n) reactions go on up to energy values of ~10 MeV. It is this that is the cause of some of the errors in determining the absolute values of the cross-sections of these reactions which will be examined specially below when discussing the systematics of the data obtained using the different methods. Moreover, the information published on the methodology indicates that, while the detector efficiency determined using the ^{252}Cf source was close to 1, in the actual experiments the detection system was used under time conditions that resulted in an efficiency of at most only around 0.6.

One obvious and very relevant shortcoming used at Saclay to determine the photoneutron multiplicity, which could be of decisive significance for the disagreements between the data obtained using it and the results obtained at Livermore, is the detector's high background: the high background and a substantially poorer signal/noise ratio than at Livermore complicate the procedure for identifying and eliminating the background, and the introduction of corrections for random coincidences in activation of the counters. All this results in a clear overestimation of the proportion of (γ,n) single-neutron reaction events by comparison with reaction events involving the emission of two (three or more) neutrons.

General conclusions. On the basis of the above, we may conclude that, although the detector efficiency at Livermore is in principle somewhat lower than that at Saclay, the ring-ratio technique used compensates for that shortcoming to a significant extent. Also, as noted above, in the actual experiments the Saclay detector efficiency was significantly lower than the level achievable in principle (according to tests using a neutron source). All this shows that, while there can be no justifiable objections to the neutron multiplicity determination procedure used at Livermore, there are quite a lot as regards the procedure used at Saclay. This being so, the question as to which procedure is incorrect is clearly of particular interest.

In Ref. [6] mentioned above, the QMA data for the nucleus ^{181}Ta obtained at Saclay and Livermore were analysed in conjunction with the results from Refs [39–41] for this nucleus for the reactions (e,Tn), (e,n) and (e,2n). As the nuclei's electro- and photodisintegration cross-sections can be interlinked [40, 41] using virtual photon spectra, the (e,2n) reaction cross-section can be evaluated from the (γ,2n) reaction data. An experimental cross-section for the ^{181}Ta(e,2n) reaction was obtained [39] using the obvious correlation:

$$\sigma(e,2n) = ½(\sigma(e,xn) - \sigma(e,n)), \qquad (8)$$

employing experimentally determined values of σ(e,xn) and σ(e,n). The σ(e,n) cross-section was measured twice: σ_1(e,n) — determining the neutron multiplicity; and σ_2(e,n) — using the induced activity method (decay of the nucleus ^{180}Ta → ^{180}Hf, 93.3 keV, Ge-Li detector). A value of $\langle\sigma_1(e,n)/\sigma_2(e,n)\rangle = 1.057 \pm 0.023$ was obtained for the weighted mean ratio of the measured cross-sections. The closeness of this ratio to 1 shows the reliability of the photoneutron multiplicity determination procedure used. The σ(e,2n) cross-section in expression (8) was also shown to be consistent with the data recalculated from the Livermore (γ,2n) reaction data, but not with the corresponding Saclay data: the Saclay data for the (γ,2n) reaction cross-sections are too low, while the (γ,n) reaction cross-section data are too high.

The reciprocal correction method mentioned above for the (γ,2n) reaction cross-section data was proposed in order to eliminate these disagreements and bring the data obtained in both laboratories in line with one another.

2.3. Reciprocal correction method for the data on the total and partial photoneutron reaction cross-sections

As indicated above, the data on the partial photoneutron reaction cross-sections obtained for identical reactions using almost identical facilities, which nevertheless differ dramatically from each other owing to the different photoneutron multiplicity determination procedures used (Table 4), must be specially harmonized.

To do this, we need a method for determining the 'surplus' contributions to the cross-sections of reactions with a multiplicity of 1 and for returning them to the cross-sections of reactions with a multiplicity of 2. A reciprocal correction method of this kind for the cross-sections of the (γ,2n) partial photonuclear reactions obtained using QMA photon beams at Livermore and Saclay was proposed in Ref. [6]. We have developed this method and extended it to reciprocally correct the cross-sections of the other partial reaction (γ,n) and (in some special cases) the cross-sections of the total photoneutron reaction (γ,xn) as well.

Taking into account what has been stated above, the reciprocal correction method for the Saclay and Livermore data is essentially as follows:

- after appropriate correction of the energy scales of the cross-sections to be compared using data on the cross-sections of the (γ,xn) reaction (shift of the cross-sections obtained at Livermore by ΔE to the Saclay data), the coefficient $R = R(xn) = \sigma^{int}_{Saclay}(\gamma,xn)/\sigma^{int}_{Livermore}(\gamma,xn)$ in expression (6) is determined which, in fact, coincides with the coefficient R(n) in expression (5) and normalizes the cross-sections of the total photoneutron reaction to one another in the energy region up to B(2n);
- since (γ,xn) = (γ,n) + 2(γ,2n), the coefficient R can be used to obtain a correlation which is used to return — as discussed — part of the cross-section of the (γ,n) reaction obtained at Saclay to the new (corrected) (γ,2n) reaction cross-section:

$$R = \sigma^{xn}_S/\sigma^{xn}_L = (\sigma^{n}_S + 2\sigma^{2n}_S)/(\sigma^{n}_L + 2\sigma^{2n}_L), \quad (9)$$

$$\sigma^{xn}_S = (\sigma^{n}_S + 2\sigma^{2n}_S) = R\sigma^{xn}_L = R(\sigma^{n}_L + 2\sigma^{2n}_L) \quad (10)$$

and, thus,

$$R\sigma^{2n}{}_L = \sigma^{2n}{}_S{}^* = \sigma^{2n}{}_S + 1/2(\sigma^{n}{}_S - R\sigma^{n}{}_L). \quad (11)$$

The right-hand side of expression (11) (the main correlation in the method for correcting the (γ,2n) reaction cross-section data obtained at Saclay) has the same meaning as discussed above: part of the (γ,n) reaction cross-section ($1/2(\sigma^{n}{}_S - R\sigma^{n}{}_L)$), determined taking into account the coefficient R and using the data on the (γ,xn) reaction cross-sections, is added to the (γ,2n) reaction cross-section value determined at Saclay $\sigma^{2n}{}_S$. Here it is important to note that, if the disagreement between the Livermore and Saclay data is caused only by the Saclay photoneutron multiplicity error, the left-hand side of expression (11) should also apply: the recalculated Saclay cross-section $\sigma^{2n}{}_S{}^*$ should agree with the Livermore cross-section $\sigma^{2n}{}_L$, multiplied by the coefficient R = R(xn) in expression (6).

3. Joint evaluation (correction) of the data on the partial photoneutron reaction cross-sections obtained at Saclay and Livermore

Based on the data in Fig. 4 and Table 4, we pointed out above that all the cases studied can be divided essentially into 3 groups:

- Group 1 — the 'standard situation' — comprises 13 nuclei (^{51}V, ^{89}Y, ^{115}In, $^{116, 117, 118, 120}$Sn, ^{133}Cs, ^{159}Tb, ^{181}Ta, ^{197}Au, ^{208}Pb and ^{232}Th) for which a 'standard' reciprocally inverse correlation is observed between the (γ,n) and (γ,2n) reaction cross-section values: the coefficients R(n) in expression (5) have values greater than 1 and the coefficients R(2n) in expression (7) have values less than 1;
- Group 2 — 'special cases' — comprise 4 nuclei for which the ratios of the (γ,n) and (γ,2n) reaction cross-section values are different (R(2n) > 1): ^{75}As, ^{127}I and ^{165}Ho, and also ^{90}Zr ('non-standard' ratio of (γ, xn) reaction cross-sections);
- Two nuclei, ^{124}Sn and ^{238}U, which also essentially belong to the 'special cases', can be allocated to group 3, since for both the correlation R(n) ≈ R (2n) holds; the case of ^{124}Sn ((R(n) ≈ R(2n) ≈ 1) can to some extent be viewed as 'ideal', i.e., not requiring application of the correction.

It would seem sensible to examine these three groups of nuclei separately.

Above, the assumption was put forward that, for one of the nuclei from group 2 — ^{75}As, the 'unusually' large (γ,2n) reaction cross-section value could be caused (Fig. 4) by certain additional errors in the cross-section of the total photoneutron reaction (γ,xn). In this connection, it is useful for all four nuclei in group 2 to look closely at the correlations of the (γ,xn) reaction cross-sections.

The results obtained for all 19 nuclei examined are shown in the figures and in the tables sorted by Z and A.

Cross-sections of the (γ,2n) reaction

3.1.1. 'Standard situation'

As stated above, the data for all nuclei in groups 1 and 3 was processed using the method described in Section 2.3. The data processing for the nuclei in these groups involved several stages.

Analysis of the R(xn) ratios. The aim of analysing the energy dependence of the ratio of the (γ,xn) reaction cross-sections ($R(xn) = \sigma^{int}_{Saclay}(\gamma,xn)/\sigma^{int}_{Livermore}(\gamma,xn)$ — expression (6)) is to obtain confirmation that, over the whole energy region studied, the results measured directly in the experiment at both laboratories differ only in the normalization. The results (Figs 5a, 7a-14a, 16a, 17a, 19a-23a) for all nuclei in groups 1 and 3 do confirm this: in all cases the correlation $R(xn) \approx R(n) \approx$ const holds. Furthermore, the actual values of a specific coefficient R agree on the whole fairly well with the data of the corresponding full systematics (Fig. 2). Thus, the data obtained confirm the recommendation in [8, 9] for bringing the Livermore total photoneutron reaction cross-section data into line with the data of other laboratories: multiplication by the coefficient $r = R^{int}_{syst} = \sigma^{int}_{various\ laboratories}(\gamma,xn)/\sigma^{int}_{Livermore}(\gamma,xn)$, the mean value for which determined in Ref. [22] using the full systematics (Fig. 8), is $\langle R^{int}_{syst} \rangle = 1.122$. However, based on a detailed analysis of the specific situation for each nucleus studied, we propose more accurate values for the coefficient R (Fig. 4 and Table 4).

Recalculation of the Saclay data for the (γ,2n) reaction. Since Saclay and Livermore data on the cross-sections of the total photoneutron (γ,xn) reaction do in fact differ over the whole energy region studied only in the normalization, as stated above the data on the (γ,2n) reaction cross-sections obtained at Saclay must be corrected. The method proposed in Ref. [6] is used to correct them: expression (11) is used to calculate the proportion of the (γ,2n) reaction cross-sections obtained at Saclay which, owing to the error in the photoneutron multiplicity determination procedure, was mistakenly attributed to the (γ,n) reaction and should therefore be 'returned' to the (γ,2n) reaction cross-section. The evaluated (corrected) Saclay data $\sigma_S^*(\gamma,2n)$ for all 16 nuclei in groups 1 and 3 are shown (points with error margins) in Figs 5c, 7c-12c and 16c-23c. For the purposes of comparison, each figure also gives the original Saclay data ($\sigma_S(\gamma,2n)$ — continuous line) and the evaluated (corrected) Livermore data $R\sigma_L(\gamma,2n)$. These data clearly show that the evaluated data agree well with each other. Mathematical confirmation of the effectiveness of the method used to harmonize the data is presented in Table 6, which gives the integral cross-section values calculated for coinciding integration limits and corresponding data before and after correction.

3.1.2. 'Special cases'

As noted above, the nuclei ^{75}As, ^{90}Zr, ^{127}I and ^{165}Ho must be examined separately.

^{75}As. For this nucleus the coefficients R(n) in expression (5) and R(2n) in expression (7) have the values 1.214 and 1.222 (Table 4) respectively, i.e., — and this is very important — they are both in the range of values characteristic for values of the coefficient R(n) for nuclei in the main group. The 'normal' value of the coefficient R(n) and the 'abnormally high' value of the coefficient R(2n) in this instance indicate that the (γ,xn) reaction cross-sections have a

'normal' relation to each other only in the energy region up to the B(2n) threshold of the (γ,2n) reaction. However, in the higher energy region, the Saclay cross-section 'abnormally' exceeds the Livermore cross-section. Since this 'abnormally' large contribution cannot be attributed to anything other than the (γ,2n) reaction cross-section we must conclude that the Saclay cross-section for this reaction 'abnormally' exceeds the Livermore cross-section. The energy dependence of the coefficient R(E) in expression (4), which is given for ^{75}As in Fig. 6b demonstrates precisely this: the relations between Saclay and Livermore data on the total photoneutron reaction cross-sections for this nucleus differ substantially in the energy regions below and above the B(2n) threshold of the (γ,2n) reaction: while the ratio in expression (4) is approximately constant in the lower energy region, in the energy region higher than B(2n) the $\sigma_S(\gamma,xn)$ reaction cross-section increases substantially (Fig. 6b) compared with $\sigma_L(\gamma,xn)$. As was noted in section 1.3 above, in the case of ^{75}As, the closeness of the energy where the additional disagreement occurs to the B(2n) value of the ^{75}As(γ,2n)^{73}As reaction threshold, and the closeness of the contribution of the additional amount by which the Saclay cross-section exceeds the Livermore cross-section to the ^{75}As(γ,2n)^{73}As reaction cross-section suggests that these disagreements might also be connected in some way with the processes for registering neutrons with a multiplicity other from one, i.e. the products of the (γ,2n) reaction in particular. It is clear that the approach described above should, in this special case, include a further stage for correction of the original (γ,xn) reaction cross-sections, i.e. replacement of values of the coefficient in expression (11) by the energy dependence R/R(E). The results of using the same reciprocal cross-section correction method in this way for both the total, and both partial photoneutron reactions for ^{75}As are shown in Figs 6a, c and d respectively, and in Table 5.

Table 5

Integral cross-section values of the reciprocally corrected (γ,xn), (γ,n) and (γ,2n) reaction cross-sections for coinciding integration limits

No.	Nucleus	σ^{int}_S, (Saclay)			σ^{int}_L, (Livermore)		
		Reactions					
		(γ,xn)	(γ,n)	(γ,2n)	(γ,2n)	(γ,n)	(γ,xn)
1	^{51}V	643 ± 2	469 ± 3	104 ± 3	106 ± 2	469 ± 3	639 ± 4
2	^{75}As	1248 ± 6	809 ± 2	242 ± 3	239 ± 2	808 ± 2	1188 ± 3
3	^{89}Y	1428 ± 3	1205 ± 3	113 ± 3	107 ± 1	1206 ± 3	1416 ± 6
4	^{90}Zr	1371 ± 3	1128± 2	92 ± 2	88 ± 1	1211 ± 2	1454 ± 4
5	^{115}In	1857 ± 3	1298 ± 3	365 ± 3	358 ± 1	1298 ± 3	1865 ± 4
6	^{116}Sn	1661 ± 3	1359 ± 4	234 ± 4	238 ± 1	1359 ± 5	1706 ± 5
7	^{117}Sn	1688 ± 4	1262 ± 2	234 ± 3	244 ± 1	1261 ± 2	1719 ± 3
8	^{118}Sn	1820 ± 3	1281 ± 2	299 ± 2	320 ± 1	1281 ± 2	1878 ± 2
9	^{120}Sn	2123 ± 3	1283 ± 2	444 ± 2	460 ± 1	1282 ± 2	2161 ± 2
10	^{124}Sn	1991 ± 4	1043 ± 3	511 ± 4	503 ± 1	1042 ± 3	1962 ± 4
11	^{127}I	2363 ± 6	1568 ± 6	342 ± 7	347 ± 2	1568 ± 5	2585 ± 10
12	^{133}Cs	2464 ± 3	1620 ± 3	432 ± 3	414 ± 2	1618 ± 4	2444 ± 9
13	^{159}Tb	3157 ± 16	1485 ± 10	634 ± 7	676 ± 3	1485 ± 10	3380 ± 19
14	^{165}Ho	3663 ± 12	1954 ± 5	848 ± 7	839 ± 3	1954 ± 5	3714 ± 8
15	^{181}Ta	3599 ± 13	1616 ± 6	520 ± 7	560 ± 6	1616 ± 7	3704 ± 33
16	^{197}Au	3548 ± 7	2145 ± 7	367 ± 7	345 ± 3	2142 ± 9	3549 ± 22
17	^{208}Pb	3257 ± 5	2275 ± 12	611 ± 16	626 ± 6	2274 ± 12	3161 ± 12
18	^{232}Th	3668 ± 20	1309 ± 7	908 ± 10	969 ± 2	1305 ± 4	3902 ± 6
19	^{238}U	4614 ± 31	863 ± 3	966 ± 6	855 ± 3	855 ± 3	5481 ± 9

^{90}Zr. The pronounced maximum (Fig. 8) in the ratio R(E) makes the situation for this nucleus analogous, to some extent, to that for ^{75}As.

^{127}I. From the point of view of the proposed correction method, this case is entirely analogous to the previous one, the only difference being that, unlike ^{75}As, in the energy region above the B(2n) threshold of the (γ,2n) reaction the $\sigma_S(\gamma,xn)$ reaction cross-section decreases substantially (Fig. 15b) compared with $\sigma_L(\gamma,xn)$.

The results of using the same reciprocal cross-section correction method for both the total, and both partial photoneutron reactions for ^{127}I are shown in Figs 15a, 15c and 15d respectively. The corresponding quantitative characteristics of the procedure for correcting the photoneutron reaction data for this special case are also given in Table 5.

^{165}Ho. From the point of view of the proposed correction method, this case is entirely analogous with the preceding one (Fig. 18b).

The results of using the same reciprocal cross-section correction method for both the total, and both partial photoneutron reactions for ^{165}Ho are shown in Figs 18a, 18c and 18d respectively.

The corresponding characteristics of the procedure for correcting the photoneutron reaction data for this special case are also given in Table 5.

^{124}Sn and ^{238}U. The reason why ^{124}Sn and ^{238}U are allocated to special group 3 is that for them the coefficients R(n) from expression (5) and R(2n) from expression (7) have very similar values (0.939 and 0.919, and 0.765 and 0.793 respectively). This indicates that, for some reason in the case of ^{124}Sn and ^{238}U, unlike all 17 cases examined above, the normalization of the data at Livermore is close to the normalization of the data at Saclay, and the sorting of data by multiplicity was carried out at Saclay correctly.

A possible reason for this could be the photoneutron energy spectrum shape which allows correct sorting by multiplicity and at a relatively low detector efficiency. Moreover, in the case of ^{124}Sn, both the coefficient R(n) from expression (5) and coefficient R(2n) from expression (7) are very close to 1. As stated above, the correlations R(n) $\approx$ (R(2n) $\approx$ 1 make the case of ^{124}Sn generally close to the 'ideal': processing using the method described should result in noticeable correction of data. The corresponding data in Figs 14 and 23 and Table 5 fully confirm the suggested interpretation, demonstrating the internal consistency of the approach used.

Thus, the data given in Tables 4 and 5, Figs 5c, 7c-14c, 16c, 17c and 19c-23c ('standard situation') and Figs 6d, 15d and 18d ('special cases') refine and substantially supplement the results of Ref. [6] for the 12 nuclei studied therein (Table 3). They all show that, by taking into account the inaccuracies in the procedure for determining the photoneutron multiplicity at Saclay, the data on the (γ,2n) reaction can be corrected and brought into line with the Livermore data.

3.2. Cross-sections of the (γ,n) reaction

Since the reciprocal correction method used involves, essentially, returning to the (γ,2n) reaction cross-section the part mistakenly attributed to the (γ,n) reaction cross-section, in addition to what was done in Ref. [6] the (γ,n) reaction cross-sections obtained at Saclay can also be corrected. To do this, the part mistakenly attributed to the (γ,n) reaction cross-section must be removed from it and transferred using expression (11) to the (γ,2n) reaction cross-section.

The corrected (γ,n) reaction cross-section should, based on expression (11), take the following form:

$$R\sigma^{n}_{L} = \sigma^{n}_{S}{}^{*} = \sigma^{n}_{S} - (\sigma^{n}_{S} - R\sigma^{n}_{L}), \qquad (12)$$

where the difference $(\sigma^{n}_{S} - R\sigma^{n}_{L})$ is calculated in the energy region above B(2n).

The corrected Saclay data (σ_S*(γ,n)) and the original cross-sections for all 19 nuclei studied are shown in Figs 5b, 7b-14b, 16b, 17b and 19b-23b ('standard situation') and Figs 6c, 15c and 18c ('special cases'). For the purposes of comparison, for the 'standard situation' each figure also gives the original Saclay data (σ_S(γ,n)) and the Livermore evaluated data ($R\sigma_L$(γ,n)). We can see clearly that the evaluated data agree well with each other, which is confirmed by the data in Table 5 on the integral cross-sections of the reciprocally corrected (γ,xn), (γ,n) and (γ,2n) reaction cross-sections obtained at Saclay and Livermore for coinciding integration limits.

It should be noted in particular that, in the cases of ^{118,120}Sn, ^{181}Ta, ^{197}Au and ^{208}Pb (Figs 12, 13, 19-21), the correction of the energy scales (shift by ΔE) resulted in appreciable disgreements in the region of the B(2n) threshold and, consequently, discontinuities in the corrected cross-sections. In these cases the corrected cross-sections cannot be used as evaluated cross-sections.

A clear picture of the results of applying the reciprocal data correction method is given in Table 6, which partly repeats the data from Table 3. It clearly shows that, instead of the reciprocally inverse significant mismatch of the original cross-sections of the (γ,n) and (γ,2n) reactions, and the (γ,xn) reactions, the corrected Saclay and Livermore data agree well with each other within the limits of error. The 'after' ratios for the seven nuclei studied in addition — ^{51}V, ^{75}As, ^{90}Zr, ^{116}Sn, ^{127}I, ^{232}Th, ^{238}U — are just as close to 1.

3.3. Cross-sections of the (γ,xn) reaction

The (γ,xn) reaction cross-sections obtained at Saclay for the nuclei in group 2 ('special cases') ^{75}As, ^{127}I and ^{165}Ho, corrected in the manner described above, are shown in Figs 6a, 15a and 18a, and their integral cross-sections for coinciding integration limits are also given in Table 5.

The integral cross-sections calculated for all the (γ,xn), (γ,n) and (γ,2n) reaction cross-sections evaluated in this paper for all 19 nuclei studied are given in Table 7.

Table 6

Integral cross-sections of the (γ,n) and (γ,2n) partial photoneutron reactions obtained at Saclay and Livermore, before (data from Ref. [6]) and after reciprocal correction

Nucleus	$\sigma^{int}_S(\gamma,n)/\sigma^{int}_L(\gamma,n)$, both — MeV·mb		$\sigma^{int}_S(\gamma,2n)/\sigma^{int}_L(\gamma,2n)$, both — MeV·mb	
	Before [6]	After	Before [6]	After
^{89}Y	1279/960 = 1.33	1205.3/1206.1 = 1.00	74/99 = 0.75	112.6/107.3 = 1.05
^{115}In	1470/1354 = 1.09	1298.0/1298.2 = 1.00	278/508 = 0.55	364.6/358.3 = 1.02
^{117}Sn	1334/1380 = 0.97	1261.6/1261.4 = 1.00	220/476 = 0.46	234.1/243.6 = 0.96
^{118}Sn	1377/1302 = 1.06	1281.3/1281.4 = 1.00	258/531 = 0.49	298.9/320.4 = 0.93
^{120}Sn	1371/1389 = 0.99	1282.7/1282.6 = 1.00	399/673 = 0.59	444.5/460.2 = 0.97
^{124}Sn	1056/1285 = 0.82	1042.5/1042.4 = 1.00	502/670 = 0.75	511.5/502.6 = 1.02
^{133}Cs	1828/1475 = 1.24	1619.5/1618.5 = 1.00	328/503 = 0.65	431.8/413.7 = 1.04
^{159}Tb	1936/1413 = 1.37	1485.3/1485.4 = 1.00	605/887 = 0.68	633.9/675.7 = 0.94
^{165}Ho	2090/1735 = 1.20	2040.7/2040.7 = 1.00	766/744 = 1.03	825.6/803.4 = 1.03
^{181}Ta	2180/1300 = 1.68	1616.4/1615.7 = 1.00	790/881 = 0.90	520.1/559.9 = 0.93
^{197}Au	2588/2190 = 1.18	2144.6/2142.4 = 1.00	479/777 = 0.62	367.0/345.0 = 1.06
^{208}Pb	2731/1776 = 1.54	2274.5/2273.8 = 1.00	328/860 = 0.38	611.0/626.0 = 0.98

Table 7

Integral cross-sections calculated for the evaluated (reciprocally corrected) photoneutron reaction cross-sections obtained at Saclay and Livermore (by the (γ,n) reaction we in fact mean the (γ,n) + (γ,np) reactions)

No.	Nucleus	Reaction	Threshold, MeV	Laboratory	E^{int}_{min}, MeV	E^{int}_{max}, MeV	σ^{int} MeV·mb	$\Delta\sigma^{int}$, MeV·mb
1	^{51}V	(γ,xn)		S	13.21	27.84	678.4	2.3
				L	10.26	27.78	693.9	4.4
		(γ,n)	11.3	S	13.21	27.78	468.8	3.0
				L	10.26	27.78	480.3	3.2
		(γ,2n)	20.4	S	20.4	27.84	104.4	3.1
				L	20.4	28.78	105.7	1.8
2	^{75}As	(γ,xn)		S	9.92	26.18	1312.9	6.0
				L	10.03	29.54	1377.1	5.2
		(γ,n)	10.2	S	9.92	26.18	809.2	2.0
				L	10.03	29.54	834.8	2.2
		(γ,2n)	18.2	S	18.2	26.18	242.2	3.0
				L	18.2	29.54	301.4	3.0
3	^{89}Y	(γ,xn)		S	10.95	27.02	1429.0	3.1
				L	11.27	27.99	1451.4	6.1
		(γ,n)	11.5	S	10.95	27.02	1206.7	3.5
				L	11.27	28.1	1205.6	4.2
		(γ,2n)	20.8	S	20.8	27.02	112.6	3.1
				L	20.8	27.99	124.6	1.4
4	^{90}Zr	(γ,xn)		S	12.17	25.93	1306.3	2.0
				L	12.12	27.60	1466.4	4.2
		(γ,n)	12.0	S	12.17	25.93	1127.7	1.9
				L	12.12	27.60	1213.6	2.4
		(γ,2n)	21.3	S	21.57	25.93	91.7	1.8
				L	21.57	27.60	125.7	1.5
5	^{115}In	(γ,xn)		S	8.87	24.05	2025.4	3.3
				L	9.10	31.09	2347.1	10.1
		(γ,n)	9.0	S	8.87	24.05	1321.2	5.5
				L	9.10	31.09	1320.6	5.5
		(γ,2n)	16.3	S	16.46	24.05	364.6	3.1
				L	16.3	31.09	493.6	3.5
6	^{116}Sn	(γ,xn)		S	9.45	22.12	1834.5	3.0
				L	9.63	29.61	2345.2	10.2
		(γ,n)	9.6	S	9.45	22.12	1361.7	4.3
				L	9.63	29.61	1417.9	10.7
		(γ,2n)	17.1	S	17.1	22.12	234.1	3.7
				L	17.1	29.61	462.3	3.0
7	^{117}Sn	(γ,xn)		S	8.87	21.06	3022.2	4.3
				L	9.72	31.09	2462.4	12.3
		(γ,n)	6.9	S	8.87	21.06	1283.9	2.2
				L	9.72	31.09	1379.9	6.4
		(γ,2n)	16.5	S	16.73	21.06	232.8	2.7
				L	16.5	31.09	484.6	4.6
8	^{118}Sn	(γ,xn)		S	10.13	21.57	1896.5	3.1
				L	9.1	30.78	2606.5	11.3
		(γ,n)	9.3	S	Difficulty in evaluating data			
				L	9.3	30.78	1404.4	5.5

No.	Nucleus	Reaction	Threshold, MeV	Laboratory	E^{int}_{min}, MeV	E^{int}_{max}, MeV	σ^{int} MeV·mb	$\Delta\sigma^{int}$, MeV·mb
		(γ,2n)	16.3	S	16.3	21.57	298.9	2.2
				L	16.3	30.78	557.4	4.2
9	^{120}Sn	(γ,xn)		S	9.04	22.39	2174.3	3.4
				L	8.94	29.85	2772.4	6.7
		(γ,n)	9.1	S	Difficulty in evaluating data			
				L	9.10	29.85	1372.5	3.7
		(γ,2n)	15.6	S	15.60	22.39	444.5	2.5
				L	15.60	29.85	668.8	2.7
10	^{124}Sn	(γ,xn)		S	9.41	21.61	2053.3	4.5
				L	8.48	31.09	2606.0	11.7
		(γ,n)	8.5	S	9.41	21.61	1043.7	2.9
				L	8.50	31.09	1210.9	6.1
		(γ,2n)	14.4	S	14.56	21.61	506.8	3.8
				L	14.40	31.09	621.2	4.3
11	^{127}I	(γ,xn)		S	8.89	24.89	2387.2	6.3
				L	8.79	29.54	2905.9	17.5
		(γ,n)	9.1	S	9.1	22.49	1562.6	5.5
				L	9.1	29.54	1763.4	11.5
		(γ,2n)	16.3	S	16.3	31.2	359.8	19.1
				L	16.3	29.54	479.1	5.8
12	^{133}Cs	(γ,xn)		S	9.18	24.16	2474.4	2.6
				L	9.1	29.54	2465.0	8.9
		(γ,n)	9.0	S	9.18	24.16	1619.5	3.3
				L	9.1	29.54	1623.8	6.4
		(γ,2n)	16.2	S	16.2	24.16	431.8	2.7
				L	16.2	29.54	556.0	3.8
13	^{159}Tb	(γ,xn)		S	7.8	27.39	3192.2	16.5
				L	8.63	27.99	3421.4	21.4
		(γ,n)	8.1	S	8.1	26.03	1497.2	9.9
				L	8.63	26.13	1482.6	10.2
		(γ,2n)	14.9	S	14.9	28.48	867.4	13.6
				L	14.9	27.99	960.1	5.5
14	^{165}Ho	(γ,xn)		S	7.26	26.84	3669.3	12.3
				L	8.17	28.92	4038.9	10.4
		(γ,n)	8.0	S	8.0	26.84	2044.8	5.2
				L	8.17	28.92	2040.7	5.0
		(γ,2n)	14.7	S	14.7	28.48	812.3	8.5
				L	14.7	28.92	811.0	3.5
15	^{181}Ta	(γ,xn)		S	7.26	25.21	3803.5	15.0
				L	8.17	24.58	3832.3	34.9
		(γ,n)	7.6	S	Difficulty in evaluating data			
				L	8.17	17.46	1615.7	6.8
		(γ,2n)	14.2	S	14.2	26.57	1092.5	16.7
				L	14.2	24.58	1084.7	13.0
16	^{197}Au	(γ,xn)		S	8.08	21.68	3558.8	6.7
				L	8.72	24.70	3765.8	28.1
		(γ,n)	8.1	S	Difficulty in evaluating data			
				L	8.72	17.94	2142.5	9.0
		(γ,2n)	14.7	S	14.7	27.12	952.6	19.6
				L	14.7	24.7	774.0	9.2
		(γ,xn)		S	7.5	20.8	3643.6	6.3
				L	8.48	26.44	4310.1	33.1
			7.4	S	Difficulty in evaluating data			

No.	Nucleus	Reaction	Threshold, MeV	Laboratory	E^{int}_{min}, MeV	E^{int}_{max}, MeV	σ^{int} MeV·mb	$\Delta\sigma^{int}$, MeV·mb
17	^{208}Pb	(γ,n)		L	8.48	26.44	2441.3	23.1
		(γ,2n)	14.1	S	14.1	20.85	660.7	12.8
				L	14.1	26.44	1055.0	12.7
18	^{232}Th	(γ,xn)		S	9.28	16.33	3902.1	6.3
				L	5.27	18.26	4763.0	9.0
		(γ,n)	6.4	S	9.28	16.33	1275.6	6.3
				L	6.4	18.26	1431.9	3.9
		(γ,2n)	11.6	S	11.6	16.33	908.4	10
				L	11.6	18.26	1210.7	2.1
19	^{238}U	(γ,xn)		S	7.8	18.30	4812.8	31.8
				L	5.27	18.26	5748.5	9.2
		(γ,n)	6.2	S	7.8	18.26	1009.8	3.7
				L	6.2	18.26	1047.3	3.2
		(γ,2n)	11.3	S	11.3	18.35	971.6	6.3
				L	11.3	18.26	854.8	2.4

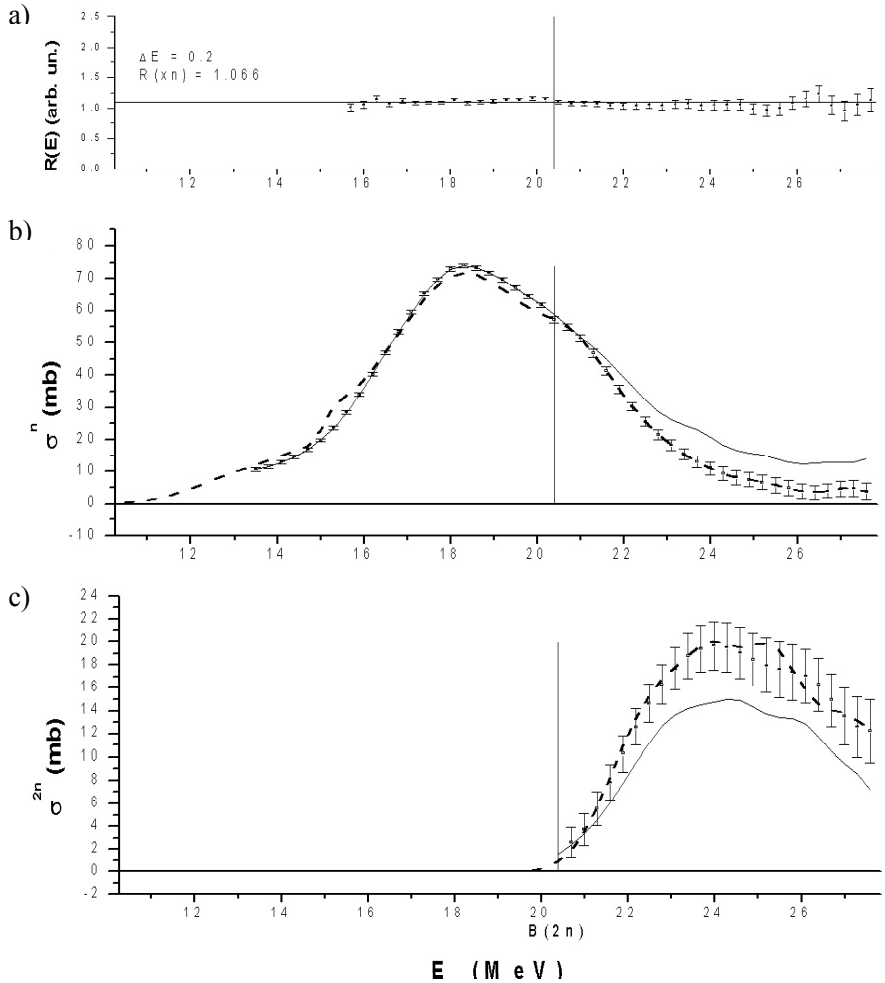

Fig. 5. Results of the reciprocal correction ('standard situation') of the total and partial photoneutron reaction cross-sections obtained at Saclay and Livermore for ^{51}V:

a) R(E) ratios for the (γ,xn) reaction cross-sections; ΔE and R(xn) values are given;

b) Data for the (γ,n) reaction cross-sections:
- Continuous line — original Saclay data σ^{n}_{S};
- Points with error margins — **evaluated** Saclay data (12) σ^{n}_{S}*;
- Dotted line — **evaluated** Livermore data $R\sigma^{n}_{L}$;

c) Data for the (γ,2n) reaction cross-sections:
- Continuous line — original Saclay data σ^{2n}_{S};
- Points with error margins — **evaluated** Saclay data ((9) – (11)) σ^{2n}_{S}*;
- Dotted line — **evaluated** Livermore data $R\sigma^{2n}_{L}$.

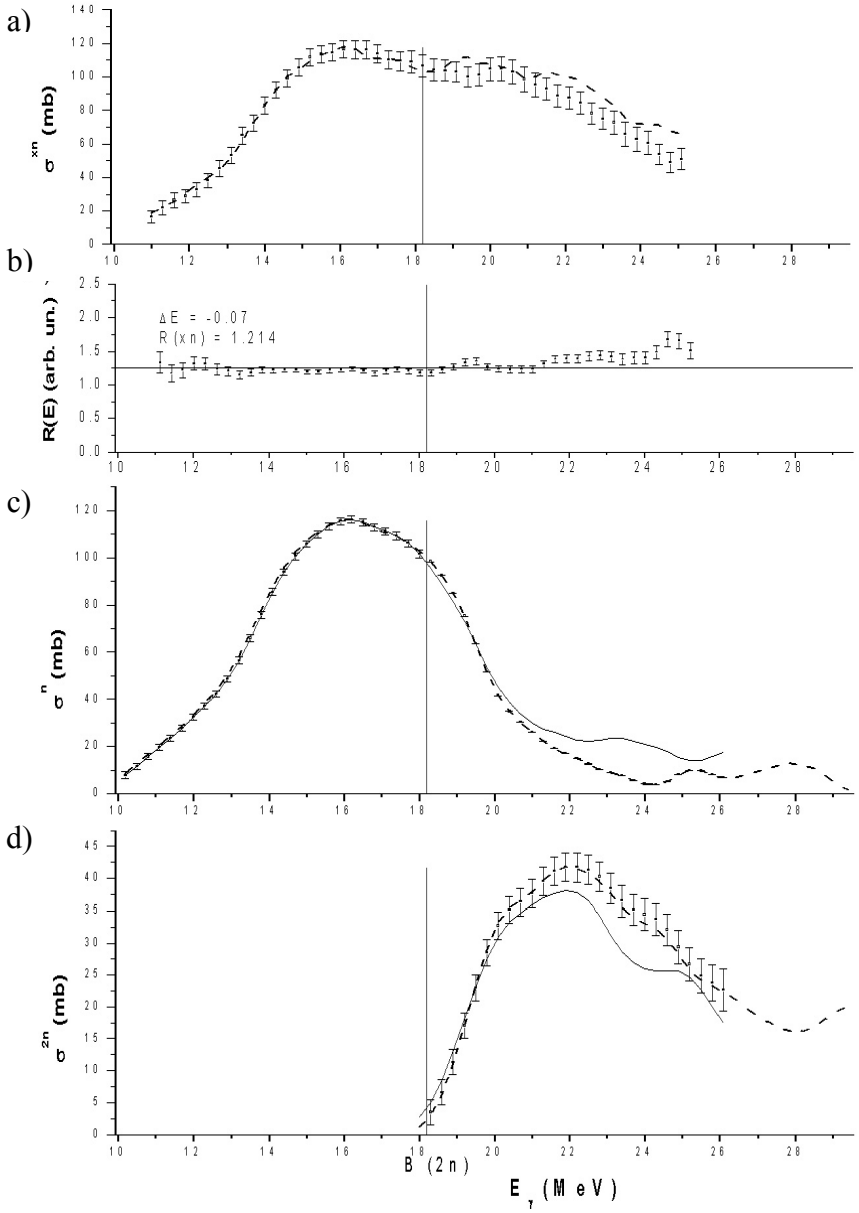

Fig. 6. Results of the reciprocal correction ('special case') of the reaction cross-sections obtained at Saclay and Livermore for ^{75}As:

a) Saclay (γ,xn) reaction cross-section data (dotted line — original $\sigma^{xn}{}_S$; points with error margins — corrected $\sigma^{xn}{}_S^* = \sigma^{xn}{}_S\, R/R(E)$);

b) R(E) ratios for the (γ,xn) reaction cross-sections: ΔE and R(xn) values given;

c) Data for the (γ,n) reaction cross-sections: continuous line — original Saclay data $\sigma^{n}{}_S$; points with error margins — **evaluated** Saclay (12) data $\sigma^{n}{}_S^*$; dotted line — **evaluated** Livermore data $R\sigma^{n}{}_L$;

d) Data for the (γ,2n) reaction cross-sections: continuous line — original Saclay data $\sigma^{2n}{}_S$; points with error margins — **evaluated** ((9) – (11)) Saclay data $\sigma^{2n}{}_S^*$; dotted line — **evaluated** Livermore data $R\sigma^{2n}{}_L$.

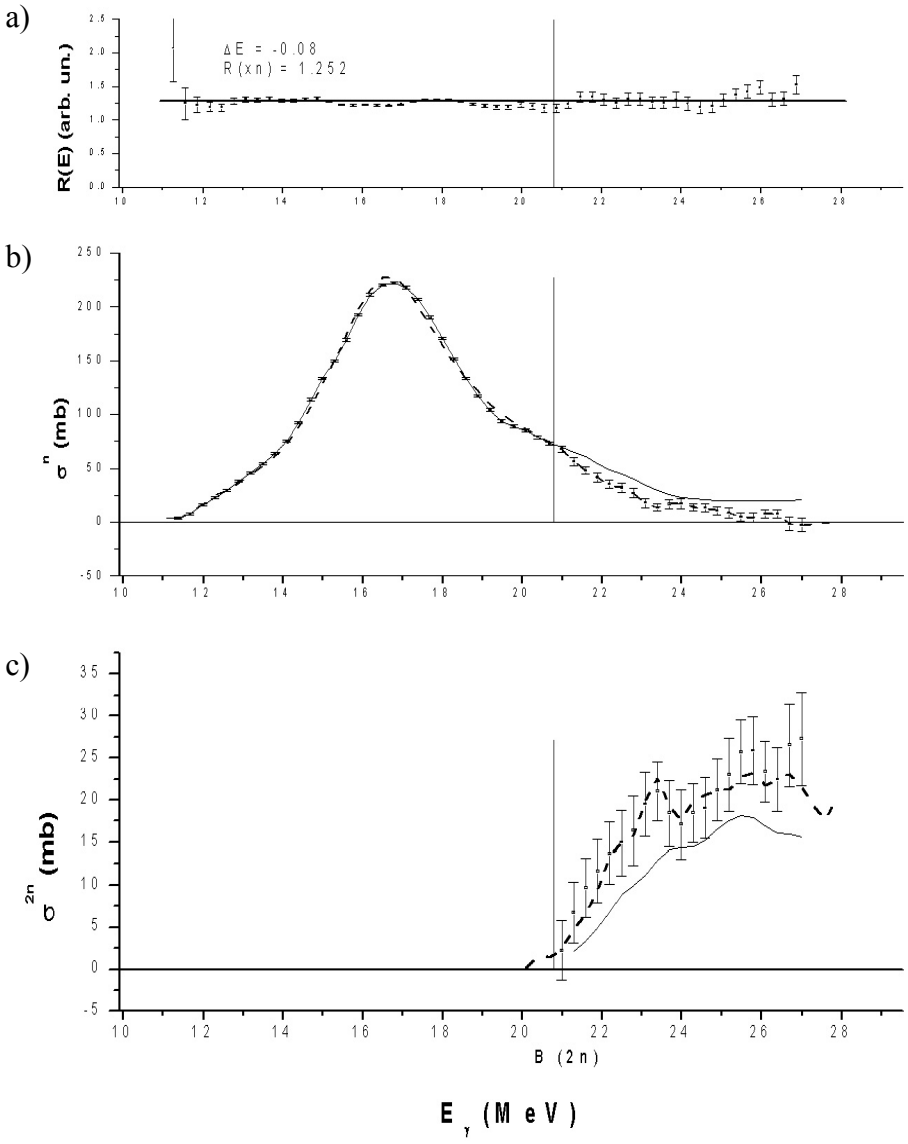

Fig. 7. Results of the reciprocal correction ('standard situation') of the total and partial photoneutron reaction cross-sections obtained at Saclay and Livermore for ^{89}Y:

a) R(E) ratios for the (γ,xn) reaction cross-sections; ΔE and R(xn) values given;

b) Data for the (γ,n) reaction cross-sections:
- Continuous line — original Saclay data σ^{n}_{S};
- Points with error margins — **evaluated** Saclay data (12) σ^{n}_{S}*;
- Dotted line — **evaluated** Livermore data $R\sigma^{n}_{L}$;

c) Data for the (γ,2n) reaction cross-sections:
- Continuous line — original Saclay data σ^{2n}_{S};
- Points with error margins — **evaluated** Saclay data ((9) – (11)) σ^{2n}_{S}*;
- Dotted line — **evaluated** Livermore data $R\sigma^{2n}_{L}$.

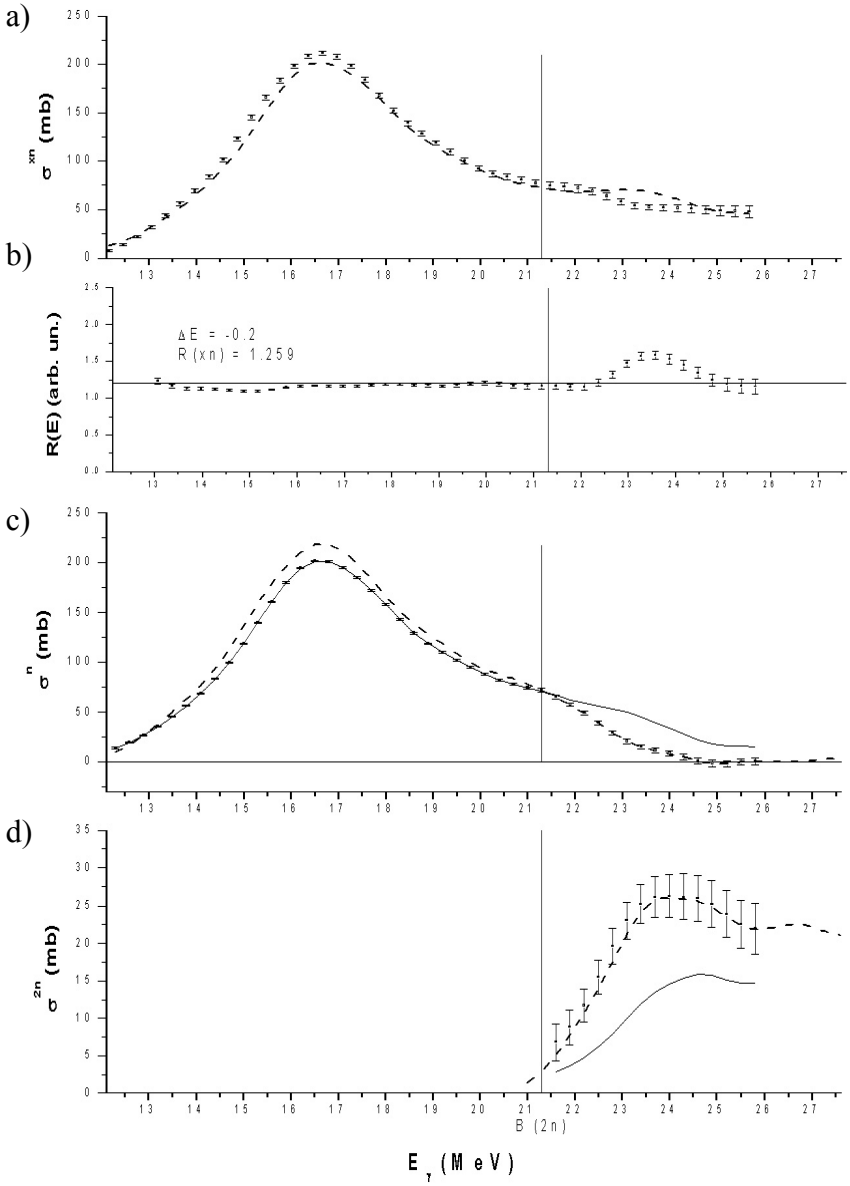

Fig. 8. Results of the reciprocal correction ('special case') of the reaction cross-sections obtained at Saclay and Livermore for ^{90}Zr:

a) Saclay (γ,xn) reaction cross-section data (dotted line — original $\sigma^{xn}{}_S$; points with error margins — corrected $\sigma^{xn}{}_S^* = \sigma^{xn}{}_S\, R/R(E)$);

b) R(E) ratios for the (γ,xn) reaction cross-sections; ΔE and R(xn) values given;

c) Data for the (γ,n) reaction cross-sections: continuous line — original Saclay data $\sigma^{n}{}_S$; points with error margins — **evaluated** (12) Saclay data $\sigma^{n}{}_S^*$; dotted line — **evaluated** Livermore data $R\sigma^{n}{}_L$;

d) Data for the (γ,2n) reaction cross-sections: continuous line — original Saclay data $\sigma^{2n}{}_S$; points with error margins — **evaluated** ((9) – (11)) Saclay data $\sigma^{2n}{}_S^*$; dotted line — **evaluated** Livermore data $R\sigma^{2n}{}_L$.

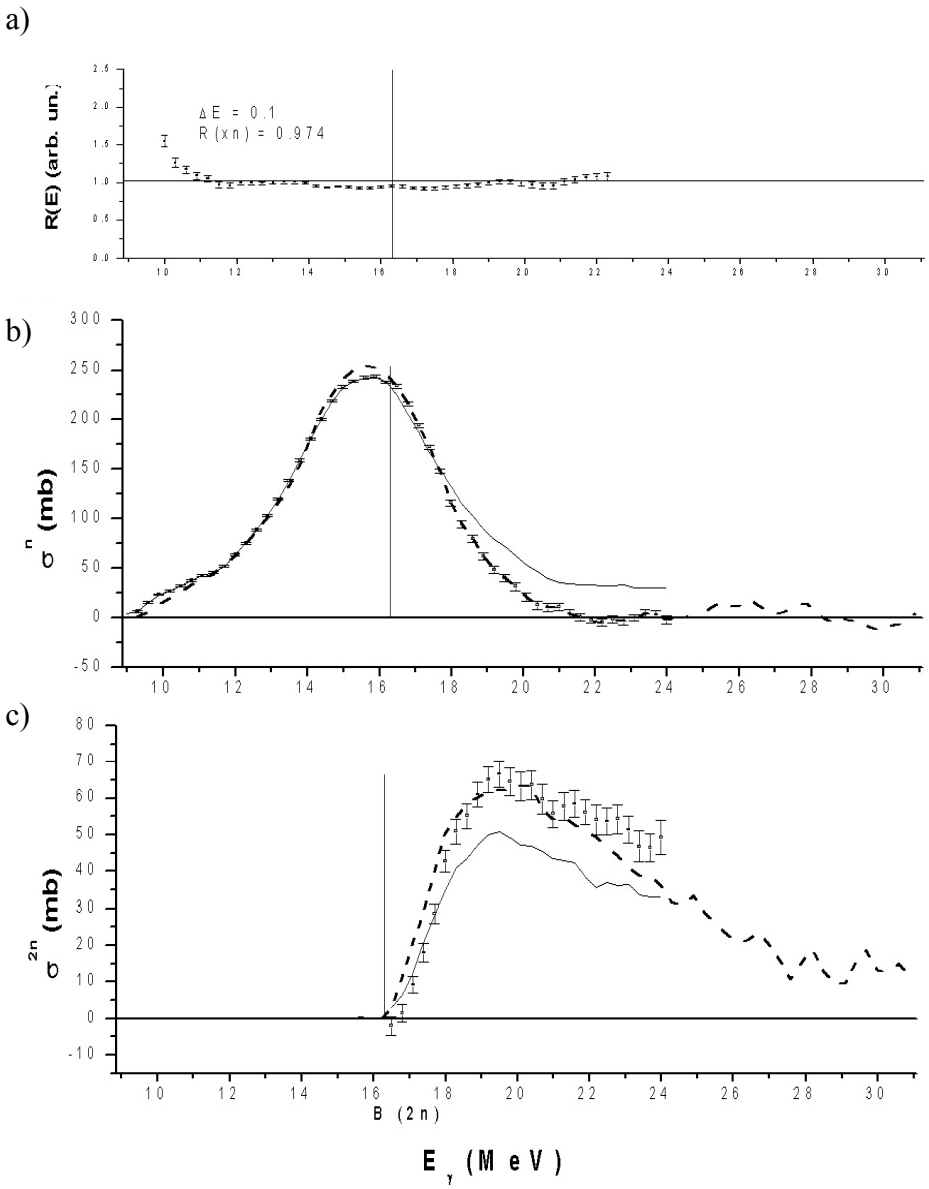

Fig. 9. Results of the reciprocal correction ('standard situation') of the total and partial photoneutron reaction cross-sections obtained at Saclay and Livermore for ^{115}In:

a) R(E) ratios for the (γ,xn) reaction cross-sections; ΔE and R(xn) values given;

b) Data for the (γ,n) reaction cross-sections:
- Continuous line — original Saclay data σ^{n}_{S};
- Points with error margins — **evaluated** Saclay data (12) σ^{n}_{S}*;
- Dotted line — **evaluated** Livermore data $R\sigma^{n}_{L}$;

c) Data for the (γ,2n) reaction cross-sections:
- Continuous line — original Saclay data σ^{2n}_{S};
- Points with error margins — **evaluated** Saclay data ((9) – (11)) σ^{2n}_{S}*;
- Dotted line — **evaluated** Livermore data $R\sigma^{2n}_{L}$.

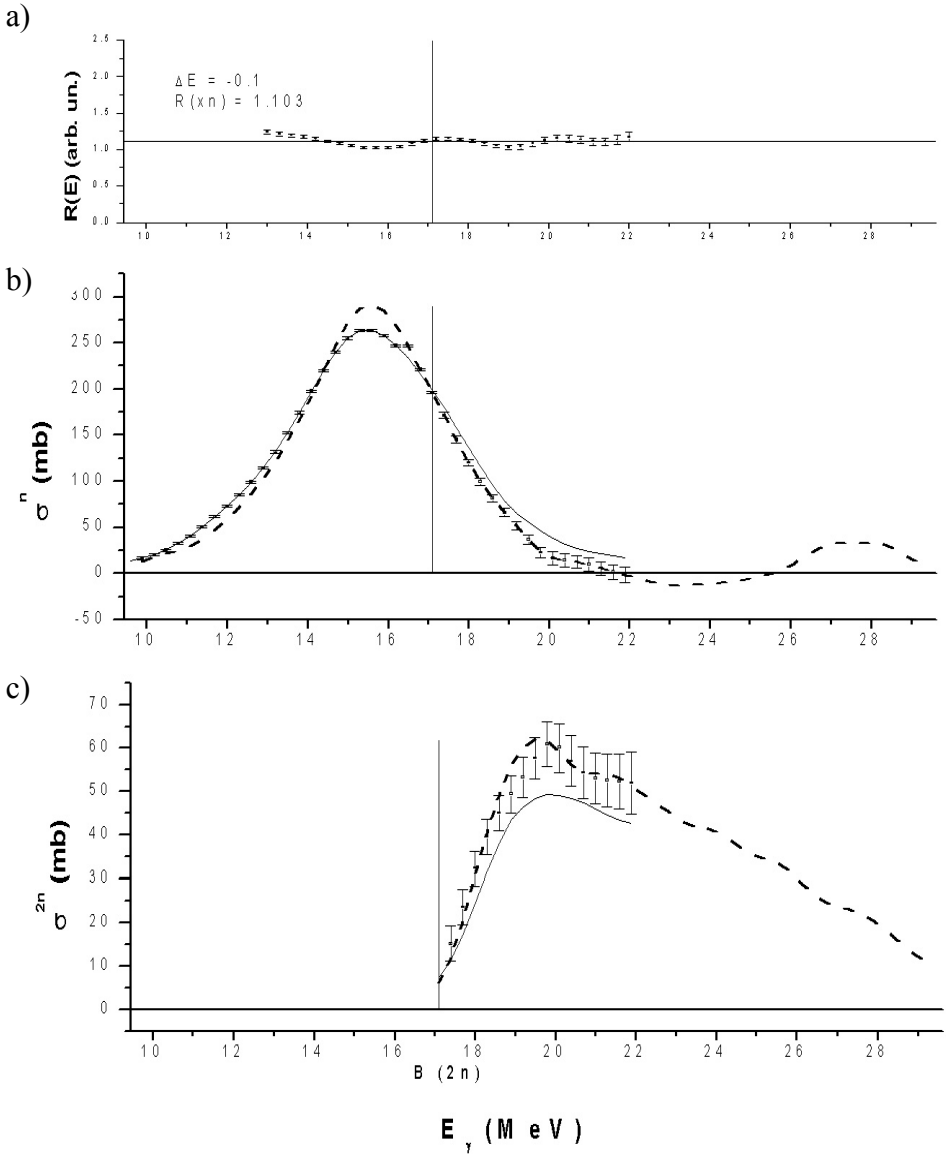

Fig. 10. Results of the reciprocal correction ('standard situation') of the total and partial photoneutron reaction cross-sections obtained at Saclay and Livermore for ^{116}Sn:

a) R(E) ratios for the (γ,xn) reaction cross-sections; ΔE and R(xn) values given;
b) Data for the (γ,n) reaction cross-sections:
   - Continuous line — original Saclay data σ^{n}_{S};
   - Points with error margins — **evaluated** Saclay data (12) σ^{n}_{S}*;
   - Dotted line — **evaluated** Livermore data $R\sigma^{n}_{L}$;
c) Data for the (γ,2n) reaction cross-sections:
   - Continuous line — original Saclay data σ^{2n}_{S};
   - Points with error margins — **evaluated** Saclay data ((9) – (11)) σ^{2n}_{S}*;
   - Dotted line — **evaluated** Livermore data $R\sigma^{2n}_{L}$.

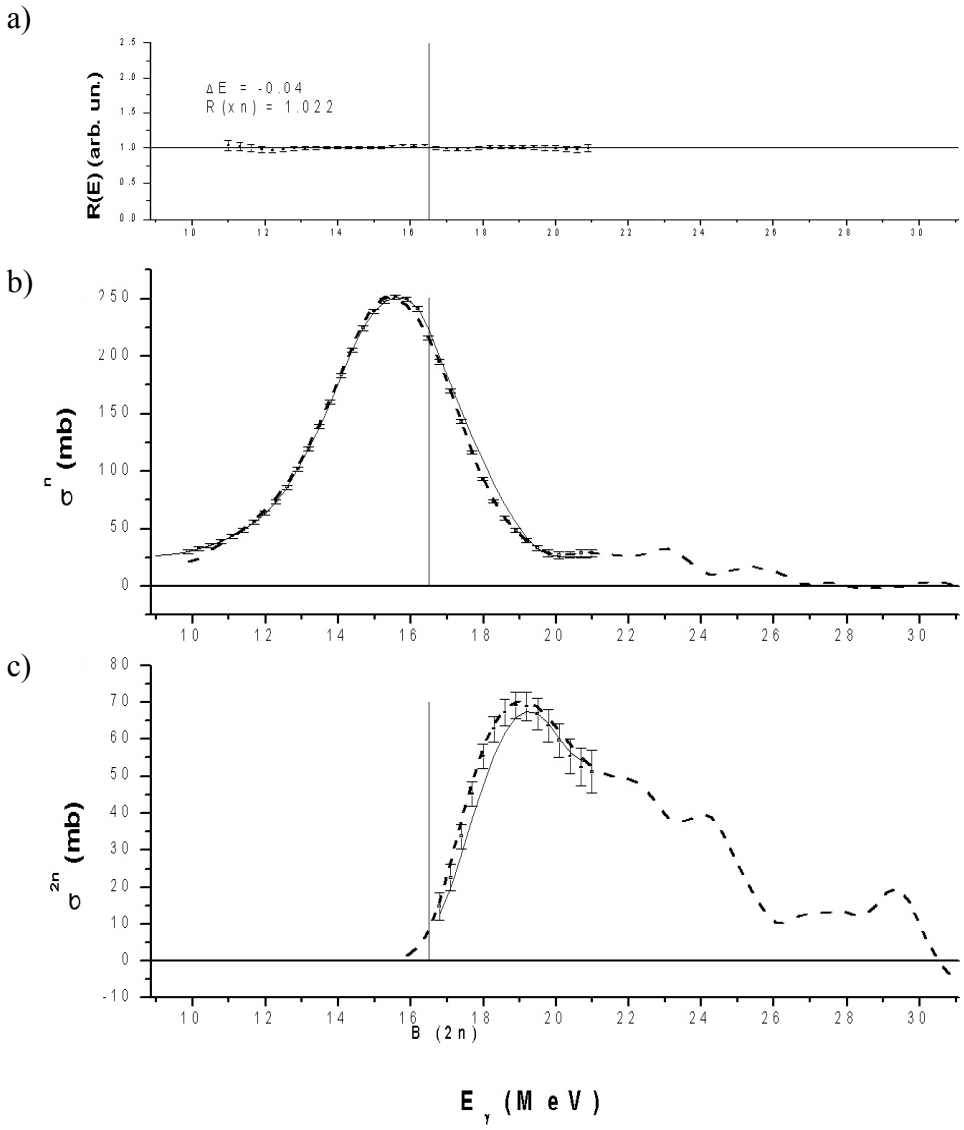

Fig. 11. Results of the reciprocal correction ('standard situation') of the total and partial photoneutron reaction cross-sections obtained at Saclay and Livermore for ^{117}Sn:

a) R(E) ratios for the (γ,xn) reaction cross-sections; ΔE and R(xn) values given;
b) Data for the (γ,n) reaction cross-sections:
   - Continuous line — original Saclay data σ^{n}_{S};
   - Points with error margins — **evaluated** Saclay data (12) σ^{n}_{S}*;
   - Dotted line — **evaluated** Livermore data $R\sigma^{n}_{L}$;
c) Data for the (γ,2n) reaction cross-sections:
   - Continuous line — original Saclay data σ^{2n}_{S};
   - Points with error margins — **evaluated** Saclay data ((9) – (11)) σ^{2n}_{S}*;
   - Dotted line — **evaluated** Livermore data $R\sigma^{2n}_{L}$.

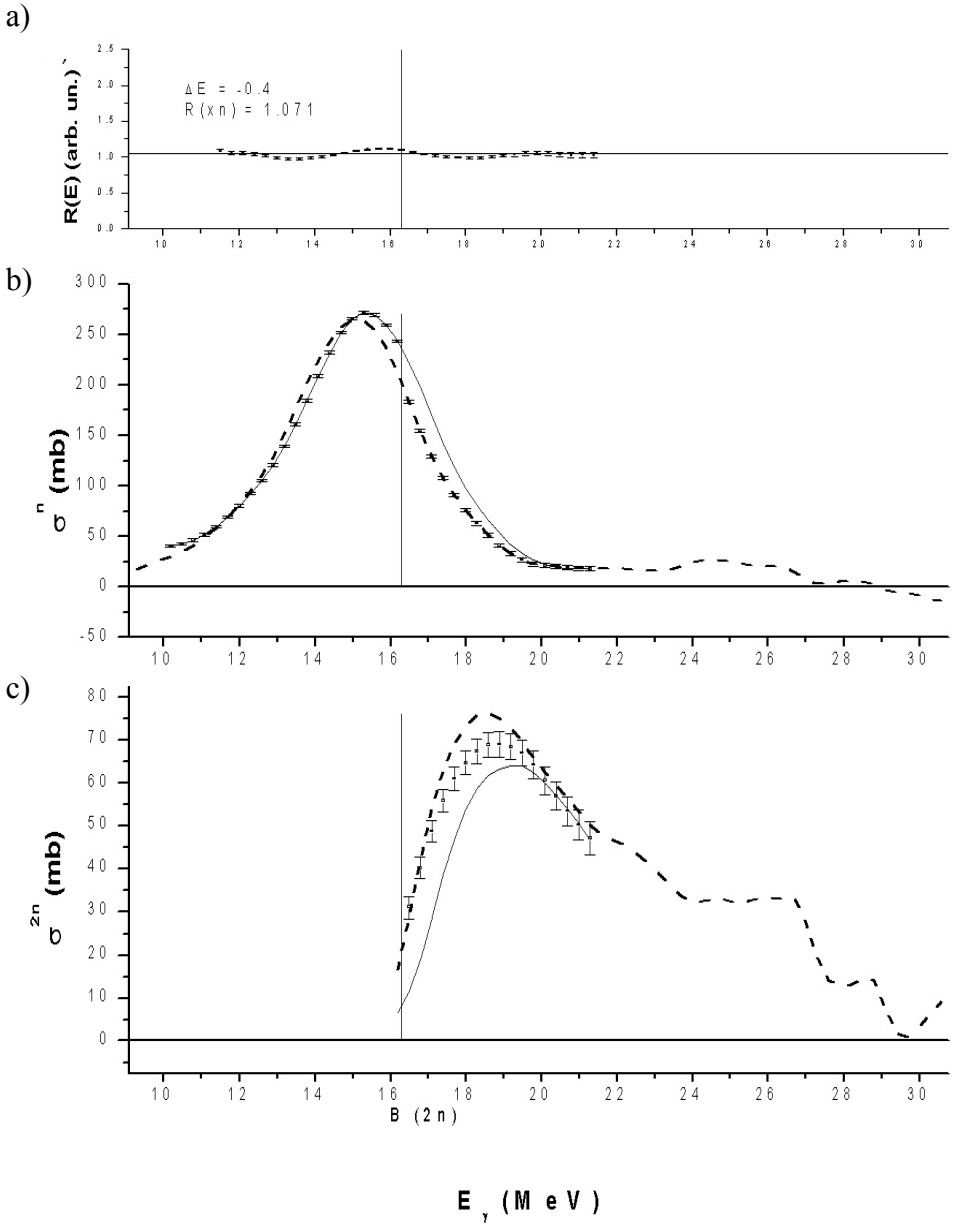

Fig. 12. Results of the reciprocal correction ('standard situation') of the total and partial photoneutron reaction cross-sections obtained at Saclay and Livermore for ^{118}Sn:

a) R(E) ratios for the (γ,xn) reaction cross-sections; ΔE and R(xn) values given;

b) Data for the (γ,n) reaction cross-sections:
- Continuous line — original Saclay data σ^{n}_{S};
- Points with error margins — **evaluated** Saclay data (12) σ^{n}_{S}*;
- Dotted line — **evaluated** Livermore data $R\sigma^{n}_{L}$;

c) Data for the (γ,2n) reaction cross-sections:
- Continuous line — original Saclay data σ^{2n}_{S};
- Points with error margins — **evaluated** Saclay data ((9) – (11)) σ^{2n}_{S}*;
- Dotted line — **evaluated** Livermore data $R\sigma^{2n}_{L}$.

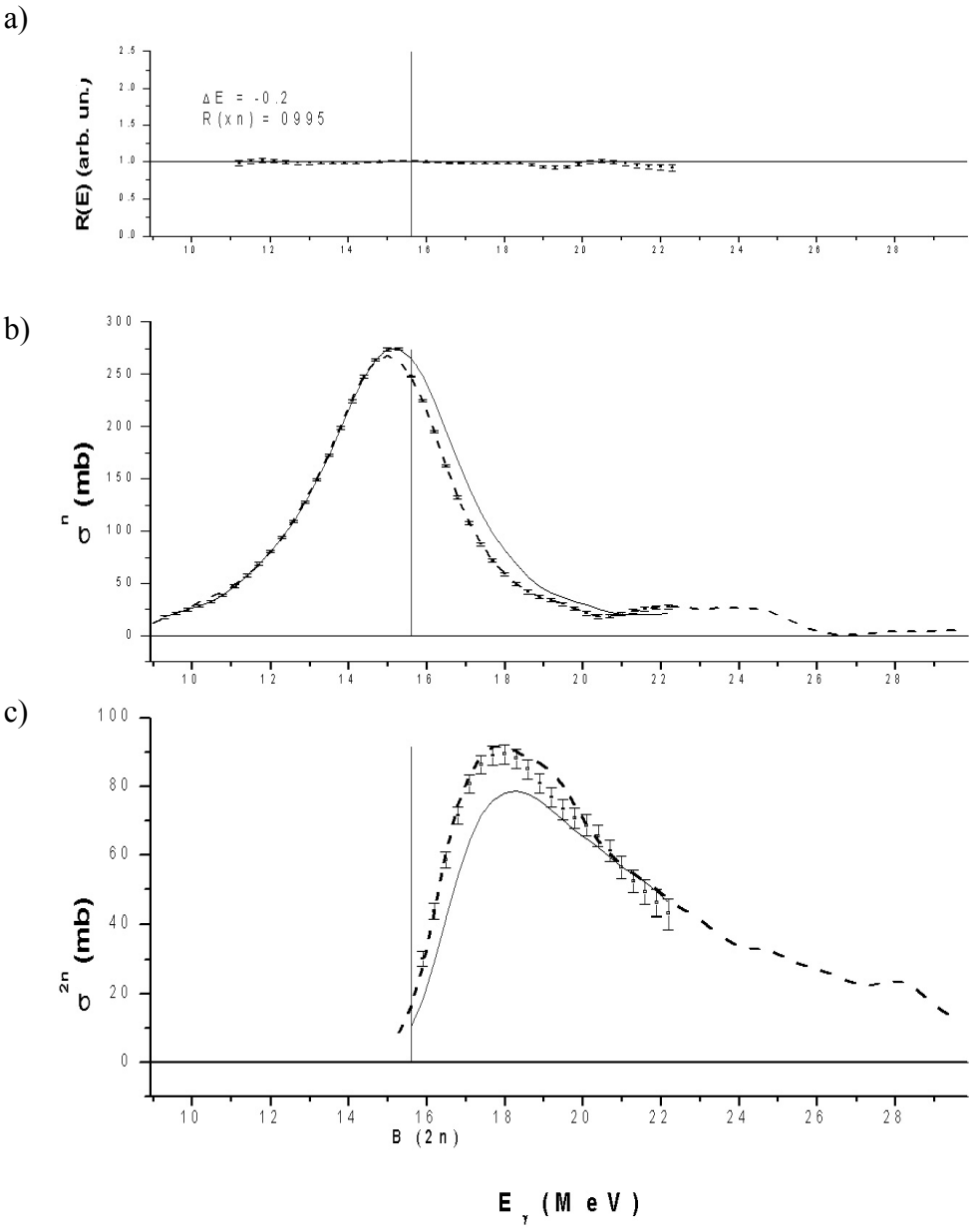

Fig. 13. Results of the reciprocal correction ('standard situation') of the total and partial photoneutron reaction cross-sections obtained at Saclay and Livermore for ^{120}Sn:

a) R(E) ratios for the (γ,xn) reaction cross-sections; ΔE and R(xn) values given;

b) Data for the (γ,n) reaction cross-sections:
- Continuous line — original Saclay data σ^{n}_{S};
- Points with error margins — **evaluated** Saclay data (12) σ^{n}_{S}*;
- Dotted line — **evaluated** Livermore data $R\sigma^{n}_{L}$;

c) Evaluated data for the (γ,2n) reaction cross-sections:
- Continuous line — original Saclay data σ^{2n}_{S};
- Points with error margins — **evaluated** Saclay data ((9) – (11)) σ^{2n}_{S}*;
- Dotted line — **evaluated** Livermore data $R\sigma^{2n}_{L}$.

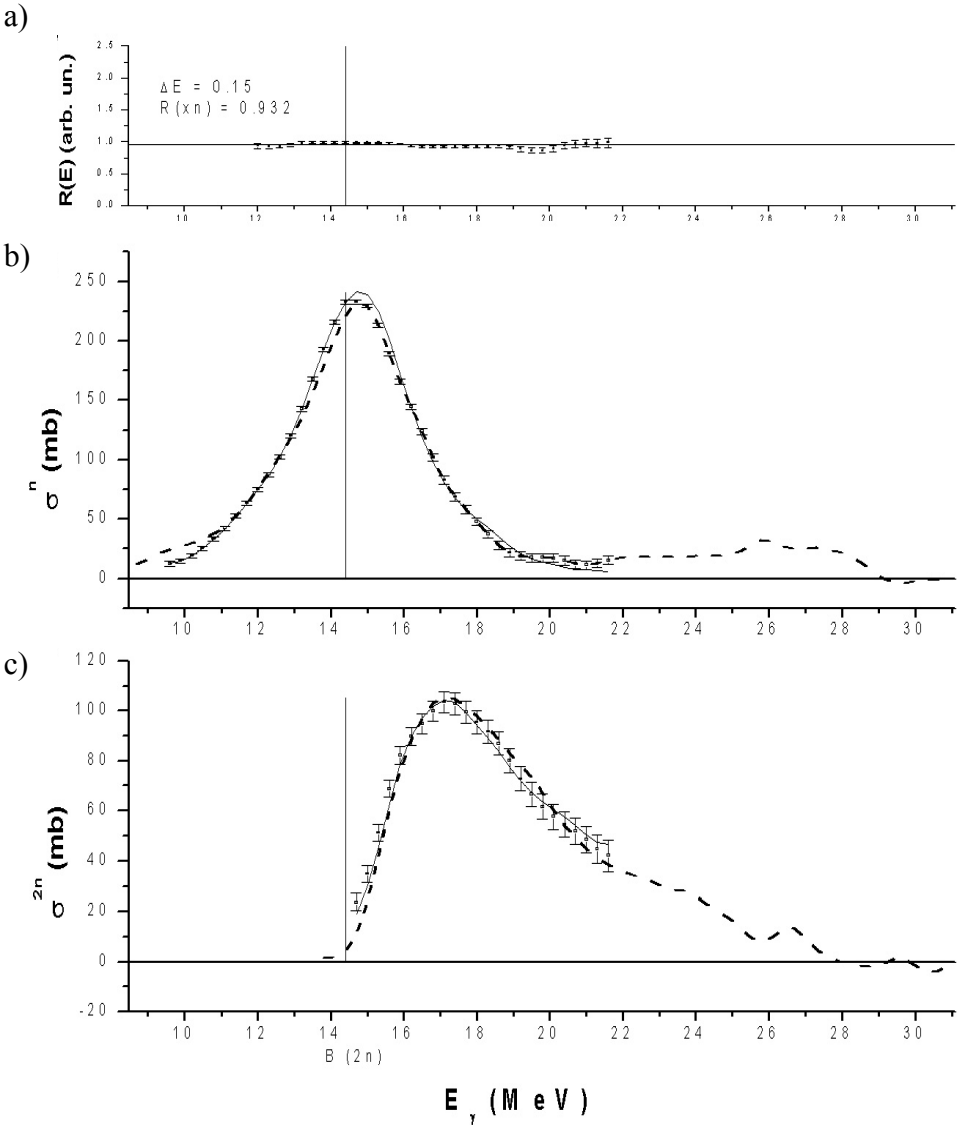

Fig. 14. Results of the reciprocal correction ('ideal case') of the total and partial photoneutron reaction cross-sections obtained at Saclay and Livermore for ^{124}Sn:

a) R(E) ratios for the (γ,xn) reaction cross-sections; ΔE and R(xn) values given;

b) Data for the (γ,n) reaction cross-sections:
- Continuous line — original Saclay data σ^{n}_{S};
- Points with error margins — **evaluated** Saclay data (12) σ^{n}_{S}*;
- Dotted line — **evaluated** Livermore data $R\sigma^{n}_{L}$;

c) Data for the (γ,2n) reaction cross-sections:
- Continuous line — original Saclay data σ^{2n}_{S};
- Points with error margins — **evaluated** Saclay data ((9) – (11)) σ^{2n}_{S}*;
- Dotted line — **evaluated** Livermore data $R\sigma^{2n}_{L}$.

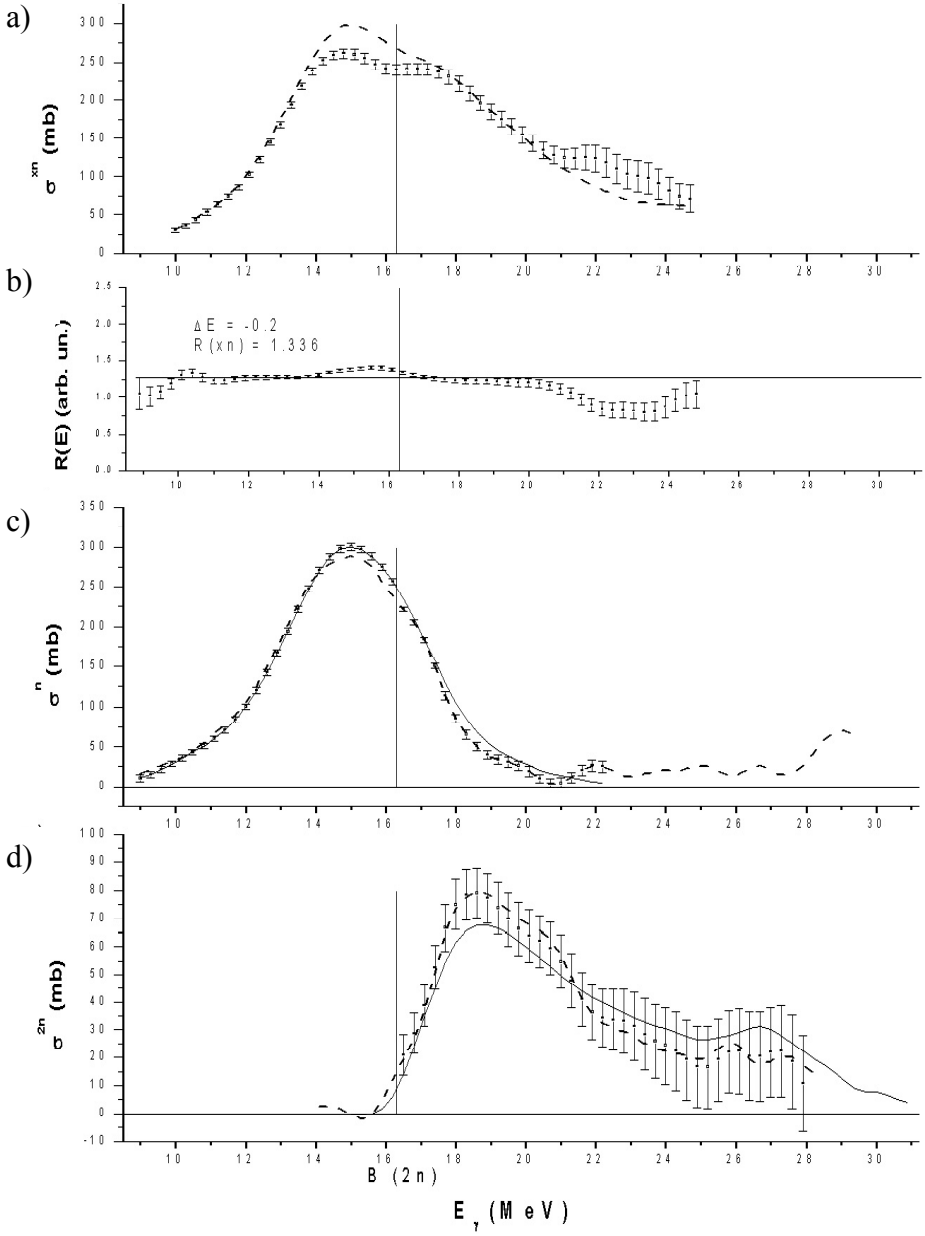

Fig. 15. Results of the reciprocal correction ('special case') of the reaction cross-sections obtained at Saclay and Livermore for ^{127}I:

a) Saclay (γ,xn) reaction cross-section data (dotted line — original $\sigma^{xn}_{S;}$ points with error margins — corrected $\sigma^{xn}* = \sigma^{xn}_S$ R/R(E));

b) R(E) ratios for the (γ,xn) reaction cross-sections; ΔE and R(xn) values given;

c) Data for the (γ,n) reaction cross-sections: continuous line — original Saclay data σ^{n}_S; points with error margins — **evaluated** (12) Saclay data σ^{n}_S*; dotted line — **evaluated** Livermore data $R\sigma^{n}_L$;

d) Data for the (γ,2n) reaction cross-sections: continuous line — original Saclay data σ^{2n}_S; points with error margins — **evaluated** ((9) – (11)) Saclay data σ^{2n}_S*; dotted line — **evaluated** Livermore data $R\sigma^{2n}_L$.

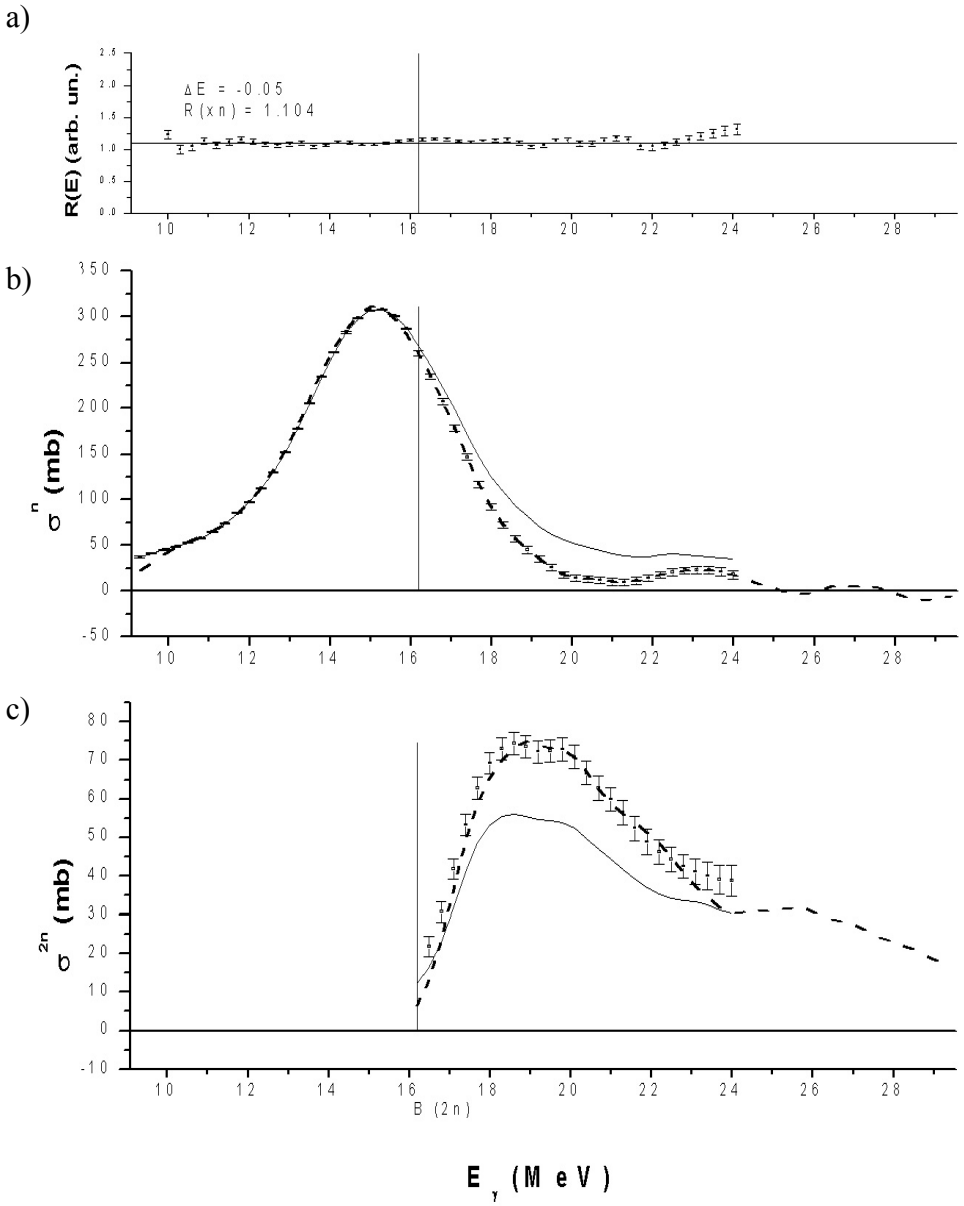

Fig. 16. Results of the reciprocal correction ('standard situation') of the total and partial photoneutron reaction cross-sections obtained at Saclay and Livermore for ^{133}Cs:

a) R(E) ratios for the (γ,xn) reaction cross-sections; ΔE and R(xn) values given;

b) Data for the (γ,n) reaction cross-sections:
- Continuous line — original Saclay data σ^{n}_{S};
- Points with error margins — **evaluated** Saclay data (12) σ^{n}_{S}*;
- Dotted line — **evaluated** Livermore data $R\sigma^{n}_{L}$;

c) Data for the (γ,2n) reaction cross-sections:
- Continuous line — original Saclay data σ^{2n}_{S};
- Points with error margins — **evaluated** Saclay data ((9) – (11)) σ^{2n}_{S}*;
- Dotted line — **evaluated** Livermore data $R\sigma^{2n}_{L}$.

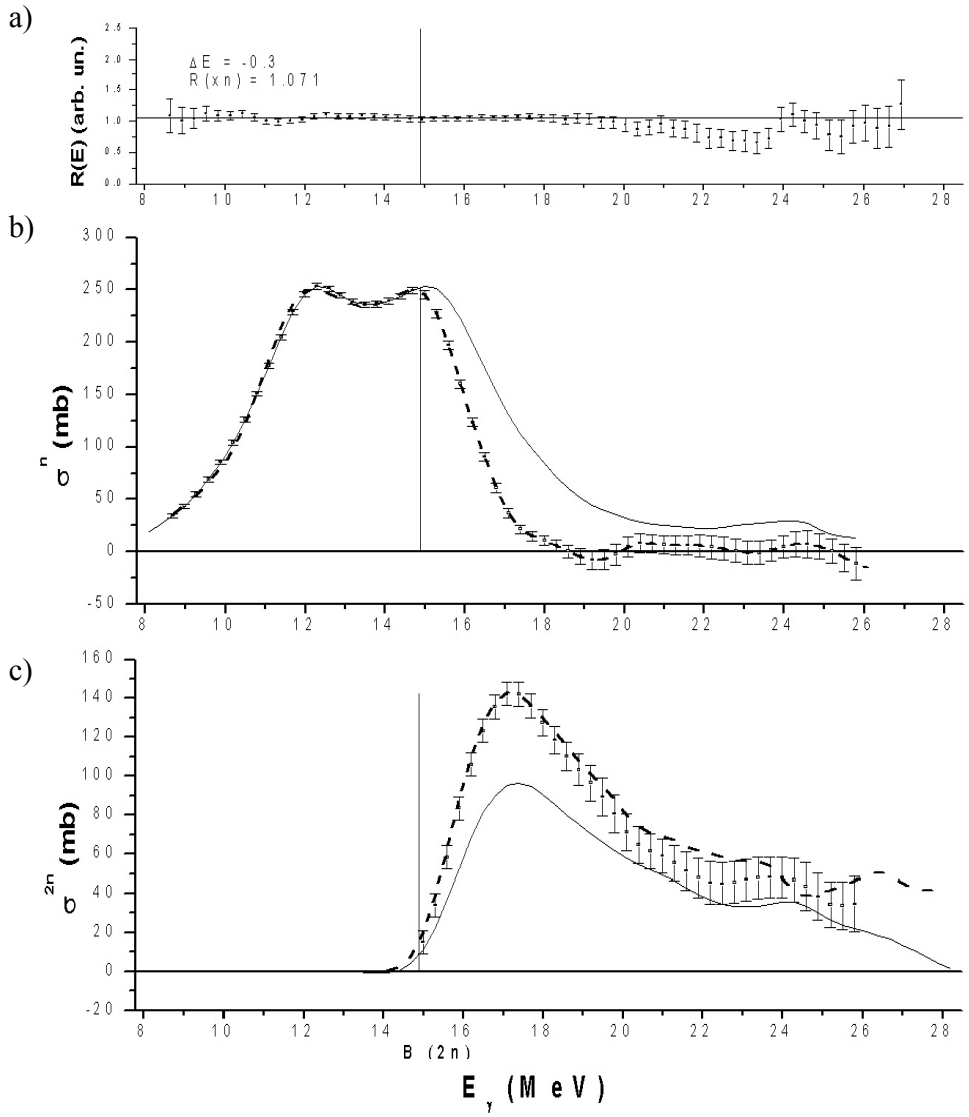

Fig. 17. Results of the reciprocal correction ('standard situation') of the total and partial photoneutron reaction cross-sections obtained at Saclay and Livermore for ^{159}Tb:

a) R(E) ratios for the (γ,xn) reaction cross-sections; ΔE and R(xn) values given;

b) Data for the (γ,n) reaction cross-sections:
- Continuous line — original Saclay data σ^{n}_{S};
- Points with error margins — **evaluated** Saclay data (12) σ^{n}_{S}*;
- Dotted line — **evaluated** Livermore data $R\sigma^{n}_{L}$;

c) Data for the (γ,2n) reaction cross-sections:
- Continuous line — original Saclay data σ^{2n}_{S};
- Points with error margins — **evaluated** Saclay data ((9) – (11)) σ^{2n}_{S}*;
- Dotted line — **evaluated** Livermore data $R\sigma^{2n}_{L}$.

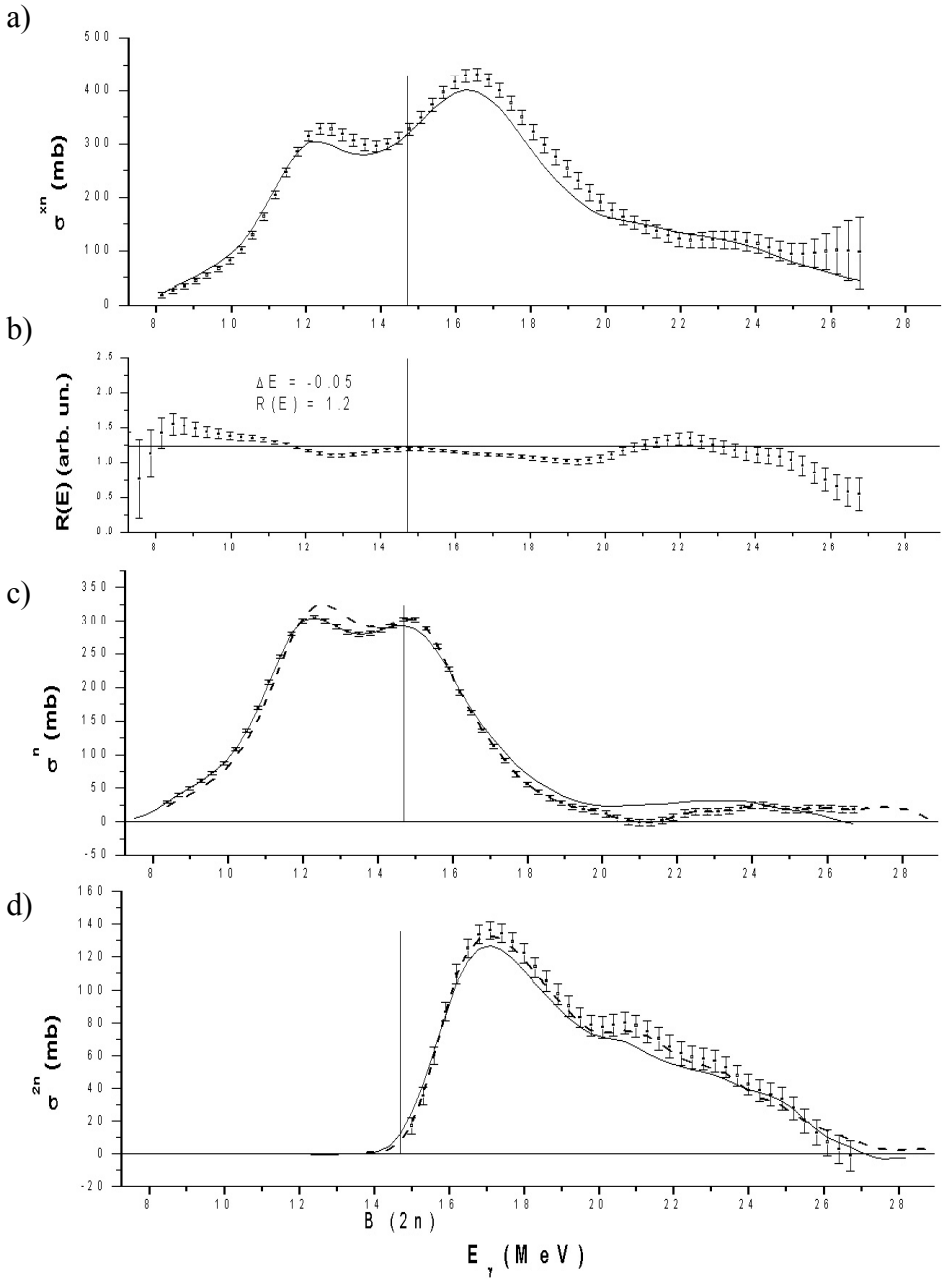

Fig. 18. Results of the reciprocal correction ('special case') of the reaction cross-sections obtained at Saclay and Livermore for ^{165}Ho:

a) Saclay (γ,xn) reaction cross-section data (dotted line — original $\sigma^{xn}_{S;}$ points with error margins — corrected $\sigma^{xn}_S{}^* = \sigma^{xn}_S\, R/R(E)$);

b) R(E) ratios for the (γ,xn) reaction cross-sections; ΔE and R(xn) values given;

c) Data for the (γ,n) reaction cross-sections: continuous line — original Saclay data σ^{n}_S; points with error margins — **evaluated** (12) Saclay data $\sigma^{n}_S{}^*$; dotted line — **evaluated** Livermore data $R\sigma^{n}_L$;

d) Data for the (γ,2n) reaction cross-sections: continuous line — original Saclay data σ^{2n}_S; points with error margins — **evaluated** ((9) – (11)) Saclay data $\sigma^{2n}_S{}^*$; dotted line — **evaluated** Livermore data $R\sigma^{2n}_L$.

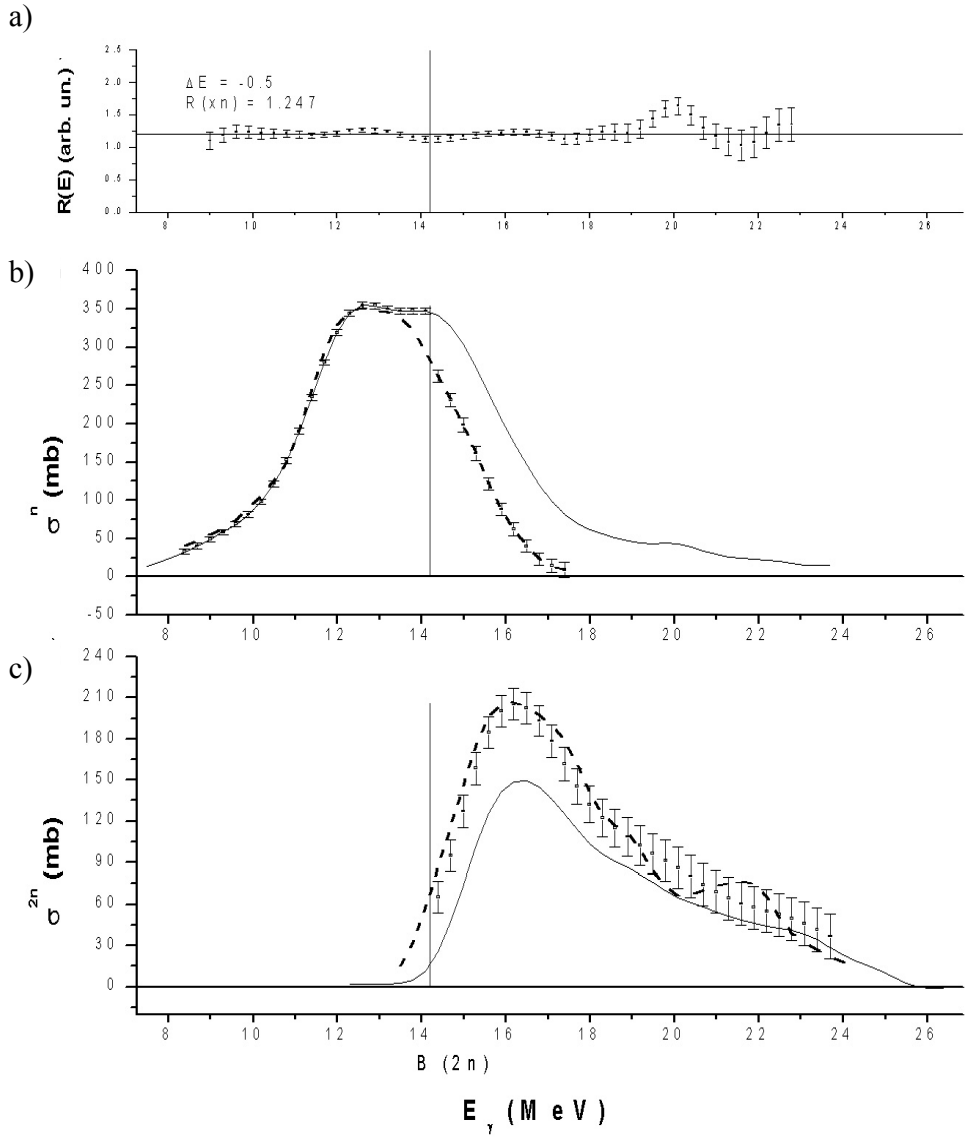

Fig. 19. Results of the reciprocal correction ('standard situation') of the total and partial photoneutron reaction cross-sections obtained at Saclay and Livermore for ^{181}Ta:

a) R(E) ratios for the (γ,xn) reaction cross-sections; ΔE and R(xn) values given;

b) Data for the (γ,n) reaction cross-sections:
- Continuous line — original Saclay data σ^{n}_{S};
- Points with error margins — **evaluated** Saclay data (12) σ^{n}_{S}*;
- Dotted line — **evaluated** Livermore data $R\sigma^{n}_{L}$;

c) Data for the (γ,2n) reaction cross-sections:
- Continuous line — original Saclay data σ^{2n}_{S};
- Points with error margins — **evaluated** Saclay data ((9) – (11)) σ^{2n}_{S}*;
- Dotted line — **evaluated** Livermore data $R\sigma^{2n}_{L}$.

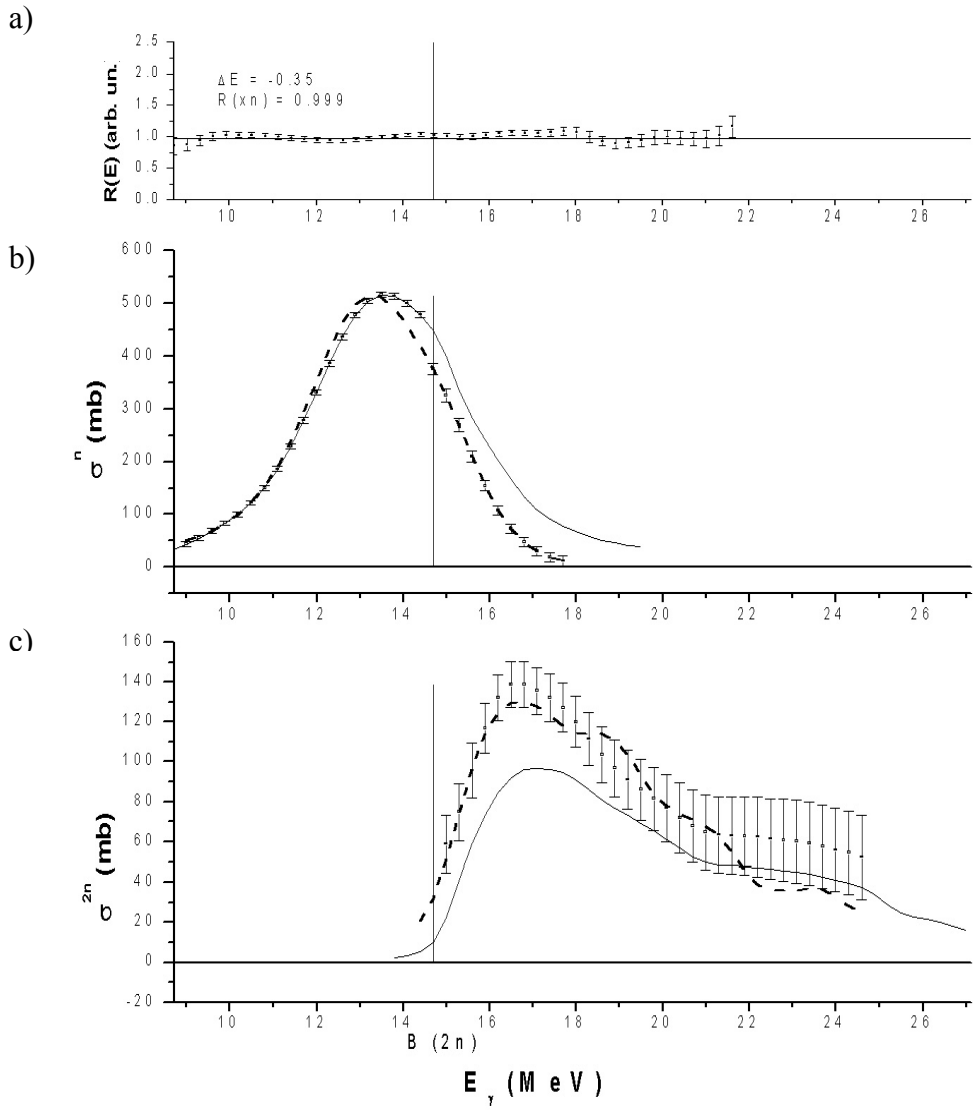

Fig. 20. Results of the reciprocal correction ('standard situation') of the total and partial photoneutron reaction cross-sections obtained at Saclay and Livermore for ^{197}Au:

a) R(E) ratios for the (γ,xn) reaction cross-sections; ΔE and R(xn) values given;
b) Data for the (γ,n) reaction cross-sections:
   - Continuous line — original Saclay data σ^{n}_{S};
   - Points with error margins — **evaluated** Saclay data (12) σ^{n}_{S}*;
   - Dotted line — **evaluated** Livermore data $R\sigma^{n}_{L}$;
c) Data for the (γ,2n) reaction cross-sections:
   - Continuous line — original Saclay data σ^{2n}_{S};
   - Points with error margins — **evaluated** Saclay data ((9) – (11)) σ^{2n}_{S}*;
   - Dotted line — **evaluated** Livermore data $R\sigma^{2n}_{L}$.

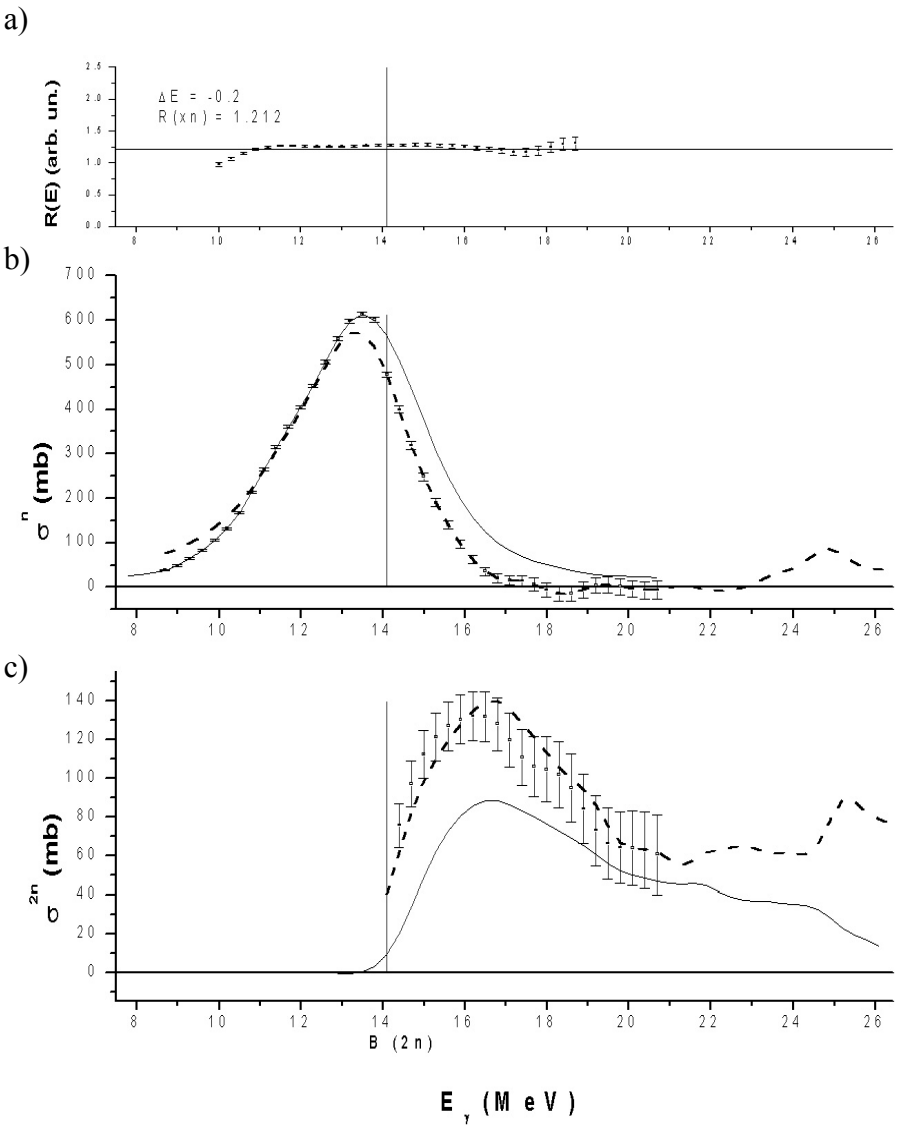

Fig. 21. Results of the reciprocal correction ('standard situation') of the total and partial photoneutron reaction cross-sections obtained at Saclay and Livermore for ^{208}Pb:

a) R(E) ratios for the (γ,xn) reaction cross-sections; ΔE and R(xn) values given;

b) Data for the (γ,n) reaction cross-sections:
- Continuous line — original Saclay data σ^{n}_{S};
- Points with error margins — **evaluated** Saclay data (12) σ^{n}_{S}*;
- Dotted line — **evaluated** Livermore data $R\sigma^{n}_{L}$;

c) Data for the (γ,2n) reaction cross-sections:
- Continuous line — original Saclay data σ^{2n}_{S};
- Points with error margins — **evaluated** Saclay data ((9) – (11)) σ^{2n}_{S}*;
- Dotted line — **evaluated** Livermore data $R\sigma^{2n}_{L}$.

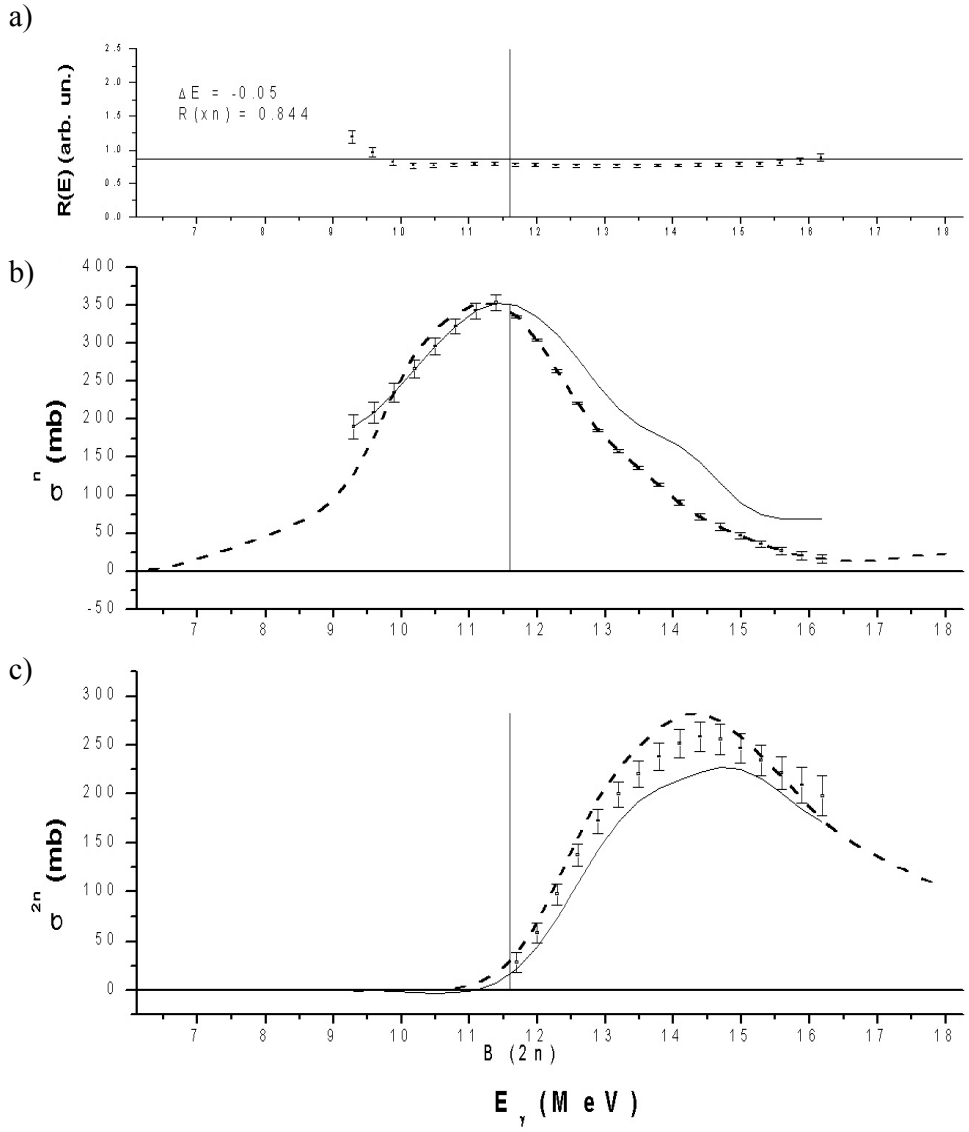

Fig. 22. Results of the reciprocal correction ('standard situation') of the total and partial photoneutron reaction cross-sections obtained at Saclay and Livermore for ^{232}Th:

a) R(E) ratios for the (γ,xn) reaction cross-sections; ΔE and R(xn) values given;

b) Data for the (γ,n) reaction cross-sections:
- Continuous line — original Saclay data σ^{n}_{S};
- Points with error margins — **evaluated** Saclay data (12) σ^{n}_{S}*;
- Dotted line — **evaluated** Livermore data $R\sigma^{n}_{L}$;

c) Data for the (γ,2n) reaction cross-sections:
- Continuous line — original Saclay data σ^{2n}_{S};
- Points with error margins — **evaluated** Saclay data ((9) – (11)) σ^{2n}_{S}*;
- Dotted line — **evaluated** Livermore data $R\sigma^{2n}_{L}$.

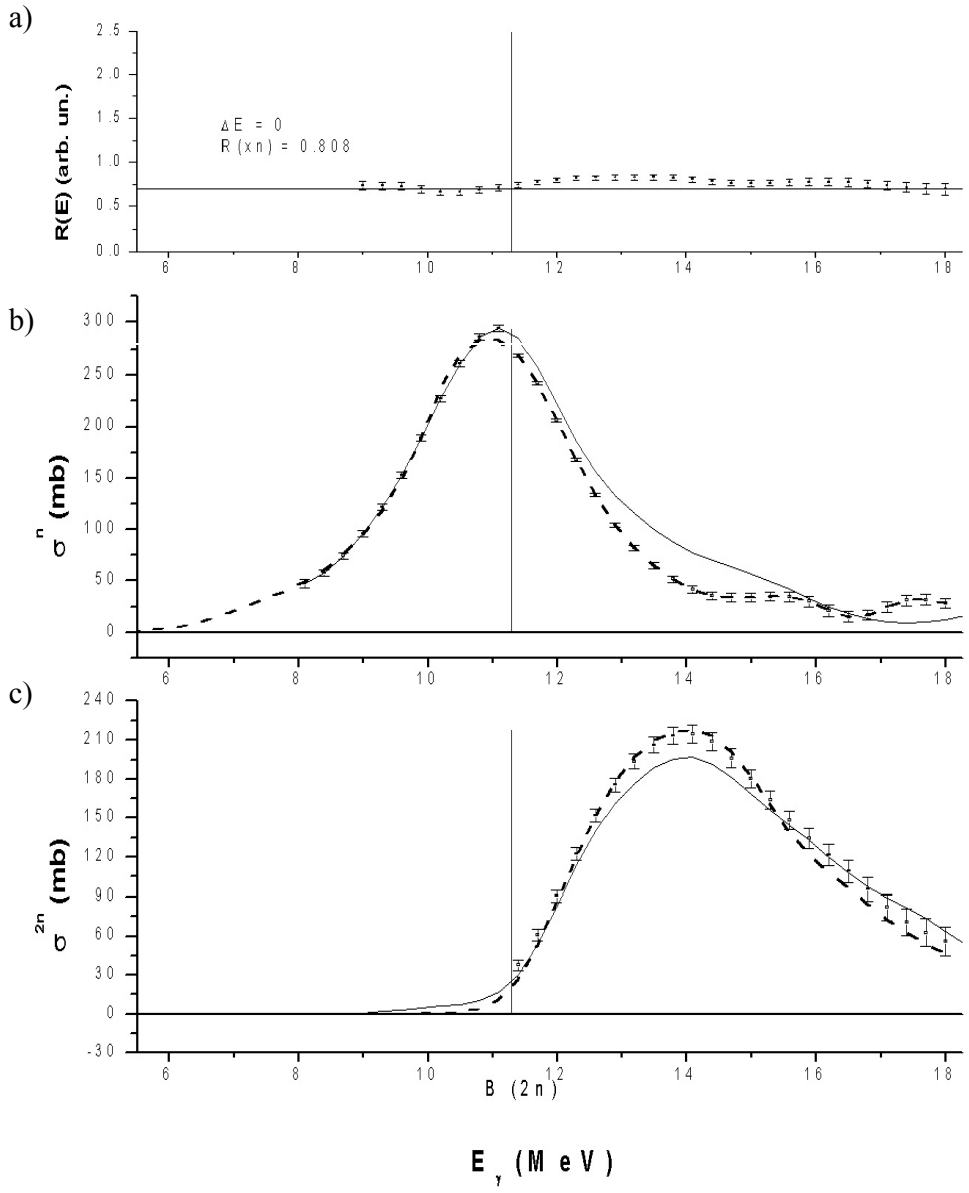

Fig. 23. Results of the reciprocal correction ('standard situation') of the total and partial photoneutron reaction cross-sections obtained at Saclay and Livermore for ^{238}U:

a) R(E) ratios for the (γ,xn) reaction cross-sections; ΔE and R(xn) values given;

b) Data for the (γ,n) reaction cross-sections:
- Continuous line — original Saclay data σ^{n}_{S};
- Points with error margins — **evaluated** Saclay data (12) σ^{n}_{S}*;
- Dotted line — **evaluated** Livermore data $R\sigma^{n}_{L}$;

c) Data for the (γ,2n) reaction cross-sections:
- Continuous line — original Saclay data σ^{2n}_{S};
- Points with error margins — **evaluated** Saclay data ((9) – (11)) σ^{2n}_{S}*;
- Dotted line — **evaluated** Livermore data $R\sigma^{2n}_{L}$.

Conclusion

The main assertions and recommendations that can be made on the basis of the research carried out and the results obtained are as follows.

1. The experimental data on the total photoneutron reaction cross-sections (γ,xn) obtained at Livermore disagree with the data from other laboratories. They can be made to agree with most of the data by additional normalization using the coefficients R = R(xn) in expression (6). For the 19 nuclei studied in this paper (^{51}V, ^{75}As, ^{89}Y, ^{90}Zr, ^{115}In, ^{116,117,118,120,124}Sn, ^{127}I, ^{133}Cs, ^{159}Tb, ^{165}Ho, ^{181}Ta, ^{197}Au, ^{208}Pb, ^{232}Th, ^{238}U), evaluated (γ,xn) reaction cross-sections were obtained using the data in Table 4. In other cases, the coefficient $\langle R^{int}_{syst} \rangle = 1.222$, which was obtained in Ref. [22] on the basis of major systematics data, can be used without further research.
2. The experimental data on the (γ,n) and (γ,2n) partial photoneutron reaction cross-sections obtained at Livermore do agree with each other and with the data on the total photoneutron reaction cross-sections (γ,xn). Thus, evaluated cross-sections for these can be obtained by simple normalization using the same values of R (or $\langle R^{int}_{syst} \rangle$).
3. The experimental data on the total photoneutron reaction cross-sections (γ,xn) obtained at Saclay agree with the data of other laboratories and can be used as evaluated cross-data without additional normalization.
4. The experimental data on the (γ,n) and (γ,2n) partial photoneutron reaction cross-sections obtained at Saclay are incorrect and must be recalculated using the proposed reciprocal correction method. Using the method described above, the data obtained at Saclay and Livermore on the (γ,n) and (γ,2n) partial reaction cross-sections can be brought into agreement (Tables 5 and 6). This is achieved by increasing the cross-sections of the two-neutron reactions by decreasing the single-neutron reaction cross-sections obtained at Saclay in the energy region above the B(2n) threshold. It should be noted in particular that, after correction, for both reactions the Saclay data agree with the corresponding Livermore data multiplied by the coefficient R.
5. The poorer agreement between the Livermore data and the single-neutron reaction cross-sections obtained at Saclay in the energy region above the B(2n) threshold casts doubt on the suggested interpretation [5, 31, 34, 42] of high energy 'tails' of these cross-sections as the result of contributions from fast neutrons (non-statistical processes). The fact that the single-neutron reaction cross-sections obtained at Saclay do not drop to 0 in the energy region at ~ 2 MeV above the threshold of the two-neutron reaction B(2n), as they should according to the predictions of the statistical model, has also resulted in a very high (~ 25%) evaluation of the proportion of non-statistical processes in the (γ,n) reaction cross-section. The research carried out indicates that the non-statistical component of the giant dipole resonance does not exceed 10%, and thus decay of the giant dipole resonance is largely primarily statistical. Clearly this means that the total photoabsorption cross-section data obtained subsequently at Saclay using the photoneutron reaction data also require substantial correction.

6. In the light of what has been said, it would be interesting to compare the corrected and harmonized Saclay and Livermore data on the partial photoneutron reaction cross-sections (particularly the (γ,2n) reaction cross-sections which have changed considerably) with the results of research carried out using other methods. Unfortunately, such a comparison is not a very easy task:
   - Only in very few cases do the data on the (γ,2n) reactions obtained at Saclay and Livermore overlap with any other data;
   - Individual (γ,2n) reaction cross-sections obtained using GB beams and the induced-activity method (analogous data on the (γ,n) reaction cannot be used directly since, in the Saclay and Livermore data, we are essentially dealing with [(γ,n) + (γ,np)]) reaction cross-sections) have error levels that exceed to an even greater degree the mismatch between the original Saclay and Livermore data.

References

1. Ishkhanov, B.S., Kapitonov, I.M., Interaction of electromagnetic radiation with atomic nuclei, Moscow University Press, Moscow (1979) [in Russian].
2. Fuller, E.G., Gerstenberg, H., Photonuclear Data — Abstracts Sheets 1955–1982, NBSIR 83-2742, USA, National Bureau of Standards (1986).
3. Varlamov, V.V., Sapunenko, V.V., Stepanov, M.E., Photonuclear Data Index 1976–1995, Izdatel'stvo Moskovskogo Universiteta, Moscow (1996).
4. Dietrich, S.S., Berman, B.L., Atomic Data and Nuclear Data Tables, 38 (1988) 199.
5. Bergere, R.L., Beil, H., Veyssiere, A., Nucl. Phys., A121 (1968) 463.
6. Wolynec, E., Martins, M.N., Revista Brasileira Fisica, 17 (1987) 56.
7. Varlamov, V.V., Efimkin, N.G., Lenskaja, N.A., Chernjaev, A.P., The Investigation of the Reasons for Discrepancies in Results of Photonuclear Experiments at the Beams of Bremsstrahlung and Quasimonoenergetic Gamma-Quanta, The Problem of Interpretation, MSU INP Preprint-89-66/143, Moscow (1989).
8. Varlamov, V.V., Ishkhanov, B.S., Analysis of systematic discrepancies in the cross-sections of photonuclear reactions in the GDR region, Abstracts of the International Conference on 'Properties of the Excited States of Atomic Nuclei and Nuclear Reaction Mechanisms', LI Conference on Nuclear Spectroscopy and the Structure of the Nucleus, 3–8 September 2001, Sarov 2001, p. 180 [in Russian].
9. Varlamov, V.V., Ishkhanov, B.S., Study of Consistency Between (γ,xn), [(γ,n) + (γ,np)] and (γ,2n) Reaction Cross Sections Using Data Systematics, Vienna, Austria, INDC(CCP)-433, IAEA NDS, Vienna, Austria, 2002.
10. Boboshin, I.N., Varlamov, V.V., Ivanov, E.M., Ivanov, S.V., Peskov, N.N., Stepanov, M.E., Chesnokov, V.V., Relational Nuclear Databases Upon the MSU INP CDFE Web-site and Nuclear Data Centres Network CDFE Activities, Report on the IAEA Consultant's Meeting on the Co-ordination of Nuclear Reaction Data Centres (Technical Aspects), 28–30 May 2001, Vienna, Austria. INDC(NDS)-427, IAEA NDS, Vienna, Austria, 2001, p. 49.
11. Boboshin, I.N., Varlamov, V.V., Komarov, S.Yu., Peskov, N.N., Semin, S.B., Stepanov, M.E., Chesnokov, V.V., Universal electronic information system on atomic nuclei and nuclear reactions, Proceedings of the All-Russia Scientific and Methodological Conference 'Telematika' 2002', 3–6 June 2002, St. Petersburg,

ISBN 5-7577-0103-X, St. Petersburg, 'University Telecommunications', 2002, p. 148 [in Russian].

12. Varlamov, V.V., Ivanov, S.V., Peskov, N.N., Stepanov, M.E., New search engine for experimental data on nuclear reactions from the international EXFOR system, Collected Materials of the Third All-Russian Conference on Digital Libraries, RCDL' 2001, Digital Libraries: Advanced Methods and Technologies, Digital Collections, Petrozavodsk, 11–13 September, 2001, ISBN 5-9274-0055-8, Karelian Research Centre of the Russian Academy of Sciences, 2001, p. 166 [in Russian].
13. Relational nuclear data database of the Centre for Photonuclear Experiments Data of the Scientific Research Institute for Nuclear Physics, Moscow State University, URL: http://depni.sinp.msu.ru/cdfe [in Russian].
14. Ed. by Pronyaev, V.G., The Nuclear Data Centres Network, IAEA Nuclear Data Section, INDC(NDS)-401, IAEA, Vienna, Austria, 1999.
15. Pronyaev, V., Winchell, D., Zerkin, V., Muir, D., Arcilla, R., Requirements for the Next Generation of Nuclear Databases and Services, International Conference on Nuclear Data for Science and Technology, Embracing the Future at the Beginning of the 21st Century (October 7–12, 2001), Tsukuba, Japan, Japan Atomic Energy Research Institute, 2001, p. 263.
16. Ed. by V.McLane, EXFOR Systems Manual, Nuclear Reaction Data Exchange Format, BNL-NCS-63330, BNL, NNDC, USA, 1996.
17. Ishkhanov, B.S., Kapitonov, I.M., Lazutin, E.V., Piskarev, I.M., Sopov, V.S., Shevchenko, V.G., Yadernaya Fizika, 12 (1970) 892 [in Russian].
18. Veyssiere, A., Beil, H., Bergere, R., Carlos, P., Lepretre, A., De Miniac, A., Nucl. Phys., A227 (1974) 513.
19. Bramblett, R.L., Caldwell, J.T., Harvey, R.R., Fultz, S.C., Phys. Rev., 133 (1964) B869.
20. Pywell, R.E., Thompson, M.N., Berman, B.L., Nucl. Instr. and Meth., 178 (1980) 149.
21. Woodworth, J.G., McNeill, K.G., Jury, J.W., Alvarez, R.A., Berman, B.L., Faul, D.D., Meyer, P., Phys. Rev., C19 (1979) 1667.
22. Varlamov, V.V., Efimkin, N.G., Ishkhanov, B.S., Sapunenko, V.V., Voprosy atomnoj nauki i tekhniki, Ser.: Yadernye konstanty, 1 (1993) 52 [in Russian].
23. Berman, B.L., Pywell, R.E., Dietrich, S.S., Thompson, M.N., McNeill, K.G., Jury, J.W., Phys. Rev., C36 (1987) 1286.
24. Carlos, P., Beil, H., Bergere, R., Fagot, J., Lepretre, A., Veyssiere, A., Solodukhov, G.V., Nucl. Phys., A259 (1976) 365.
25. Berman, B.L., Bramblett, R.L., Caldwell, J.T., Davis, H.S., Kelly, M.A., Fultz, S.C., Phys. Rev., 177 (1969) 1745.
26. Fultz, S.C., Bramblett, R.L., Caldwell, J.T., Hansen, N.E., Jupiter, C.P., Phys. Rev., 128 (1962) 2345.
27. Lepretre, A., Beil, H., Bergere, R., Carlos, P., Veyssiere, A., Sugawara, M., Nucl. Phys., A175 (1971) 609.
28. Berman, B.L., Caldwell, J.T., Harvey, R.R., Kelly, M.A., Bramblett, R.L., Fultz, S.C., Phys. Rev., 162 (1967) 1098.
29. Lepretre, A., Beil, H., Bergere, R., Carlos, P., Miniac, A.De., Veyssiere, A., Nucl. Phys., A219 (1974) 39.
30. Fultz, S.C., Berman, B.L., Caldwell, J.T., Bramblett, R.L., Kelly, M.A., Phys. Rev., 186 (1969) 1255.
31. Bergere, R., Beil, H., Carlos, P., Veyssiere, A., Nucl. Phys., A133 (1969) 417.

32. Bramblett, R.L., Caldwell, J.T., Berman, B.L., Harvey, R.R., Fultz, S.C., Phys. Rev., 148 (1966) 1198.
33. Berman, B.L., Kelly, M.A., Bramblett, R.L., Caldwell, J.T., Davis, H.S., Fultz, S.C., Phys. Rev., 185 (1969) 1576.
34. Bramblett, R.L., Caldwell J.T., Auchampaugh, G.F., Fultz, S.C., Phys. Rev., 129 (1963) 2723.
35. Veyssiere, A., Beil, H., Bergere, R., Carlos, P., Lepretre, A., Nucl. Phys., A159 (1970) 561.
36. Fultz, S.C., Bramblett, R.L., Caldwell, J.T., Kerr, N.A., Phys. Rev., 127 (1962) 1273.
37. Harvey, R.R., Caldwell, J.T., Bramblett, R.L., Fultz, S.C., Phys. Rev., B136 (1964) 126.
38. Veyssiere, A., Beil, H., Bergere, R., Carlos, P., Lepretre, A., Kernbach, K., Nucl. Phys., A199 (1973) 45.
39. Caldwell, J.T., Dowdy, E.J., Berman, B.L., Alvarez, R.A., Meyer, P., Phys. Rev., C21 (1980) 1215.
40. Berman, B.L., Fultz, S.C., Rev. Mod. Phys., 47 (1975) 713.
41. Gargaro, W.W., Onley, D.S., Phys. Rev., C4 (1971) 1032.
42. Soto Vargas, C.W., Onley, D.S., Wright, L.E., Nucl.Phys., A288 (1977) 45.
43. Dodge, W.R., Hayward, E., Wolinec, E., Phys. Rev., C28 (1983) 150.
44. Beil, H., Bergere, R., Carlos, P., Lepretre, A., Nucl. Phys., A227 (1974) 427.

04-10281 (195) [4]
Translated from Russian

UDC 546.79

INTERACTIVE INFORMATION SYSTEM ON THE TRANSMUTATION OF NUCLIDES IN NUCLEAR REACTORS

V.I. Plyaskin, *R.A. Kosilov*
State Technical University of Nuclear Power Engineering, Obninsk, Russia

G.N. Manturov
State Scientific Centre - A.I. Leipunsky Institute for Physics and Power Engineering, Obninsk, Russia

INTERACTIVE INFORMATION SYSTEM ON THE TRANSMUTATION OF NUCLIDES IN NUCLEAR REACTORS. An information system which can be used to calculate nuclide transmutation in nuclear reactors is described. The algorithms developed are based on a directed nuclide transformation graph and improve the speed of the calculations. The calculations are performed using a nuclear physics constants database with the latest evaluations which improves the reliability of the results obtained.

Introduction

When irradiated with neutrons, the nuclide composition of materials changes. These changes, known as transmutations, used to be calculated in a wide range of theoretical research and practical work related to nuclear reactors, in particular for irradiation of targets to obtain radionuclides. The information system in question can be used for the following:

- automatic plotting and display on screen of a diagram of the nuclide transformations resulting from reactions caused by neutrons in a nuclear reactor and radionuclide decay;
- calculation of the number of nuclei of the desired nuclide in target irradiation and cooling modes;
- calculation of the specific radioactivity of the target and the energy release from decaying radionuclides as a function of time in irradiation and cooling modes;
- calculation of the neutron flow rate characteristic of the number of neutrons absorbed in the target to produce a certain quantity of the desired radionuclide;
- determination of the spectra of the different types of radiation from both an individual radionuclide and all radionuclides in the target as a whole at a given moment;
- selection of the optimum target irradiation and cooling mode depending on the hardness of the reactor neutron spectrum and the parameters of the target.

To calculate the transmutation of nuclides in nuclear reactors, the cross-sections for thermal neutrons, the resonance integrals and the Westcott factors must be known. In this information system, the calculations are based on a recent evaluation of these nuclear physics constants [1], which improves the reliability of the results obtained.

In general, calculating the transmutation parameters of a substance of arbitrary composition in a nuclear reactor is a complex and resource-intensive task even for modern computers, because the space-energy and nuclide burnup problems must be solved simultaneously. In Refs. [2, 3], the theory underlying the nuclide transmutation calculations is presented at some length, but the calculation algorithms proposed are rather complex, making them unsuitable for creating an **interactive** information system. The algorithms given below speed up the calculation of the basic parameters for transmutation of substances in a nuclear reactor and they are based on calculations using a nuclide transformation graph [4].

1. Use of a directed transformation graph when calculating nuclide transformations during transmutation

The time characteristics of nuclide transmutation processes in a reactor are determined by the rates of the nuclear reactions and radioactive decays involved. By the reaction rate S_n^i, for transformation of the nuclide i into the nuclide n, we mean the proportion of nuclei of the nuclide i which have transformed into the nuclide n over a unit of time.

For radioactive decay processes, $S_n^i = k_n^i \lambda_i$, where λ_i is the decay constant of the nuclide i and k_n^i is the proportion of the radioactive decay of the nuclide i resulting in the formation of the nuclide n relative to the total number of radioactive transformations of the nuclide i.

For reactions induced by neutrons, the reaction field S_n^i depends on the properties of the nucleus i and the spectrum neutron. Below we use the binomial representation $S_n^i = \sigma_n^i \Phi_T + I_n^i \Phi_R$, where σ_n^i and I_n^i are the effective thermal cross-section and the resonance integral of the reaction, and Φ_T and Φ_R are the thermal and resonance neutron flux densities respectively.

Let x_n equal the number of nuclei of the nuclide n. The equations describing the change over time of the value of x_n are derived from the equilibrium condition and take the form:

$$\begin{cases} \dfrac{dx_n}{dt} = \sum\limits_{i \neq n} S_n^i x_i - S_n x_n, \quad n = 1..N \end{cases} \tag{1}$$

where N is the total number of nuclides in the transmutation chain, x_n is the number of nuclei of the nuclide n, S_n is the total annihilation rate of the nuclide n, S_n^i is the rate of formation of the nuclide n from the nuclide i.

Clearly, the total annihilation rate S_n is given by the correlation:

$$S_n = \sum_i S_i^n ,$$

where the summation is performed for all products of nuclear reactions of the nuclide n.

It should be noted that the value x_n may have different physical meanings. The dimension and physical meaning of x_n will depend on what normalization is selected: if x_n is simply the number of nuclei of the nuclide n, x_n is dimensionless; if x_n is the density of the number of nuclei, the dimension of x_n = [cm^{-3}]. In this paper we assume that x_n is the number of nuclei of the nuclide n calculated for 1 g of the target substance. Then the dimension of x_n=[g^{-1}].

Based on the normalization selected, the starting conditions for the transmutation problem are written as follows:

$$x_i(0) = \begin{cases} x_{i,0}, \text{ if the nuclide is contained in the original substance} \\ 0, \quad \text{if it is not} \end{cases} \tag{2}$$

where $x_{i,0}$ is the number of nuclei of the nuclide i in 1 g of the target substance at the starting point.

In general, solving problem (1), (2) requires a lot of time and computing resources, because reaction rates S_n^i are non-uniform and exhibit a complex dependence on all the values of x_n. The most simple example of problem (1), (2) is where the nuclide transformation diagram is a linear chain. Then problem (1), (2) can be written as follows:

$$\begin{cases} \dfrac{dx_1}{dt} = -S_1 x_1 \\ \dfrac{dx_n}{dt} = S_n^{n-1} x_{n-1} - S_n x_n, \quad n = 2..N \end{cases} \tag{3}$$

with the following starting conditions:

$$\begin{cases} x_1(0) = x_{1,0} \\ x_n(0) = 0, \quad n = 2..N \end{cases} \tag{4}$$

Problem (3),(4) has a simple analytical solution:

$$\begin{cases} x_1(t) = x_{1,0} \exp(-S_1 t) \\ x_n(t) = x_{1,0} S_2^1 \ldots S_n^{n-1} \displaystyle\sum_{j=1}^{n} \frac{\exp(-S_j t)}{\displaystyle\prod_{k \neq j}^{n} (S_k - S_j)}, \quad n = 2..N \end{cases} \tag{5}$$

The traditional method for calculating nuclide transmutation parameters presupposes a numerical solution to the system of differential equations in expression (1), which is a complex and resource-intensive problem (particularly if thermal and resonance shielding are taken into account). The problem is complicated in particular by the fact that, when the system

is numerically integrated, the magnitude of the integration step, using the roughest estimates, cannot be greater than:

$$h \le \min_{i=1..N} \frac{\ln 2}{\widetilde{S}_i},$$

where h is the magnitude of the integration step; N is the total number of nuclides in the transmutation chain; $\widetilde{S}_i$ is the intensity of the "strongest" reaction of the nuclide i.

In the case of radioactive decay, this means that the integration step cannot be greater than the half-life of the shortest-lived nuclide in the chain. This significantly increases the time needed for the calculations when making long-term forecasts. An appealing way out of this situation is to attempt an analytical solution like the correlations in expression (5). As mentioned above, however, these correlations only apply for linear chains and where the reaction rates are uniform and are not dependent on any values of x_i.

In this interactive information system, a somewhat different approach to solving the transmutation problem is examined. It is based on the assumption that the branchings in the nuclide transformation diagram during the transmutation process occur independently of one another. Based on this assumption, we can use the nuclide transformation diagram to separate out linear chains and then calculate the transmutation parameters, using the formulae in expression (5).

To illustrate the above, we shall examine the following example: if a nuclide transformation diagram is plotted (Fig. 1), based on the assumptions made, the number of nuclei of the nuclide ^{134}Xe at a point in time t can be obtained as the sum of the number of nuclei of this nuclide calculated for all the linear chains leading from the start nuclide to the nuclide ^{134}Xe, thus:

$$({}^{134}_{52}Te \rightarrow {}^{134m}_{53}I \rightarrow {}^{134m}_{54}Xe \rightarrow {}^{134}_{54}Xe), ({}^{134}_{52}Te \rightarrow {}^{134m}_{53}I \rightarrow {}^{134}_{53}I \rightarrow {}^{134}_{54}Xe) \text{ and } ({}^{134}_{52}Te \rightarrow {}^{134}_{53}I \rightarrow {}^{134}_{54}Xe).$$

Apart from allowing us to separate out linear chains and use the formulae in expression (5), the transformation diagram allows us to display the decay chain on a monitor screen or print it out on a printer, which is a definite advantage for information systems.

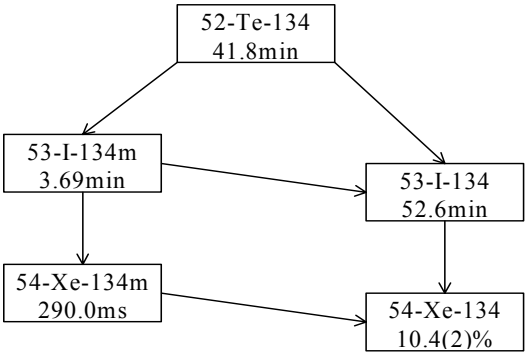

Fig. 1. Decay diagram for the radionuclide ^{134}Te

The reason for using a nuclide transformation diagram is that, from a mathematical point of view, this diagram is a directed graph whose vertices are the nuclides in the chain and whose edges correspond to the relative transformations of the nuclides during the transmutation process. The direction of the edges corresponds to the direction of transformation of the nuclides from parent to daughter nuclide.

Some definitions follow.

A *start vertex* (nuclide) is a vertex to which no edge leads. Start vertices correspond to nuclides in the chain at the starting point. In the case of radioactive decay, the transformation graph contains one start vertex. In the case of target irradiation in a reactor, the set of start vertices represents the initial isotopic composition of the target.

An *end vertex* (nuclide) is a vertex from which no edge leads. End vertices represent the "stable" nuclides at the time of the calculation, i.e. the nuclides whose total annihilation rate can be disregarded. In the case of radioactive decay, the end vertices correspond to the stable nuclides in the chain.

A *goal vertex* (nuclide) is a vertex whose parameters used to be calculated, or a vertex of particular significance for a problem.

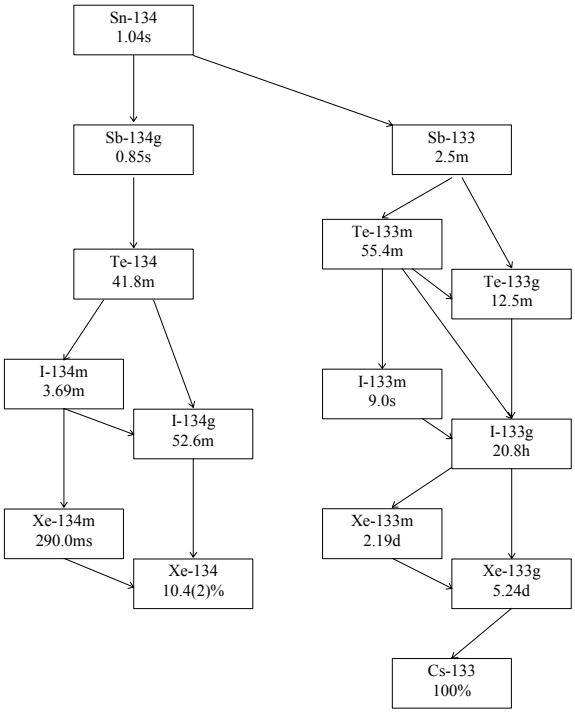

Fig. 2. Directed nuclide transformation graph representing the decay of the nuclide ^{134}Sn.

The characteristic features of a transformation graph representing the radioactive decay of a nuclide are as follows: a single start vertex; one or more end vertices; at least one path leading from the start vertex to any of the other vertices in the graph; no cycles (Fig. 2).

The characteristic features of a transformation graph representing the transmutation of a target substance of arbitrary composition in the neutron flux of a nuclear reactor are as follows: one or more start vertices representing the nuclides of the original target; one or more end vertices; at least one path leading to a given vertex from one of the start vertices (this may otherwise be expressed as follows: "the given vertex must be the 'progeny' of one or more of the start vertices, but does not have to be the progeny of all the start vertices"); possible cycles (Fig. 3).

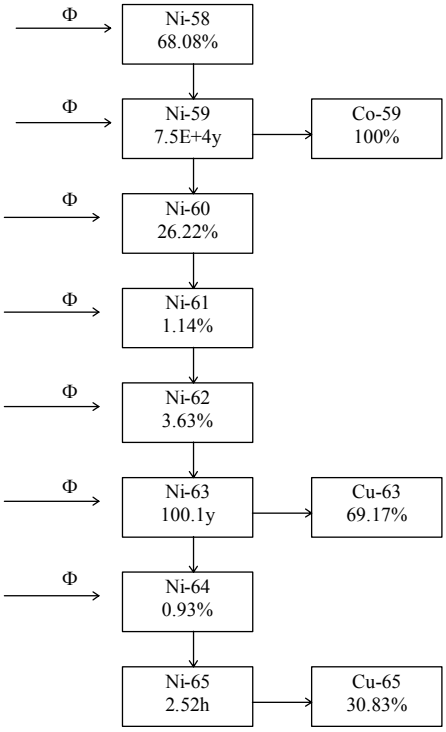

Fig. 3. Directed nuclide transformation graph representing nuclide transmutation during irradiation of a target made of a natural mixture of nickel isotopes

2. Calculation of the parameters of nuclide transmutation chains in a neutron flux using a directed transformation graph

The interactive information system implements an algorithm for solving the combined problem (1)–(2), which is based on use of the directed transformation graph described above, plotted using the starting conditions (2).

With the directed transformation graph, the number of nuclei x_n of a specific nuclide n at a moment in time T can be obtained as follows:

$$x_n(T) = \sum_l x_n^{(l)}(T), \qquad (6)$$

where the summation is performed for all the linear chains leading from the nuclides of the original target to the nuclide n. It is not difficult to produce a list of all the linear chains in question from the transformation graph. Solution (5) to problem (3), with the starting conditions ($x_1(0)=x_1^{(0)}$, $x_i(0)=0$, $i=2..N$) is used to find $x_n^{(l)}(T)$. To take account of the change in reaction rates caused by the effect of the thermal and resonance shielding during the transmutation process, the problem is solved by breaking down the calculation period $[O,T]$ into a series of intervals in which the rates are taken to be constant. Then, for each interval, a solution is obtained using the formulae in expression (5), assuming that the reaction rates remain the same as they are at the start of the interval.

3. Calculation of the parameters for producing radionuclides by irradiating targets in reactors

One of the most important practical applications of the problem of transmutation of substances in a nuclear reactor is for calculating the specifications when producing radionuclides by irradiating targets. The main indicators for this process are as follows: the number of nuclei of the desired nuclide, specific activity of the desired nuclide and all secondary nuclides, and the neutron flow rate.

The number of nuclei of the desired nuclide $x_m(t)$, calculated for only one nucleus of the main starting nuclide, is determined by solving problem (1),(2). The activity of the radionuclide according to that determination is the number of radionuclide decays per unit of time.

The specific activity Q of a radionuclide in the target calculated for one gram of the starting chemical element, is

$$Q_i(t) = \lambda_i N_A C_s x_i(t) / M \,, \tag{7}$$

where λ_i is the decay constant of the i-th radionuclide; N_A is the Avogadro number; C_s is the isotope content (enrichment) of the main starting nuclide; $x_i(t)$ is the number of nuclei of the i-th radionuclide at the moment in time t; M is the mean atomic mass of the starting chemical element. Because we can calculate the specific activity of the secondary radionuclides, we can analyse the process for producing a radionuclide and select the optimal parameters for the irradiation and cooling mode.

The neutron flow rate R is a value characterizing the number of neutrons absorbed in the target to produce one nucleus of the desired nuclide. Where there are no fissile nuclei in the transformation diagram, the neutron flow rate can be obtained using the formula

$$R = \frac{1}{x_m(T)} \sum_i \int_0^T \hat{S}_i x_i(t) dt \,, \tag{8}$$

where $x_m(T)$ is the number of nuclei of the desired nuclide at the point in time T; $x_i(t)$ is the number of nuclei of nuclide i at the point in time t; $\hat{S}_i$ is the total rate of the reactions of the

nuclide i induced by the neutron flux: $\hat{S}_i = \sum_k \left(\sigma_k^i g_{W_k}^i p + \gamma q_i I_k^i \right) \Phi_T$ (the summation is performed for all products of the nuclear reactions of the nuclide i).

If there are fissile nuclides in the target, the formula for calculating the neutron flow rate must be adjusted to take account of fission neutrons:

$$R = \frac{1}{x_m(T)} \sum_i \int_0^T (1 - \nu_i) \hat{S}_i x_i(t) dt \,, \qquad (9)$$

where ν_i is the number of fission neutrons per capture.

The algorithm for solving problem (1), (2) proposed in this paper can also be used to obtain an analytical expression for the integrals on the right-hand side of formulae (8) and (9), which substantially speeds up the calculation of those values.

Conclusion

An interactive information system has been developed which can be used to calculate transmutation of nuclides in nuclear reactors on a personal computer. Algorithms have been proposed for calculating the main parameters of nuclide transmutation in a reactor, which are based on a directed nuclide transformation graph and help speed up the calculation. The calculations are performed using databases of nuclear physics constants with the latest evaluations, which improves the reliability of the results obtained.

The research was conducted with financial support from the Russian Foundation for Fundamental Research and the administration of the Kaluga region (project No. 02-07-96005), and a grant from the Ministry of Education of the Russian Federation for fundamental research on technical science (No. T02–01.31383).

References

1. Ignatyuk A.V., Plyaskin I.V., Popov Yu.P., New Series: Numerical data and functional relationships in science and technology, Group I: Elementary particles, nuclei and atoms, Volume 16: Low energy neutron physics, Subvolume A: Low energy neutrons and their interaction with nuclei and matter, Part 1, Springer-Verlag, 2000, chapter 8.
2. Kruglov A.K., Rudik A.P., Reactor production of radionuclides, Moscow, Ehnergoatomizdat, 1985, pp. 64–108 [in Russian].
3. Gerasimov A.S., Zaritskaja T.S., Rudik A.P., Handbook on the production of nuclides in nuclear reactors, Moscow, Ehnergoatomizdat, 1989, p. 258 [in Russian].
4. Plyaskin V.I., Kosilov R.A., Manturov G.N., Interactive information system on the nuclear physics properties of nuclides and radioactive decay chains, IAEA, INDC(CCP)-450, Vienna, 2001, p. 27-32.

Nuclear Data Section
International Atomic Energy Agency
P.O. Box 100
A-1400 Vienna
Austria

e-mail: services@iaeand.iaea.org
fax: (43-1) 26007
cable: INATOM VIENNA
telex: 1-12645
telephone: (43-1) 2600-21710

Online: TELNET or FTP: iaeand.iaea.org
username: IAEANDS for interactive Nuclear Data Information System
usernames: ANONYMOUS for FTP file transfer;
FENDL2 for FTP file transfer of FENDL-2.0;
RIPL for FTP file transfer of RIPL;
NDSONL for FTP access to files saved in “NDIS” Telnet session.
Web: http://www-nds.iaea.org